

LAURA MELCHIONDA

Matr. N°. 067170

New genes involved in mitochondrial and
neurodegenerative diseases identified by whole
exome sequencing

Coordinator: Prof. Andrea Biondi

Tutor: Dr. Massimo Zeviani

Table of Contents

Chapter 1: general introduction	1
NEURODEGENERATIVE DISEASES	2
Misfolded protein	3
Calcium homeostasis	5
Oxidative stress	7
Mitochondrial dysfunction	9
Axonal transport	11
Inflammation	14
AMYOTROPHIC LATERAL SCLEROSIS	15
LEUKODYSTROPHIES	18
Alexander disease	20
MITOCHONDRIAL DISEASES	21
Genetics of mitochondrial diseases	23
mtDNA mutations	23
nDNA mutations	28
Treatment of mitochondrial diseases	38
NEXT GENERATION SEQUENCING	40
Scope of the thesis	46

References	48
Chapter 2:	57
Adult-onset Alexander disease, associated with a mutation in an alternative GFAP transcript, may be phenotypically modulated by a non-neutral HDAC6 variant	
Chapter 3:	87
Mutations of the Mitochondrial-tRNA Modifier <i>MTO1</i> Cause Hypertrophic Cardiomyopathy and Lactic Acidosis	
Chapter 4:	123
<i>MTO1</i> Mutations are Associated with Hypertrophic Cardiomyopathy and Lactic Acidosis and Cause Respiratory Chain Deficiency in Humans and Yeast	
Chapter 5: Summary, conclusions and future perspectives	163
Summary	165
Discussion and conclusions	171
Future perspectives	176
References	180

CHAPTER 1

General introduction:

Neurodegenerative and Mitochondrial diseases

NEURODEGENERATIVE DISEASES

The term “neurodegeneration” is defined as “any pathological condition primarily affecting neurons” or “disease process in which neurons are selectively and gradually destroyed, leading to a progressive loss of nervous system structure and function” (Przedborski S et al., 2003; Deuschl G and Elble R, 2009).

It is currently estimated that the number of neurodegenerative diseases is approximately a few hundred. Their classification is based on the predominant clinical feature or the topography of the principal lesion, or often on a combination of both. Accordingly, neurodegenerative disorders of the central nervous system (CNS) may, for example, be first grouped into diseases affecting the cerebral cortex, the basal ganglia, the brainstem and cerebellum, or the spinal cord. Then, within each group, a given disease may be further classified based on its main clinical features (Przedborski S et al. 2003).

However, clinical and pathological features among different neurodegenerative disorders often overlap, making their practical classification quite demanding.

One of the main debates about the aetiology of these disorders concerns the relative roles of genetic and environmental factors in the initiation of these diseases. Some cases have a clear familial occurrence suggesting a genetic basis, but others, the largest amount, are essentially sporadic. For example, this claim is true for Parkinson’s disease (PD), Alzheimer disease (AD) and Amyotrophic Lateral Sclerosis (ALS).

Despite numerous progresses in understanding the aetiopathogenesis of neurodegenerative diseases have been done, the precise pathway that firstly leads to neuronal dysfunction and then to death isn't yet known. However, there are several hypothesis related to pathogenesis of these diseases: accumulation of misfolded proteins, proteasomal and autophagy dysfunction, oxidative stress, impaired calcium homeostasis, axonal transport deficits, mitochondrial dysfunction, inflammation, and white matter alterations are postulated to play a role in almost every neurodegenerative disorder. Anyway, many of these mechanisms are likely to be connected, so that a defect in one cellular pathway will have a “domino effect” leading to multiple stresses for the cell.

In the following paragraphs I have reported the main pathogenetic mechanisms related to neurodegenerative disorders, with a final focus on amyotrophic lateral sclerosis; leukodystrophies (in particular Alexander disease), and mitochondrial disorders that are the subjects of my PhD projects

Misfolded proteins

Many neurodegenerative diseases are caused by accumulation of specific protein aggregates in the brain with a regional pattern specific to each disease. AD is characterized by extracellular deposition of amyloid- β ($A\beta$) protein in the form of senile plaques and by intraneuronal accumulation of hyperphosphorylated tau as

neurofibrillary tangles. (Hardy, 2006; Selkoe, 2004). In PD, the synaptic protein α -synuclein accumulates in neuronal cell bodies and axons; these aggregates are referred to as Lewy bodies and Lewy neuritis, respectively (Goedert, 2001). In Huntington's disease (HD) and other diseases with the expansion of triplet repeats, proteins with expanded polyglutamine (polyQ) accumulate in the nucleus and cytoplasm (Ross and Poirier, 2004). Accumulation of misfolded prion proteins also occurs in Creutzfeldt–Jakob disease (CJD) (Prusiner, 2001). The proteins that accumulate in neurodegenerative diseases are typically misfolded and yield a β -sheet structure that promotes aggregation and fibril formation (Soto C 2003; Ross Ca et al. 2004). Genetic factors, including gene mutations, gene dose and promoter polymorphisms, may affect protein levels and conformation. In the same way environmental factors, such as oxidative or metabolic stress, can increase the production of misfolded proteins.

In eukaryotic cells there are two main pathways responsible for protein and organelle clearance: the ubiquitin-proteasome system (UPS) and the autophagy-lysosome system.

Proteasome are barrel-shaped multiprotein complexes that predominantly degrade short-lived nuclear and cytosolic proteins after their C-terminal ubiquitination.

Autophagy, literally “self-eating”, describes a catabolic process in which cell constituents such as organelles and proteins are delivered to the lysosomal compartment for degradation.

Increasing evidences suggest that impairment in UPS and autophagy is a common feature in several brain diseases (McNaught KS et al.

2001; Keller JN et al. 2000). These dysfunctions may be caused directly by mutations in genes that encode proteins involved these pathways; for example, mutations in the *PARK2/PARKIN* gene, that encode an E3 ubiquitin ligase, one of the three enzymes involved in the conjugation of ubiquitin to proteins targeted to UPS, caused inherited forms of PD (Kitada T et al., 1998). Another possibility is that the abnormal protein accumulation may further overwhelm degradative systems and, as a result, even more proteins start accumulating within the cells (Bence NF et al. 2001).

If unfolded proteins cannot be refolded and targeted for degradation, they may be sequestered into a specific cellular site to generate an intracellular inclusion body, as an aggresome (Johnston JA et al., 1998). According to current knowledge, the formation of this aggresome would have a protective function, reducing the random accumulation of potential toxic protein oligomers and aggregates and preventing abnormal interactions of these aberrant species with other proteins or cell organelles (Chen B et al., 2011).

Calcium homeostasis

Neurons are excitable cells that process and transmit the information through an electrochemical signal in highly controlled spatio-temporal manner. Calcium, as Ca^{2+} cation, is the major intracellular messenger that mediates the physiological response of neurons to chemical and electrical stimulation. Under resting conditions, free cytosolic Ca^{2+} levels in neurons are maintained around 200 nM, but their concentration can rise to low micromolar values upon electrical or

receptor-mediated stimulation. Calcium can be released from intracellular stores or influx from extracellular space, where the concentrations are several magnitudes higher compared to cytosolic calcium levels.

Ca^{2+} can influx into the cell through voltage-dependent channels and ligand-gated channels such as glutamate and acetylcholine receptors (Berridge MJ et al. 2003). The main intracellular calcium store is the endoplasmic reticulum (ER) from where calcium can be released into the cytosol via activation of inositol 1,4,5-triphosphate receptors (InsP3Rs) or ryanodine receptors (RyRs). Basal cytosolic Ca^{2+} levels are maintained partly by powerful calcium-binding and calcium-buffering proteins (e.g. calbindin or parvalbumin) and partly by an active uptake into internal stores by the Sarco/ER calcium-ATPase (SERCA) at the ER membrane or by the mitochondrial uniporter (Berridge MJ et al. 2003).

Usually, this finely tuned control of Ca^{2+} fluxes and Ca^{2+} load is compromised in normal aging and even more in pathological states. The major factor responsible for impairment of neuronal Ca^{2+} homeostasis is oxidative stress. This situation makes neurons vulnerable to a form of Ca^{2+} -mediated death, called excitotoxicity, in which glutamate receptors are over activated leading to rise of intracellular Ca^{2+} concentrations beyond tolerable levels (Arundine M and Tymianski M, 2003). Mitochondria play an important role in the regulation of Ca^{2+} levels. It has been demonstrated that both genetic manipulations and pharmacological treatments, enhancing

mitochondrial Ca^{2+} sequestration, can protect neurons against excitotoxicity (Duchen MR, 2000).

Alterations of Ca^{2+} homeostasis are observed in several neurodegenerative diseases including PD, AD, ALS and HD. Rare examples support a direct role of Ca^{2+} homeostasis deregulation as the first hit towards neurodegeneration, however there are evidences that highlights the presence and the importance of calcium deregulation in progression of several neurodegenerative process (Wojda U et al. 2008).

Oxidative stress

Oxygen is necessary for the normal function of eukaryotic organisms, but paradoxically, as a result of its metabolism it produces reactive oxygen species (ROS), which can be extremely toxic to cells. ROS include both free radicals, such as superoxide ($\text{O}_2^{\cdot-}$), nitric oxide (NO^{\cdot}) and hydroxyl (OH^{\cdot}) radicals and other molecular species, such as hydrogen peroxide (H_2O_2) and peroxynitrite (ONOO^{\cdot}). ROS can interact with different substrates in the cell, such as proteins, lipids and DNA. Oxidation of proteins may involve structural alterations or destroy the active sites of enzymes. Other examples of protein modifications caused by ROS are nitration, carbonylation, and protein-protein cross linking, generally leading to protein loss of function and accumulation into cytoplasmic inclusions with alterations of degradation systems (Dalle-Donne et al., 2005).

Oxidative modification of unsaturated fatty acids can result in lipid peroxides, which in some cases disrupt both the plasma membrane and membranes of subcellular organelles, such as mitochondria.

Oxidation of DNA may lead to mutations. In fact, it is known that the frequency of mtDNA mutations is higher than nDNA, because it is exposed to the action of ROS produced by oxidative phosphorylation (OXPHOS), the metabolic pathway in which the mitochondria produce energy in the form of ATP.

The cell has evolved several defense and repair mechanisms against oxidized species based on antioxidant enzymes, including superoxide dismutase (SOD), glutathione peroxidase, and catalase.

SOD plays a crucial role in scavenging $O_2^{\cdot-}$. Three distinct isoforms of SOD are identified: copper-zinc-containing cytoplasmic SOD (SOD1), manganese-containing mitochondrial SOD (SOD2) and extracellular SOD (SOD3).

Glutathione peroxidase is the general name for a family of multiple isoenzymes that catalyze the reduction of H_2O_2 or organic hydroperoxides in water or corresponding alcohols using glutathione (GSH) as an electron donor.

Catalase, a ferriheme-containing enzyme, is responsible for the conversion of hydrogen peroxide to water and it is localized especially in peroxisomes.

In addition there are non enzymatic antioxidant compounds, such as GSH and vitamin E. GSH is the most abundant small non protein molecule in cells and it is the main antioxidant in CNS. Reduced GSH can interact directly with free radicals for their removal. Vitamin E

appears to neutralize the effect of peroxide and to prevent lipid peroxidation in membranes.

The brain is considered to be particularly susceptible to ROS damaging. In fact, even if it represents only ~2% of the total body weight, the brain accounts over than 20% of the total consumption of oxygen (Halliwell B. et al., 2006). Therefore, oxidative stress can be important in aetiology of various neurodegenerative diseases. In fact postmortem brain tissues from patients with different neurodegenerative diseases demonstrated increased ROS in affected brain regions. A clear example from genetics is the presence of *SOD1* mutations in 20% of familial cases of ALS.

Mitochondrial dysfunction

Mitochondria play a central role in many functions including ATP generation, intracellular Ca^{2+} homeostasis, ROS formation and apoptosis. Therefore, decrease of ATP synthesis due to mitochondrial respiratory chain deficiency, increase of oxidative stress, accumulation of mitochondrial DNA (mtDNA) mutations, and Ca^{2+} homeostasis deregulation can be considered as signs of mitochondrial dysfunction.

Mitochondria produce more than 90% of our cellular energy (ATP) by OXPHOS which occurs at the level of mitochondrial respiratory chain (MRC), composed of five enzymatic multi-heteromeric complexes (I, II, III, IV, V) embedded in the inner membrane of mitochondria. Mutations in genes encoding MRC subunits or assembly factors of

mitochondrial complexes result in ATP synthesis deficiency. But also drugs can inhibit complex activities. For example, the first evidence for complex I dysfunction in PD was the observation that drug abusers who were accidentally exposed to 1-methyl 4-phenyl 1,2,3,6-tetrahydropyridine (MPTP) developed PD (Langston JW et al., 1983). The proper functioning of mitochondria is essential. In fact, energy metabolism plays a decisive role in life/death of the cells. In particular, neuronal function and survival depend on a continuous supply of glucose and oxygen, used to generate ATP through glycolysis and mitochondria respiration. A perturbation in energy metabolism, for instance after stroke, ischemia or brain trauma can lead to irreversible neuronal injury. An age-related decline in energy metabolism also may contribute to neuronal loss during normal aging, as well as in neurodegenerative diseases (Beal, 1995). Damage to mitochondria is caused primarily by ROS generated by the mitochondria themselves (Wei et al., 1998; Duchen, 2004). It is currently believed that the majority of ROS are generated by complexes I and III (Harper et al., 2004). Amongst all the interconnected mitochondrial pathways, it is often difficult to distinguish between causes and consequences. For instance, oxidative stress induces mtDNA mutations, OXPHOS dysfunction, alteration of membrane potential, permeability transition pore activation, and calcium uptake; but, conversely, some inherited mtDNA mutations lead to respiratory chain deficiency or directly cause increased ROS production.

Faulty mitochondria have been thought to contribute to several ageing-related neurodegenerative diseases, such as PD, AD and ALS. A lot of genes associated with PD code proteins with mitochondrial localization and/or influence on mitochondrial function, for example mutations of parkin, an ubiquitin E3 ligase involved mainly in UPS, cause oxidative stress and mitochondrial impairment.

The exact role of mitochondria in the pathogenesis of AD is less clear, but there are several observations that support this link. Amyloid precursor protein (APP), when overexpressed in cells and mice, clogged mitochondrial import machinery, causing mitochondrial dysfunction and impairment of energy metabolism.

Axonal transport

Neurons are cells responsible for the reception and the transmission of nerve impulses to and from the CNS. Typically, neurons are composed of a cell body, multiple dendrites and a single axon.

Dendrites and cell bodies play a role in collection and processing of information, and the axon is responsible for the transmission of information to other neurons via synapses.

Unlike dendrites, that are in close proximity with the neuronal cell body, axons can extend from a few millimeters to one meter or more. Being axons devoid of a specific apparatus for protein synthesis, axonal proteins are synthesized in the cell bodies and subsequently transported into axons and synapses. This process is called axonal transport and occurs along the cellular cytoskeleton. There are three

major components of the neuronal cytoskeleton: microtubules, actin and intermediate filaments.

Microtubules are formed from the dynamic polymerization of $\alpha\beta$ -tubulin dimers. Microtubules polymerize outward from the centrosome, then undergo a stochastic transition, resulting in a very rapid depolymerization. This dynamic behavior is required for the normal outgrowth of axons and growth cones, specialized ends of growing axons (or dendrites) that generate the motive force for elongation.

Also the cytoskeletal actin provides both dynamics and stability to this structure. Actin monomers assemble into a flexible helical polymer with two distinct ends: one fast growing extremity and one with a slower growth.

The third major component of the cellular cytoskeleton includes intermediate filaments, the most common of which are neurofilaments in mature motor neurons. Once assembled, these filaments lack overall polarity, and do not undergo the dramatic remodeling characteristic of actin and microtubules. Neurofilaments primarily provide structural stabilization to the cell, and regulate the radial growth of axons. It is interesting to note that aggregation of neurofilaments is a common marker of neurodegenerative disease (Liu Q et al., 2004)

Molecular motors, specialized enzymes that use ATP hydrolysis energy to move along the cellular cytoskeleton, are responsible for active transport in neurons. Long distance travel within the motor neuron is driven primarily by microtubule-based motor proteins, while

actin filament-based motors drive shorter distances, or dispersive movements. Microtubules motors include members of the kinesin superfamily and cytoplasmic dynein; myosin drive transport of vesicles and organelles along actin filaments. Conventional kinesins are the major species of plus-end directed molecular motors in the brain (Wagner et al., 1989), being involved in anterograde transport (from cell body to synapses) of various membrane-bounded organelles, including mitochondria, synaptic vesicles and axolemmal precursors, among others (Leopold et al., 1992; Elluru et al., 1995). Conventional kinesin is a heterotetramer composed of two heavy chains (kinesin-1s, KHCs) and two light chains (KLCs) (DeBoer et al., 2008). Retrograde transport (from axonal end to cell body) is carried out by the multisubunit motor protein complex cytoplasmic dynein (CDyn) (Susalka and Pfister, 2000). This transport consists mainly of endosomal/lysosomal organelles that carry corrupted proteins back to the cell bodies for degradation but also neurotrophic factors required for neuronal survival.

A lot of evidence suggests that neurodegenerative diseases may be a direct consequence of axonal transport alterations. Mutations have been found in various subunits of conventional kinesin (Reid et al., 2002) and CDyn (Hafezparast et al., 2003; Farrer et al., 2009) resulting in selective degeneration of specific neuronal subtypes. Moreover other mechanisms, such as abnormal activation of protein kinases and aberrant patterns of protein phosphorylation, that are not associated with mutations in molecular motors, represent major hallmarks in neurodegenerative diseases (Wagey and Krieger, 1998).

Inflammation

The immune system plays important roles in the maintenance of tissue homeostasis and in the response to infection and injury. The CNS has developed strategies to limit the entry of immune elements as well as to limit the emergence of immune activation within the tissue itself. This phenomenon is called 'immune privilege' and is partially reliable on the blood-brain barrier (BBB), which is designed to limit the entry of solutes and ions into the CNS (Amor S et al., 2010).

Microglial cells are the major resident immune cells in the brain, where they constantly survey the microenvironment and produce factors that influence surrounding astrocytes (another type of glial cell with support functions) and neurons.

While an acute neuroinflammatory response is generally beneficial to the CNS, tending to minimize further injury and contributing to the repair of damaged tissue, a chronic neuroinflammation is always detrimental. In fact, chronic neuroinflammation, as well as the standing activation of microglia and the release of inflammatory mediators, increase oxidative and nitrosative stress (Tansey MG et al., 2007).

Generally, inflammation is not a trigger factor for neurodegenerative diseases, but emerging evidence suggests that sustained inflammatory responses, involving microglia and astrocytes, may contribute to disease progression.

AMYOTROPHIC LATERAL SCLEROSIS

ALS is a neurodegenerative disease characterized by injury and death of lower motor neurons in the brainstem and spinal cord, and of upper motor neurons in the motor cortex, resulting in progressive muscle wasting and weakness. Generally, patients survive about 3 years from the onset of symptoms and death is typically associated with respiratory failure. Incidence of ALS is 2 per 100,000 individuals, the mean age of onset is 55-60 years and the disease affects more frequently men than women.

ALS is commonly a sporadic disease (SALS), only 5-10% of cases are familial (FALS), usually with an autosomal dominant inheritance. The identification of mutations in genes associated to FALS has helped to understand some key pathogenic mechanisms for this disease.

Mutations in at least 15 different genes have been attributed to FALS (table 1), the most common being in *SOD1*, *TARDBP* and *FUS*.

Biological samples from patients with *SOD1* mutations, including cerebrospinal fluid, serum and urine, show ROS elevation (Simpson E P, 2004; Mitsumoto H et al., 2008). Moreover, postmortem tissues from SALS and FALS patients presented high levels of oxidative damage of proteins, lipids and DNA and show abnormalities in mitochondrial structure, number, localization, and impaired respiratory chain complex activity. *SOD1* is mainly a cytoplasmic protein, but several studies have demonstrated that both wt *SOD1* and its mutant form localize to mitochondria in affected tissues (Vijayvergiya C et al. 2005). The interaction between *SOD1* and mitochondria suggests a number of mechanisms by which

mitochondrial function and cell survival may be affected. For example, SOD1 aggregates on the outer mitochondrial membrane may impair protein import and increase ROS production, causing oxidative damage to mitochondrial proteins and lipids (Mattiuzzi M et al. 2002). These aggregates may also contribute to apoptotic cells death promoting the release of cytochrome *c* (Takeuchi H et al. 2002) and/or sequestering the anti-apoptotic protein Bcl-2 (Pasinelli P et al. 2004).

Genetic subtype	Chromosomal locus	Gene	Onset/inheritance	Reference
<i>Oxidative stress</i>				
ALS1	21q22	Superoxide dismutase 1 (SOD1)	Adult/AD	Rosen (1993) ²⁷
<i>RNA processing</i>				
ALS4	9q34	Senataxin (SETX)	Juvenile/AD	Chen et al. (2004) ¹⁵⁴
ALS6	16p11.2	Fused in sarcoma (FUS)	Adult/AD	Kwiatkowski et al. (2009) ¹⁵² Vance et al. (2009) ¹⁵³
ALS9	14q11.2	Angiogenin (ANG)	Adult/AD	Greenway et al. (2006) ¹⁵¹
ALS10	1p36.2	TAR DNA-binding protein (TARDBP)	Adult/AD	Sreedharan et al. (2008) ⁸⁹
<i>Endosomal trafficking and cell signaling</i>				
ALS2	2q33	Alsin (ALS2)	Juvenile/AR	Yang et al. (2001) ¹⁰²
ALS11	6q21	Polyphosphoinositide phosphatase (FIG4)	Adult/AD	Chow et al. (2009) ¹⁰⁸
ALS8	20q13.3	Vesicle-associated membrane protein-associated protein B (VAPB)	Adult/AD	Nishimura et al. (2004) ¹⁰⁴
ALS12	10p13	Optineurin (OPTN)	Adult/AD and AR	Maruyama et al. (2010) ¹⁰⁵
<i>Glutamate excitotoxicity</i>				
ND	12q24	D-amino acid oxidase (DAO)	Adult/AD	Mitchell et al. (2010) ⁷⁰
<i>Ubiquitin/protein degradation</i>				
ND	9p13-p12	Valosin-containing protein (VCP)	Adult/AD	Johnson et al. (2010) ⁹⁹
ALSX	Xp11	Ubiquitin 2 (UBQLN2)	Adult/X-linked	Deng et al. (2011) ¹⁰¹
<i>Cytoskeleton</i>				
ALS-dementia-PD	17q21	Microtubule-associated protein tau (MAPT)	Adult/AD	Hutton et al. (1998) ¹²⁰
<i>Other genes</i>				
ALS5	15q15-q21	Spatacsin (SPG11)	Juvenile/AR	Orlaacchio et al. (2010) ¹⁵⁴
ALS-FTD	9p13.3	σ Non-opioid receptor 1 (SIGMAR1)	Adult/AD Juvenile/AR	Luty et al. (2010) ¹⁵⁵ Al Saif et al. (2011) ¹⁵⁶
ALS-FTD	9q21-q22	Chromosome 9 open reading frame 72 (C9ORF72)	Adult/AD	Hosler et al. (2000) ²⁴ Renton et al. (2011) ¹⁵⁰ De Jesus-Hernandez et al. (2011) ¹⁵⁷
<i>Unknown genes</i>				
ALS3	18q21	Unknown	Adult/AD	Hand et al. (2002) ¹⁵⁴
ALS7	20pter-p13	Unknown	Adult/AD	Sapp et al. (2003) ¹⁵⁶

Abbreviations: AD, autosomal dominant; ALS, amyotrophic lateral sclerosis; AR, autosomal recessive; FTD, frontotemporal dementia; PD, Parkinson disease.

Table 1. Genes associated with familial ALS (Ferraiuolo L et al., 2011)

TARDBP encodes for TDP-43, an essential nuclear RNA-binding protein involved in transcriptional repression, exon splicing inhibition and mRNA stabilization. TDP43 is a major constituent of cytoplasmic ubiquitin-positive inclusions that accumulate in the degenerating motor neuron of ALS patients and individuals with ubiquitin-positive fronto-temporal lobar degeneration.

FUS protein resembles TDP-43, and it has been implicated in alternative splicing, genomic maintenance, and transcription factor regulation. FUS cytosolic aggregates have been found in degenerating neurons of FALS patients.

The precise pathogenic mechanism of ALS is not fully determined, but protein misfolding and aggregation, defective axonal transport, mitochondrial dysfunction and excitotoxicity have been related to motor neuron dysfunction and death.

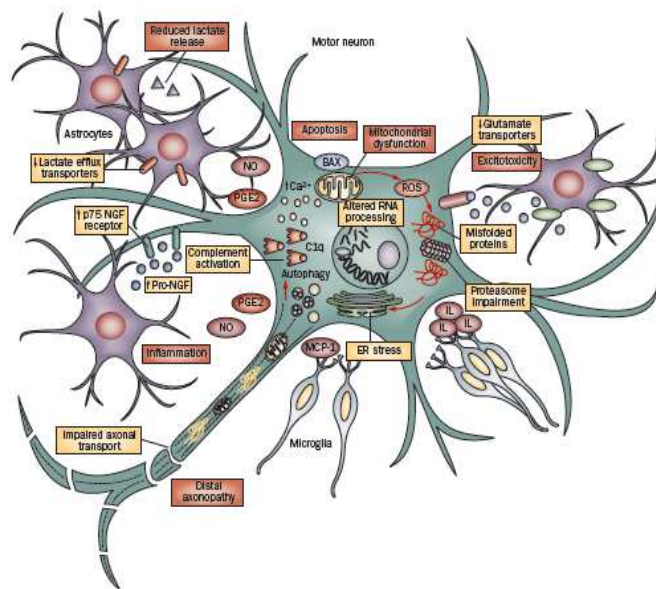


Figure 1. Molecular mechanisms of motor neuron injury in ALS (Ferraiuolo L et al., 2011)

LEUKODYSTROPHIES

Leukodystrophies are diseases characterized by a failure in myelination or hypomyelination of the white matter in CNS, and sometimes also in peripheral nerves. The term leukoencephalopathy usually refers to defects causing secondary myelin damage.

Although each leukodystrophy has distinctive clinical, biochemical, pathological and radiological features (table 2), most of these genetically inherited disorders can be classified in three categories, according to the subcellular compartment mainly affected: lysosomal storage diseases, peroxisomal disorders, and diseases caused by mitochondrial dysfunction.

Leukodystrophies can manifest in childhood or in adulthood, are generally incurable with a progressive course, leading to premature death.

The diagnosis of childhood-onset leukodystrophies is very difficult. In fact, symptoms usually progress slowly with possible periods of stagnation. Patients are generally non dysmorphic and, with the exception of infantile cases, exhibit normal early development before losing skills as myelin deteriorates. Personality changes and subtle cognitive decline may be the earliest sign and often precede the loss of previously acquired motor skills. More focal clinical signs may then appear, such as lower limb spasticity, ataxia, swallowing function, movement disorders, optic atrophy.

The 'typical' adult with leukodystrophy presents progressive cognitive or neuropsychiatric difficulties, often associated with pseudobulbar palsy or progressive lower limb spasticity. Cerebral dysfunction is

typically characterized by impaired attention and forgetfulness, psychomotor slowing, impaired executive and visuospatial skills, changes in personality, and emotional disturbances typical of subcortical dementia.

A very valuable instrument for leukodystrophy diagnosis is the magnetic resonance (MR) imaging, as it plays an important role in the identification, localization, and characterization of underlying white matter abnormalities in affected patients.

Disease	Inheritance	Clinical Features	Distinct Imaging Features	Diagnostic Tests	Pathophysiology
Adrenoleukodystrophy	X-linked recessive	Cerebral: behavioral changes, motor regression, acute progression AMN: chronic progressive spastic paraparesis	Cerebral: predominantly posterior-periventricular, contrast enhancement AMN: corticospinal tract involvement	Plasma very long chain fatty acids; ABCD1 mutation	Cerebral: brain inflammation AMN: oxidative stress?
Metachromatic leukodystrophy	Autosomal recessive	Behavioral changes, pyramidal signs, ataxia	Diffuse white matter abnormalities with sparing of U-fibers	Arylsulfatase A in leukocytes; high urinary excretion of sulfatides	Accumulation of sulfatides within lipid membranes
Globoid cell leukodystrophy (Krabbe disease)	Autosomal recessive	Developmental regression, spasticity, opisthotonus; late-onset milder	Posterior-predominant periventricular; no enhancement	Galactosylceramide β -galactosidase in leukocytes	Psychosine cytotoxic to oligodendroglia?
Vanishing white matter disease	Autosomal recessive inheritance with age-dependent penetrance	Ataxia, spasticity, deterioration following minor head trauma and fibrile illness	Progressive rarefaction and cystic degeneration of white matter	Mutation in eIF2B α , β , γ , δ , or ϵ	Abnormal unfolded protein response?
Alexander disease	De novo mutations in majority	Megalencephaly, psychomotor regression, ataxia and seizures; adults with bulbar symptoms	Diffuse white matter abnormalities, often with anterior predominance	<i>GFAP</i> gene mutation	Toxic aggregates of GFAP?
Canavan disease	Autosomal recessive	Megalencephaly, hypotonia, psychomotor regression	Diffuse subcortical signal abnormalities; increased NAA on MRS	Asparinoylase gene mutation	Poorly understood
Leukodystrophy with neuroaxonal spheroids	Unclear- most cases sporadic but familial inheritance described	Adult onset disease may masquerade as MS or dementia	Symmetric confluent or multifocal white matter signal abnormalities	Neuroaxonal spheroids and pigmented glia on brain biopsy	Poorly understood
Pelizaeus Merzbacher disease	X-linked recessive	Infantile onset in majority; nystagmus, impaired vision, ataxia, seizures	Symmetric confluent white matter signal abnormalities	<i>PLP1</i> gene mutation	Poorly formed myelin
Pelizaeus-Merzbacher-like disease	Unclear, but probably autosomal recessive	Indistinguishable from PMD	Symmetric confluent abnormalities	<i>GJA12</i> gene mutation in some	Poorly understood
Megalencephalic leukoencephalopathy with subcortical cysts	Unclear, but probably autosomal recessive	Megalencephaly, slowly progressive ataxia and spasticity, seizures	Subcortical cysts in temporal poles and frontoparietal regions	<i>MCL1</i> gene mutation	Poorly understood
Leukoencephalopathy with brainstem and spinal cord involvement and elevated white matter lactate	Autosomal recessive	In early adulthood cerebellar ataxia, spasticity, cognitive impairment	Brainstem and spinal cord involvement and elevated lactate on MRS	<i>DARS2</i> gene mutation	Poorly understood
Aicardi-Goutieres syndrome	Predominantly autosomal recessive, except subtype 5 which is autosomal dominant	Neonatal form presents with microcephaly, spasticity, dystonia, marked developmental delay and regression; later-onset variants with milder phenotype	Extensive calcification, cerebral hypoplasia, white matter signal abnormalities	<i>TREX1</i> and <i>RNASEH2A-C</i> gene mutations	Dysfunctional DNA repair?

AR indicates autosomal recessive; AD, autosomal dominant; AMN, adrenomyeloneuropathy; ABCD1, ATP-binding cassette, subfamily D, member 1; eIF, eukaryotic translation initiation factor; GFAP, Glial fibrillary acidic protein; NAA, N-acetylaspartic acid; MRS, magnetic resonance spectroscopy; MS, multiple sclerosis; PMD, Pelizaeus-Merzbacher disease; PLP, protolipid protein; GJA12, gap junction protein; MCL, Megalencephalic leukoencephalopathy with subcortical cysts; DARS2, mitochondrial aspartyl-tRNA synthetase; TREX-3-prime[repair exonuclease 1; RNASEH2A-C—aspartyl-tRNA synthetase.

Table 2. Typical clinical, imaging, and pathophysiological features of the most commonly recognized leukodystrophies (Castello et al., 2009).

Alexander disease

Alexander disease (AxD) is a rare and usually fatal leukodystrophy due to mutations in glial fibrillary acidic protein (GFAP), the main intermediate filament protein of astrocyte. The hallmark of the disease is the abundant presence of Rosenthal's fibers: protein aggregates within astrocytes containing GFAP, $\alpha\beta$ -crystallin, and heat shock protein 27.

Frequently AxD affects young children before 2 years of age with motor and mental retardation, bulbar dysfunction, seizure and megalencephaly, leading to death by 10 years of age. The neuropathology of the infantile form is characterized by the absence of myelin in the frontal lobes.

In the juvenile form the onset is between 2 and 12 years of age. Patients have difficulties with coordination, speech, swallowing, but both myelin and mental ability can be relatively intact. This form has a slow progression and patients can reach the age of 40.

The adult form, with onset from teens to middle age, can be similar to the juvenile form or may mimic multiple sclerosis or a brain tumor. A typical sign is palatal myoclonus. Both juvenile and adult forms, unlike the infantile form, primarily involve the brainstem and cerebellum.

All AxD forms are associated with heterozygous mutations in *GFAP*, acting in an autosomal dominant fashion; often mutations arise *de novo*, explaining the lack of familiarity. Most mutations are missense, but recently insertions or deletions at the C-terminus of GFAP have been described.

MITOCHONDRIAL DISEASES

Mitochondria, from the Greek *mitos* (thread-like) and *khondros* (grain or granule), are bacterium-sized organelles found in all nucleated cells. In addition to their central role in ATP synthesis through the OXPHOS system, mitochondria host central metabolic pathways, like the Krebs cycle and the β -oxidation of fatty acids, but are also crucial for other cellular processes like programmed cell death (apoptosis) and signaling.

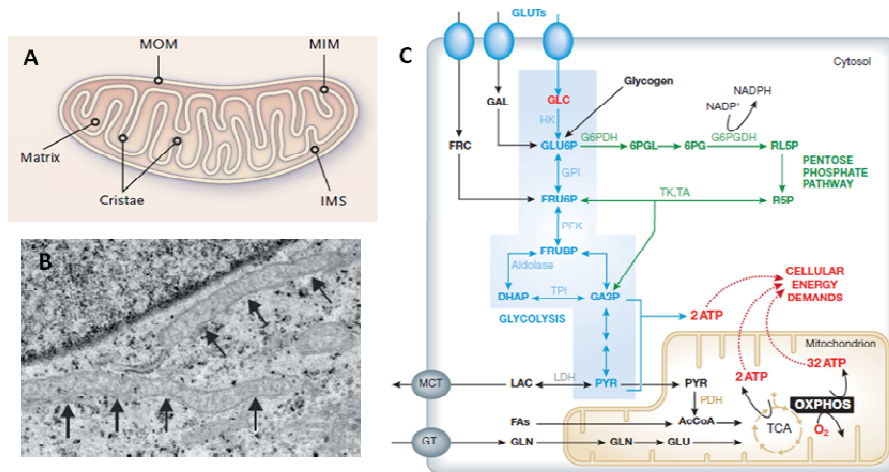


Figure 2. (A – B) Mitochondrial structure (Werner JH et al., 2012). (C) Energy metabolism in a typical mammalian cell (Werner JH Koopman et al., 2013).

Mitochondrial diseases are a group of disorders caused by dysfunctional mitochondria, in particular affecting the mitochondrial respiratory chain and Oxidative Phosphorylation (OXPHOS).

The prevalence of mitochondrial diseases is approximately 1 in 5,000 live births and their clinical manifestations are extremely heterogeneous. They may occur in infancy or adulthood, and can be either multisystemic or highly tissue-specific. However, patients with

a mitochondrial disease display a number of canonical biochemical and morphological features. Firstly, often they have defects in one or more complexes of the respiratory chain, usually detected by enzymatic assays on muscle biopsies or cultured cells (fibroblasts or myoblasts). Frequently there is an increase of resting lactic acid levels in blood and/or cerebrospinal fluid (DiMauro, S. & Schon, E. A., 2003), reflecting a block in the import of pyruvate inside impaired mitochondria with its consequent transformation in lactate. A common morphological feature of OXPHOS diseases is the presence of ragged red fibers (RRF) in muscle, due to a compensatory massive proliferation of OXPHOS-defective mitochondria (Mita, S. et al., 1989). Moreover, clinical signature trait can include skeletal myopathy, deafness, blindness, intestinal dysmotility, subacute neurodegeneration and peripheral neuropathy; the use of radiologic (RMN, PET) and electrophysiologic (EMG) tests help in the correct definition of the disease.

Patients with late-onset usually show signs of myopathy associated with variable involvement of the central nervous system (CNS), although some of them complain only of muscle weakness or wasting with exercise intolerance.

In early childhood the most common clinical and neuropathological presentation is the Leigh syndrome (LS). LS can be caused by defects in structural subunits (either mtDNA or nDNA encoded) or assembly factors of mitochondrial OXPHOS complexes, but also, for example, by disturbances in CoQ₁₀ metabolism or dysregulation in RNA/DNA maintenance. Other frequent early-onset presentations include

different encephalopathies with variable involvement of brain structures (leukodystrophies, cerebral or cerebellar atrophy, thin corpus callosum, brainstem alterations), but also cardiomyopathies and hepatopathies, although often with CNS involvement.

Genetics of mitochondrial diseases

Mitochondria contain their own DNA (mtDNA), which is maternally inherited. Every eukaryotic cell contains thousands of mitochondria, each containing 2 to 10 mtDNA molecules. The number of mitochondria depends on the specific energy demand of each cell type. For example, tissues with high capacity to perform aerobic metabolic functions, like kidney, liver, heart and skeletal muscle, have a large number of mitochondria.

Mitochondrial diseases can occur from mutations in mtDNA, but also in nuclear DNA. In fact, nDNA encode for ~ 1,500 proteins that are targeted to mitochondria and are fundamental for their proper function, including complex subunits, assembly factors and proteins involved in mitochondrial replication and transcription.

mtDNA mutations

Human mtDNA is a 16,569 base pair double stranded circular molecule constituted by two strands, the light strand (L-strand) and the heavy strand (H-strand). mtDNA contains only 37 genes, 13 of which encode for OXHOPS subunits. In particular these genes encode for seven subunits (ND1,2,3,4,4L,5,6) of complex I; cytochrome *b*

(*cytb*), that is the only mitochondrially encoded subunit of complex III; three subunits (COXI, COXII, COXIII) of complex IV and two subunits (ATP6, ATP8) of complex V. Besides OXPHOS subunits, mtDNA encodes a large and a small ribosomal RNA (12S rRNA and 16S rRNA) and 22 transfer RNAs (tRNAs). It is interesting to note that mtDNA doesn't own introns, so all the coding sequences are contiguous to each other (Anderson et al. 1981; Montoya et al. 1981).

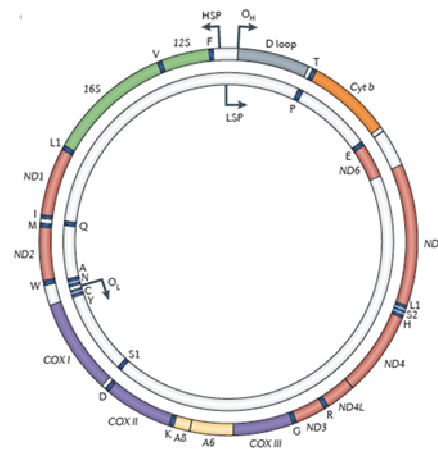


Figure 3. Human mitochondrial genome. (Schon EA et al., 2012)

The mitochondrial genotype of a normal individual consists of a single mtDNA species, a condition known as *homoplasmy*. On the contrary, most patients with mtDNA mutations are *heteroplasmic*, which means that their mitochondrial genotype is constituted by the coexistence of wildtype and mutated mtDNA species. The majority of heteroplasmic mutations don't cause clinical phenotypes. In fact, it is necessary to reach a threshold level, which has been shown to vary for different types of mutation, from 50–60% for deleted mtDNA molecules (Mita S et al., 1990; Moraes CT et al., 1992) to >90% for some tRNA point

mutations (Boulet L et al., 1992; Chomyn A et al., 1992), in order to produce a cell damage and a phenotypic manifestation.

The understanding of mitochondrial diseases is complicated by the fact that mtDNA is highly polymorphic, with several differences in sequence between individuals from the same ethnic group and more between those in different groups. mtDNA haplotypes are based upon specific patterns of polymorphisms that allow the classification of each mtDNA sequence into main haplogroups. mtDNA haplogroups seem to influence ageing, susceptibility to some diseases, and phenotypic expression/penetrance of some mtDNA mutations (Torrioni A et al., 1997; Wallace DC et al., 1999).

Mutations of mtDNA are divided in large-scale rearrangements and inherited point mutations.

Large-scale rearrangements of mtDNA

Single, large-rearrangements of mtDNA can be single partial deletions, or partial duplications. mtDNA deletions were the first mutations to be described and associated with human disease. (Holt IJ et al., 1988). Most mtDNA deletions are sporadic; they are located almost everywhere in the genome and their size can be variable. Despite that, all mtDNA deletions cause one of the following three pathological disorders:

Kearns-Sayre syndrome (KSS), characterized by an onset in the second decade of life with ophthalmoplegia, ptosis, pigmentary retinopathy and at least one of the following: cerebellar ataxia, complete block heart, or elevated cerebrospinal fluid protein.

Progressive external ophthalmoplegia (PEO), characterized by a late-onset progressive external ophthalmoplegia, ptosis, myopathy and exercise intolerance.

Pearson's syndrome, a rare disorder of early infancy characterized by marrow and pancreas abnormalities with sideroblastic anemia.

Point mutations of mtDNA

Since 1988, when the first disease-causing mtDNA mutations were reported, more than 270 point mutations have been described. mtDNA point mutations are maternally inherited and can affect either one of 13 complex subunits genes, leading to an isolate biochemical defect, or genes involved in mitochondrial protein synthesis (tRNAs, rRNAs), which may cause a general impairment of respiratory chain. Notably, more than half of these mutations are located in tRNA genes, although tRNAs represent only 10% of the whole genome. On the contrary, the polypeptide-coding genes constitute almost 70% of the genome, but they account for only about 40% of the mutations. Finally, only about 2% of the mtDNA mutations affect the two rRNA genes which constitute 15% of coding capacity.

The majority of the mtDNA point mutations are associated to few, highly defined, syndromes.

Mitochondrial encephalopathy with lactic acidosis and stroke-like episodes (MELAS) is a multisystem disorder in which the brain, muscle and endocrine system are predominantly involved, often with a fatal outcome in childhood or in young adulthood (Kaufmann P et al., 2011). This disorder is defined by the presence of stroke-like episodes

due to infarcts in the temporal and occipital lobes, angiopathy, lactic acidosis and/or RRFs. Biochemically, complex I is frequently affected, while complex IV is often normal.

The most common causal mutation is m.3243A→G in tRNA^{leu(UUR)}, but many other point mutations have been identified.

Myoclonic epilepsy with ragged red fibres (MEERF) is a maternally inherited neuromuscular disorder characterized by myoclonus, epilepsy, muscle weakness and wasting with RRFs, cerebellar ataxia, deafness, dementia and cervical lipomas. The most common mutation is m.8344A→G in the tRNA^{lys} gene (Wallace DC et al., 1988a). The main biochemical sign is CIV deficiency, although complex I can be affected too, and COX-depleted RRFs are invariably detected in the muscle biopsy.

Neurogenic weakness, ataxia and retinitis pigmentosa (NARP) is maternally inherited and characterized by ataxia, pigmentary retinopathy and peripheral neuropathy (Holt IJ et al., 1990). RRFs are consistently absent in the muscle biopsy. This disorder is associated with the heteroplasmic mutation m.8993T→G or less frequently with m.8993T→C in the ATP synthase 6 (*ATP6*) gene. Patients with NARP harbor ~ 70% mutant mtDNA.

Leigh syndrome (LS) is maternally inherited condition, characterized by a severe development delay, pyramidal signs, retinitis pigmentosa, ataxia, cerebellar and brainstem atrophy. It is caused by the same mutation m.8993T→G responsible for NARP, but in this case the mutation loads is over 90%.

Leber's hereditary optic neuropathy (LHON) is the most common mitochondrial disorder, causing subacute loss of central vision in young adults, predominantly men. The retinal ganglion cells are affected selectively. This disease is usually due to homoplasmic mutations in one of three genes encoding complex I subunits: m.11778G→A in *ND4*, m.3460G→A in *ND1* and m.14484T→C in *ND6* (Wallace DC et al., 1988b; Howell et al., 1991; Chinnery et al., 2001).

nDNA mutations

Human nDNA-encoded mutations are generally inherited in an autosomal recessive manner (Smeitink et al., 2001) and the clinical manifestation is very heterogeneous.

They can affect: structural OXPHOS subunits; OXPHOS assembly factors; Fe-S biogenesis enzymes; enzymes involved in the synthesis of CoQ₁₀ and Cyt-c; mtDNA repair enzymes; mtDNA replication, transcription and translation factors; enzymes involved in the maintenance of the mitochondrial dNTP pool; mitochondrial ribosomal proteins; mt-tRNA synthetases; nucleoid-associated proteins.

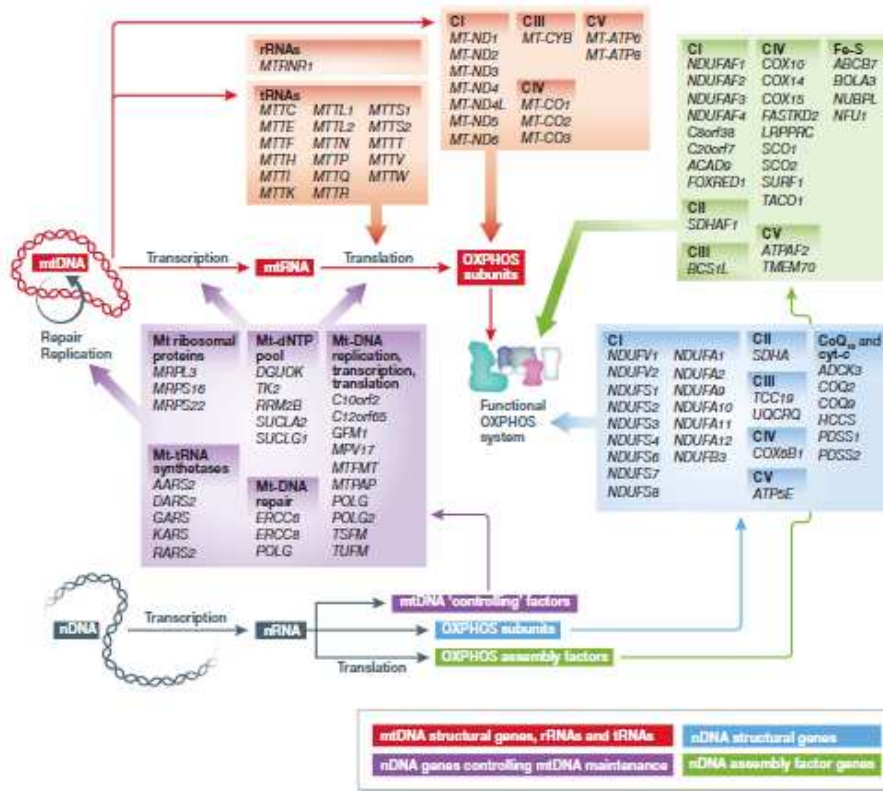


Figure 4. Biogenesis and neurodegeneration-associated mutations of the OXPHOS system. (Koopman JH et al., 2013)

Disorders due to defects in nuclear gene encoding both structural or assembly factors of OXPHOS subunits

Only 13 subunits of mitochondrial complexes are encoded by mtDNA, other 72 are encoded by nDNA, translated on cytoribosomes and transported to the mitochondrion.

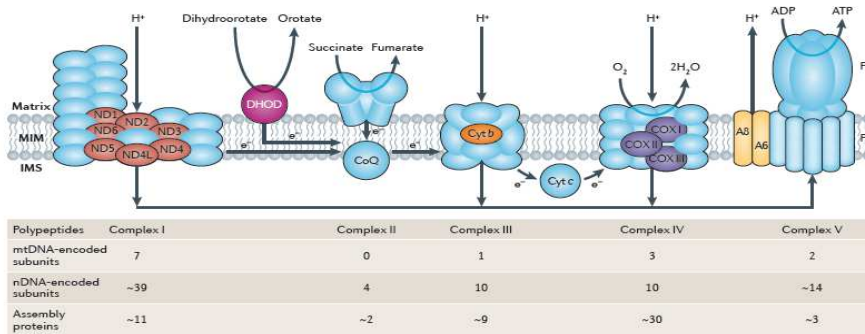


Figure 5. Oxidative phosphorylation complexes (Schon EA et al, 2012).

The respiratory chain is composed of five enzymatic multi-heteromeric complexes (I, II, III, IV, V) embedded in the inner membrane of mitochondria. **Complex I** oxidizes nicotinamide adenine dinucleotide (NADH), derived by the oxidation of fatty acid, pyruvate and aminoacids, to NAD^+ and transfers the electrons extracted from NADH to CoQ_{10} . **Complex II** oxidizes flavin adenine dinucleotide (FADH₂), derived from fatty acid and the Krebs' cycle, to FAD and also transfers the released electrons to CoQ_{10} . **Complex III** transfers electrons from reduced CoQ_{10} to cytochrome *c*. **Complex IV** catalyses the last step of electron transfer: the reduction of oxygen to water. Complexes I-IV pump NADH - and FADH_2 -derived protons from the mitochondria matrix to the mitochondrial intermembrane space (IMS), generate an electrochemical gradient (Δp_m) used by **complex V** to convert ADP and phosphate to ATP.

nDNA mutations in structural genes have been described for each of the five complexes, but remarkably they account for only a minority of the OXPHOS complex deficiency cases. This observation can be explained by their incompatibility with life.

Biochemical OXPHOS abnormalities due to mutations in assembly factors are more common. Defects of CIV activity are the most frequent; in particular mutations associated with autosomal recessive COX deficiency have been reported for the following assembly factors: SURF1, SCO1, SCO2, COX10, COX15. Patients with these mutations have usually an early onset with LS, myopathy, encephalopathy, lactic acidosis, and a rapidly progressive course with early death.

Mutations have been found also in assembly factors of the other complexes: NDUFAF2, NDUFAF3, NDUFAF4, C20ORF7, C8ORF38, NUBPL, FOXRED1, ACAD9 for CI; SDHAF1 and SDHAF2 for CII; BCS1L, TTC19 and LYRM7 for CIII; TMEM70 and ATPAF2 for CV.

Disorders due to gene defects altering the stability of mtDNA

mtDNA replication occurs in the mitochondrial matrix and it is independent from cell cycle and nuclear DNA replication, (Bogenhagen & Clayton, 1977). mtDNA replication requires a specific mitochondrial DNA polymerase, the DNA pol γ , and many other factors: the mtDNA helicase TWINKLE, the mtDNA topoisomerase I (TOPImt), a single-strand binding protein (mtSSB), the mtDNA ligase III, mitochondrial transcription factors (i.e. mtTFA) and enzymes important for the supply of deoxynucleotides, such as thymidine kinase 2 (TK2) and deoxy-guanosine kinase (dGUOK).

Typically, defects of the DNA-processive enzymes are responsible for qualitative alterations of mtDNA, such as multiple mtDNA deletions. On the contrary, mutations in genes assigned to maintenance of dNTP pools cause quantitative alterations of mtDNA, the so-called mtDNA depletion syndrome (MDS), where there is a reduction of mtDNA copy numbers.

Qualitative alterations of mtDNA are usually associated with autosomal dominant or recessive forms of progressive external

ophthalmoparesis (PEO) and autosomal recessive myoneurogastrointestinal encephalomyopathy (MNGIE).

Typical signs of PEO are progressive muscle weakness, that most severely affected the external eye muscle, RRFs and a mild reduction in the activities of respiratory chain enzymes. Additional features, present in some families, are ataxia, depression, hypogonadism, hearing loss, peripheral neuropathy and cataract (Servidei S et al., 1991). Mutations associated with autosomal dominant or recessive forms of PEO, have been found in five genes: *ANT1* (adenine nucleotide translocator), *Twinkle*, *POLG1* and *POLG2*, and *OPA1* (optic atrophy protein 1).

MNGIE is a devastating disorder with juvenile onset, characterized by ophthalmoparesis, peripheral neuropathy, leucoencephalopathy, gastrointestinal symptoms with intestinal dysmotility, and histologically abnormal mitochondria in muscle (Hirano et al., 1994).

This disorder is associated with mutations in the gene encoding thymidine phosphorylase (TP). TP is involved in the catabolism of the pyrimidine nucleoside and alterations of its function lead to imbalance of the dNTPs pool.

mtDNA depletion syndromes are a heterogeneous group of disorders and can clinically be divided in three classes: fatal infantile congenital myopathy with or without DeToni-Fanconi renal syndrome; fatal infantile hepatopathy leading to rapidly progressive liver failure; late infantile or childhood encephalomyopathy.

These diseases are mainly due to alterations in genes coding proteins involved in the maintenance of dNTP pools: thymidine kinase 2 (TK2) a deoxyribonucleoside kinase that phosphorylates thymidine, deoxycytidine and deoxyuridine; p53 controlled RR (p53R2), the major ribonucleotide reductase regulator of de novo synthesis of dNTPs; deoxyguanosine kinase (dGUOK) that carries out the phosphorylation of purine deoxyribonucleosides in mitochondria; the a (SUCLA2) and b (SUCLG1) subunits of the succinyl-CoA ligase, a Krebs cycle enzyme with a yet unexplained role in mtDNA metabolism.

Disorders due to gene defects altering mitochondrial protein synthesis

The mitochondrial transcription machinery requires a specific RNA polymerase (Tiranti *et al.* 1997) and at least three transcription factors (TFAM, TFB1M, TFB2M; Fisher & Clayton, 1985, 1988), responsible for initiation and termination of transcription. The absence of introns in mtDNA originates polycistronic primary transcripts, eventually cut by specific endonucleases to generate mature rRNAs, mRNAs and tRNAs. tRNA genes, distributed among the other genes, function as a signal driving endonucleolytic cleavage (Ojala *et al.* 1981; Montoya *et al.* 1983). Then other enzymes are in charge of polyadenylation for rRNAs and mRNAs, the addition of the CCA to the tRNA 3' end, or other processes that stabilize the corresponding RNA species.

Protein synthesis deficiency can be caused by mutations in any components of translation machinery that, except for the 22 tRNAs and 12S rRNA and 16S rRNA, are all encoded by nDNA. Usually, these mutations have maternal (for tRNAs and rRNAs) or autosomal recessive (for nDNA genes) transmission and can theoretically affect all complexes containing mitochondrial encoded subunits sparing CII.

Abnormal tRNA modification

Maturation of tRNAs is a central event of mammalian mitochondria gene expression. It involves several modifications necessary for their proper functioning, including structure stabilization, amino-acylation and codon recognition.

Mitochondrial tRNAs are processed and matured by RnaseP and RnaseZ, respectively involved in the processing of 5' and 3' end (Vilardo E et al., 2012), as well as editing enzymes, such as MTO1, PUS1, TRMU and MTFMT.

MTFMT is a methionyl-tRNA formyltransferase, which is required for the initiation of translation in mitochondria. *MTFMT* mutations have been associated with LS and combined OXPHOS deficiency (Tucker et al., 2011). Few mutations have been found in *PUS1*, coding a pseudouridine synthase that converts uridine into pseudouridine after the nucleotide has been incorporated into tRNA. *PUS1* patients show myopathy, lactic acidosis and sideroblastic anemia (MLASA; Bykhovskaya et al., 2004). TRMU is responsible for the 2-thiolation of the wobble U in tRNA^{Lys}, tRNA^{Glu}, tRNA^{Gln}, TRMU mutations

have been found in patients with acute infantile liver failure (Zeharia A et al., 2009)

Recently, mutations have been found in *MTO1*, coding the enzyme that catalyzes the 5-carboxymethylation ($\text{mnm}^{\text{S}2}\text{U34}$) of the wobble uridine base in $\text{mt-tRNA}^{\text{Gln}}$, $\text{mt-tRNA}^{\text{Glu}}$ and $\text{mt-tRNA}^{\text{Lys}}$. *MTO1* patients show variability in reduction of respiratory chain activities and hypertrophic cardiomyopathy with lactic acidosis (Ghezzi D et al., 2012; see chapter 3).

Abnormal aminoacyl-tRNA synthetases

Aminoacyl-tRNA synthetases (AARSs) catalyze the ligation of specific amino acids to their cognate tRNAs. AARSs are all encoded by nDNA and then imported into the mitochondria. Mitochondria use 20 different AARSs, three of them also acting in the cytosol (GARS, KARS, QARS). Typically, mutations in mitochondrial AARSs are associated with infantile autosomal recessive diseases. These disorders are widely heterogeneous. For example, mutations in *YARS2* present as myopathy and sideroblastic anaemia, *EARS2* mutations as leukoencephalopathy and high cerebrospinal fluid, *AARS2* mutations as hypertrophic cardiomyopathy, *SARS2* mutations as pulmonary hypertension and renal failure.

Abnormal ribosomal proteins and translation factors

The 55S mitochondrial ribosome is constituted by the small subunit (28S), containing the 12S rRNA and 30 proteins, and the large subunit (39S), containing the 16S rRNA and 48 proteins.

Mutations have been found in the following ribosomal proteins: MRPS16, associated with agenesis of the corpus callosum, muscle hypotonia and hyperlactatemia (Miller C et al., 2004); MRPS22, associated with hypotonia, cardiomyopathy and tubulopathy (Smits P et al. 2007); MRPL3, associated to hypertrophic cardiomyopathy and psychomotor retardation (Galmiche L et al., 2011) and MRPL44, associated to cardiomyopathy (Carroll CJ et al., 2013).

Mitochondrial translation is a four-step process involving nuclear encoded translation initiation (IF2, IF3), elongation (EF-Tu, EF-Ts, EF-G1 and EF-G2), termination (RF1) and ribosome recycling factors. In particular, elongation consists of the sequential addition of amino acids to the growing polypeptide chain directed by mRNA codons.

Mutations have been described in the elongation factors: EFG1; EF-Ts; EF-Tu.

Defects of mitochondrial protein import

Proteomic analysis indicates that mitochondria contain about 1500 proteins, but only 1% are encoded by mtDNA and synthesized in the matrix. The other proteins are encoded by nDNA and synthesized in the cytosol as precursors or preproteins, then are imported into mitochondria by a specific protein import machinery.

Two diseases have been associated with mutations in nuclear genes encoding for proteins involved in mitochondrial import. The first is the deafness-dystonia syndrome (Mohr-Tranebjaerg syndrome) a X-linked neurodegenerative disorder caused by mutations of the *DDP* gene, which encodes TIMM8A. This protein mediates the import and

insertion of hydrophobic membrane proteins into the MIM. The second is an autosomal recessive disorder characterized by dilated cardiomyopathy with ataxia. It is due to mutations in *DNAJC19* gene, encoding a putative mitochondrial import protein similar to yeast TIM14 (Davey et al., 2006).

Fe–S protein defects

Assembly factors, chaperones, and enzyme involved in the biosynthesis and incorporation of prosthetic groups are necessary for the correct assembly and function of mitochondrial complexes. Fe-S-clusters are important for their electron transfer activity.

Abnormalities in Fe–S cluster biosynthesis have been rarely associated with clinical conditions. This suggests the extreme importance of this prosthetic group and its incompatibility with embryonic development and extrauterine life.

Mutations in ATP-binding cassette member 7 (ABCB7), involved in the maturation of cytosolic Fe–S cluster-containing proteins, have been found in families with X-linked sideroblastic anemia with ataxia syndrome (Zeviani, 2001).

Friedreich ataxia (FRDA) is an inherited recessive disorder characterized by progressive neurological disability and heart abnormalities that may be fatal. This disorder is due to mutations in *FRDA* gene, encoding frataxin, an iron chaperon involved in the biosynthesis of Fe–S cluster and heme moieties

CoQ₁₀ deficiency

CoQ₁₀ is a lipophilic component of the electron transport chain involved in the transfer of electrons derived from CI and CII to CIII.

Disorders associated with CoQ₁₀ deficiency in muscle are characterized by recurrent myoglobinuria, brain involvement (seizures, ataxia and mental retardation) and ragged-red fibers/lipid storage in muscle. In addition, several patients with unexplained cerebellar ataxia, pyramidal signs and seizures, but with only unspecific myopathic change and no myoglobinuria, have been found to have very low levels of CoQ₁₀ in muscle (26–35% of normal). Interestingly, all patients responded to CoQ₁₀ supplementation (Musumeci et al., 2001).

Treatment of mitochondrial diseases

Therapies for mitochondrial diseases remain unsatisfactory and usually the treatment is only focused on maintaining optimal health and on mitigating symptoms. However, new treatment strategies based on genetic or metabolic/cell biological interventions are in the early stages of development. They are focused on: preventing transmission of mtDNA and nDNA gene defects; altering the balance between wild-type and mutated mtDNA; replacing mutant species (gene therapy); controlled regulation of specific transcriptional regulators; metabolic manipulation.

Among these, metabolic therapy is the most used in the treatment of mitochondrial diseases. This approach is based on the use of compounds, such as vitamins or cofactors, to promote critical enzymatic reactions, increase ATP production, reduce oxidative stress. Examples of currently used compounds are: Coenzyme Q₁₀, an electron carrier and antioxidant that has been approved for the treatment of Friedreich's ataxia (Bénil P et al., 2010); Creatine, the substrate for the synthesis of phosphocreatine, the most abundant energy storage compound in muscle, heart and brain; Dichloroacetate (DCA), a potent lactate-lowering drug.

Recently, several clinical trials, using dichloroacetate, vitamins, and a cocktail of specific food components, have been studied (Stacpoole PW et al., 2011). In spite of positive effects of some trials, none led to the filing of a New Drug Application by the Food and Drug Administration.

NEXT-GENERATION SEQUENCING IN INHERITED DISORDERS

The number of monogenic diseases is estimated >5000 and for half of them the underlying gene is unknown (McKusick VA, 2011). The identification of the gene responsible for an inherited disease represents the first step towards the understanding of pathological mechanisms, which in turn may be useful to develop therapeutic interventions.

Until a few years ago the identification of Mendelian disease genes was carried out by Sanger sequencing of candidate genes. Candidate gene association studies require an *a priori* hypothesis for the selection of the gene to be studied. However, this approach is critically dependent on previous knowledge and only a few disease genes have been identified with this approach.

Another traditional approach that has been used for years with several positive results is linkage analysis. However it can be applied only when large families with multiple affected individuals (and unaffected individuals) are available. The aim of this approach is the identification of genetic markers, such as panels of genetically variable DNA sequences (microsatellites or SNPs) with known chromosomal locations, that could be used to determine which alleles are present only in the affected individuals. Once this analysis leads to the identification of a specific genomic region, genes located inside this region are analyzed by Sanger sequencing to pinpoint the actual mutation.

The main limitation of linkage analysis is the need to have large, multi-generational pedigrees (possibly with both affected and unaffected individuals to increase the power and resolution of this analysis), besides the fact that this approach yields only regions of linkage and not the causative gene.

Homozygous mapping is another good strategy for autosomal recessive diseases in case of suspected consanguinity. In fact, assuming that the disease is caused by a homozygous variant inherited from both parents, this method can allow the identification of the genomic regions that are homozygous only in affected individuals. Nonetheless this strategy is not applicable to identify causative genes in autosomal dominant diseases or for recessive diseases caused by compound heterozygous mutations.

In the last years, next generation sequencing (NGS) technologies (figure 6) have changed the research for disease gene: whole-exome sequencing (WES) and whole-genome sequencing (WGS), by interrogating the entire exome or genome, move from hypothesis-based approaches to studies that are largely hypothesis free. Conversely, targeted NGS, i.e. the parallel sequencing of hundreds of genes related to a peculiar disease, dramatically fastened the mutational screening of candidate genes. Finally, NGS does not require large pedigrees and can also be applied to singleton patients.

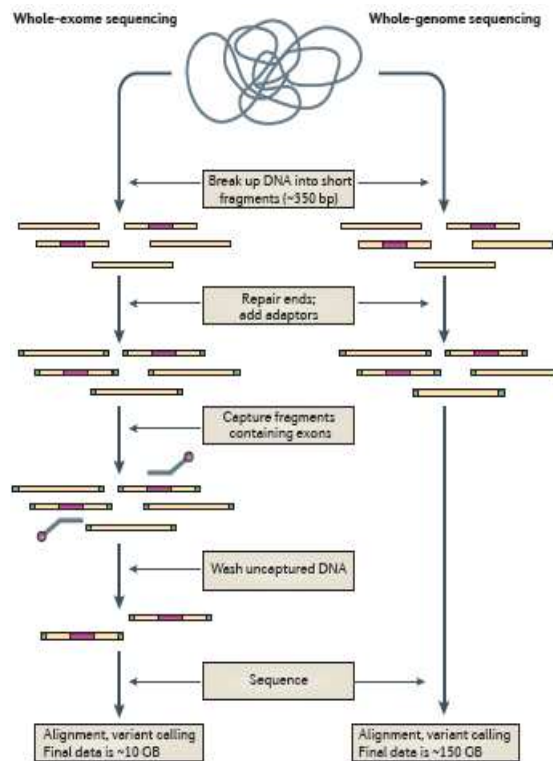


Figure 6. Simplified workflows for whole-exome and whole-genome sequencing. The initial sample preparation is identical for both whole-exome and whole-genome sequencing. Genomic DNA is broken up into small fragments and sequence adaptors, which allow each fragment to be hybridized to the flowcell where the sequencing occurs, are added. Whole-exome sequencing protocols proceed with the hybridization of the fragments to probes that are complimentary to all the known exons in the genome, which are then captured while the remaining DNA is washed away, leaving a pool of fragments containing exons. Whole-genome sequencing requires no extra steps following the addition of adaptors and the library is ready to be sequenced at that point (Bras J et al., 2012).

In NGS studies, after DNA sequencing, in-depth bioinformatics analysis is required, usually based on three general steps: (1) alignment of the short reads to the right position on a reference genome sequence; (2) variant calling, which compares aligned with known sequences to determine which positions deviate from the reference position; (3) filtering, which permits to reduce thousands of

variants to a smaller set of probably relevant nucleotide changes, and annotation, with search of known information about each variant that is detected.

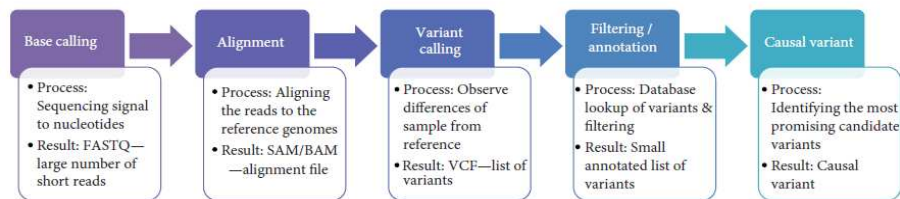


Figure 7. Next-generation sequencing bioinformatics workflow (Dolled-Filhart MP et al., 2012)

Nonetheless, NGS is not free of limitations and problems: for instance coverage of regions of interest is not complete; copy number variations are difficult to detect; GC-rich regions cause difficulties during sample preparation due to polymerase chain reaction PCR artifacts. But the real challenge of NGS is the interpretation step, because of the huge amount of variants present in each individual, almost all without any clinical relevance.

Whole-exome sequencing (WES) allows sequencing all of the known coding portions of the genome. The exome constitutes less than 1% of the whole genome, but it is estimated to contain about 85% of the disease-causing mutations of monogenic disorders; hence WES is at the moment the preferred option amongst NGS analyses because with a relatively small amount of sequenced regions it allows the

identification of most of the mutations responsible for genetic diseases.

A typical WES experiment identify between 20,000 and 50,000 variants per sequenced exome, but only one (or few) explains the Mendelian disease. In order to identify the disease gene, prioritization of variants is crucial.

Primarily, variants outside the coding regions and synonymous variants (assuming they have a minimal effect on protein) can be filtered out. This reduces the number of variants to ~ 5,000. A further reduction takes place excluding known variants (from dbSNP or other public databases, such as Exome Variant Server, or from published studies; Durbin RM et al., 2010) with a frequency in control population >1% or even lower for extremely rare diseases. With this passage 90-95% variants are removed and the remaining ~150-500 non-synonymous or splice-site variants are further filtered to select possible pathogenic variants (Ng SB et al., 2010). The hypothesized mode of inheritance of the disease has clearly a role in the selection of candidate gene: for recessive traits, only genes with homozygous or compound heterozygous variants are taken into account for further validation. Additional strategies include removal of variants not segregating with disease within the family (when additional family members are available), and prioritization of variants according to their computationally predicted consequences in terms of protein structure. However, it is important to underline that a too rigorous prioritization may discard the pathogenic variant.

Moreover, a functional validation is necessary to confirm the bioinformatic prediction. Complementation in patients' fibroblasts, in order to evaluate phenotype rescue, or creation/investigation of other models (knock-down cell lines, yeast...) is fundamental steps for the identification of the true genetic defect.

The identification of additional unrelated patients with different mutations in the same gene will further indicate the causative role of a given candidate gene and provide preliminary information on both disease frequency and genotype-phenotype correlations.

SCOPE OF THE THESIS

The scope of my thesis was the identification of genes responsible for:

- 1) an adult-onset neurological syndrome, with leukodystrophy and motor-neuron disease, in two half-siblings;
- 2) an infantile hypertrophic cardiomyopathy with lactic acidosis and mitochondrial respiratory chain defects.

Since all genetic screenings performed on the basis of clinical manifestations did not provide a diagnosis for these patients, we carried out whole exome sequencing.

My work contributed to the publications of three papers.

In the second chapter of this thesis, there is the article concerning the identification and characterization of the first *GFAP-ε* mutation, causing an adult form of Alexander disease in two affected siblings. The male presented a severe motor-neuron disease whereas his sister showed a mild movement disorder with cognitive impairment. In addition to the *GFAP-ε* mutation, we found a variant in *HDAC6* on chromosome X, present only in the male patient; *HDAC6* is a candidate MND susceptibility gene and the identified missense variant is probably responsible for his different phenotype. Cellular models were used to experimentally prove the altered functionality of mutant *GFAP-ε* and *HDAC6*.

The third chapter contains the paper reporting the first mutations in *MTO1*, responsible for a mitochondrial disorder associated with hypertrophic cardiomyopathy, lactic acidosis and mitochondrial respiratory chain defects. Then chapter four consists of the article where we described and characterized new *MTO1* mutations found in other patients. In both articles characterization of the identified mutations and validation of their deleterious effects were assessed in patients' specimens (fibroblasts) and in yeast *Saccharomyces cerevisiae*.

REFERENCES

Amor S, Puentes F, Baker D, van der Valk P. Inflammation in neurodegenerative diseases. *Immunology* (2010) Feb;129(2):154-69.

Angerer H, Zwicker K, Wumaier Z, Sokolova L, Heide H, Steger M, Kaiser S, Nübel E, Brutschy B, Radermacher M, Brandt U, Zickermann V. A scaffold of accessory subunits links the peripheral arm and the distal proton-pumping module of mitochondrial complex I. *Biochem J* (2011); 437: 279–288.

Arundine M, Tymianski M. Molecular mechanisms of calcium dependent neurodegeneration in excitotoxicity. *Cell Calcium* (2003) 34, 325–337.

Beal MF. Aging, energy, and oxidative stress in neurodegenerative diseases. *Ann Neurol.* (1995) Sep;38(3):357-66.

Bence NF, Sampat RM, Kopito RR. Impairment of the ubiquitin-proteasome system by protein aggregation. *Science*(2001); 292: 1552-1555.

Bénit P, El-Khoury R, Schiff M, Sainsard- Chanet A, Rustin P. Genetic background influences mitochondrial function: modeling mitochondrial disease for therapeutic development. *Trends Mol Med* (2010);16:210-7.

Berridge MJ, Bootman MD, Roderick HL: Calcium signalling: dynamics, homeostasis and remodelling. *Nat Rev Mol Cell Biol* (2003); 4:517-529.

Bogenhagen D, Clayton DA. Mouse L cell mitochondrial DNA molecules are selected randomly for replication throughout the cell cycle. *Cell* (1977) Aug;11(4):719-27.

Boulet L, Karpati G, Shoubridge EA. Distribution and threshold expression of the tRNA(Lys) mutation in skeletal muscle of patients with myoclonic epilepsy and ragged-red fibers (MERRF). *Am J Hum Genet* (1992); 51: 1187–1200.

Bras J, Guerreiro R, Hardy J. Use of next-generation sequencing and other whole-genome strategies to dissect neurological disease. *Nat Rev Neurosci* (2012) Jun 20;13(7):453-64.

Brière JJ, Favier J, El Ghouzzi V, Djouadi F, Bénit P, Gimenez AP, Rustin P. Succinate dehydrogenase deficiency in human *Cell Mol Life Sci* (2005); 62: 2317–2324.

Bykhovskaya Y, Casas K, Mengesha E, Inbal A, Fischel-Ghodsian N. Missense mutation in pseudouridine synthase 1 (PUS1) causes mitochondrial myopathy and sideroblastic anemia (MLASA). *Am J Hum Genet* (2004) Jun;74(6):1303-8

Carroll CJ, Isohanni P, Pöyhönen R, Euro L, Richter U, Brillhante V, Götz A, Lahtinen T, Paetau A, Pihko H, Battersby BJ, Tyynismaa H, Suomalainen A. Whole-exome sequencing identifies a mutation in the mitochondrial ribosome protein MRPL44 to underlie mitochondrial infantile cardiomyopathy. *J Med Genet*. 2013 Mar;50(3):151-9.

Chen B, Retzlaff M, Roos T, Frydman J. Cellular strategies of protein quality control. *Cold Spring Harb Perspect Biol* (2011); 3: a004374.

Chinnery PF, Brown DT, Andrews RM, Singh-Kler R, Riordan-Eva P, Lindley J, et al. The mitochondrial ND6 gene is a hot spot for mutations that cause Leber's hereditary optic neuropathy. *Brain* (2001); 124: 209–18.

Chomyn A, Martinuzzi A, Yoneda M, et al. MELAS mutation in mtDNA binding site for transcription termination factor causes defects in protein synthesis and in respiration but no change in levels of upstream and downstream mature transcripts. *Proc Natl Acad Sci USA* (1992); 89: 4221–4225.

Clason T, Ruiz T, Schägger H, Peng G, Zickermann V, Brandt U, Michel H, Radermacher M. The structure of eukaryotic and prokaryotic complex I. *J Struct Biol* (2010); 169: 81–88.

Cooper JM, Korlipara LV, Hart PE, Bradley JL, Schapira AH. Coenzyme Q10 and vitamin E deficiency in Friedreich's ataxia: predictor of efficacy of vitamin E and coenzyme Q10 therapy. *Eur J Neurol* (2008); 15: 1371–19.

Dalle-Donne I, Scaloni A, Giustarini D, Cavarra E, Tell G, Lungarella G, Colombo R, Rossi R, Milzani A. Proteins as biomarkers of oxidative/nitrosative stress in diseases: the contribution of redox proteomics. *Mass Spectrom. Rev.* (2005); 24, 55–99.

Davey KM, Parboosingh JS, McLeod DR et al. Mutation of DNAJC19, a human homologue of yeast inner mitochondrial membrane co-chaperones, causes DCMA syndrome, a novel autosomal recessive Barth syndrome-like condition. *Journal of Medical Genetics* (2006); 43: 385–393.

DeBoer SR, You Y, Szodorai A, Kaminska A, Pigino G, Nwabuisi E, Wang B, Estrada-Hernandez T, Kins S, Brady ST, Morfini G. Conventional kinesin holoenzymes are composed of heavy and light chain homodimers. *Biochemistry* (2008) ;47:4535– 4543.

Deuschl G, Elble Essential tremor—neurodegenerative or nondegenerative disease towards a working definition of ET. *Mov Disord R* (2009);24: 2033–2041

DiMauro, S. & Schon, E. A. Mitochondrial respiratory-chain diseases. *N. Engl. J. Med.* (2003); 348, 2656–2668.

Dolled-Filhart MP, Lee M Jr, Ou-Yang CW, Haraksingh RR, Lin JC. Computational and bioinformatics frameworks for next-generation whole exome and genome sequencing. *ScientificWorldJournal* (2013);2013:730210.

Duchen MR. Mitochondria and calcium: from cell signalling to cell death. *J. Physiol.* (2000) **529**, 57–68.

Duchen MR. Mitochondria in health and disease: perspectives on a new mitochondrial biology. *Mol Aspects Med.*(2004) Aug;25(4):365-451.

Durbin RM, Abecasis GR, Altshuler DL et al: A map of human genome variation from population-scale sequencing. *Nature* (2010); 467: 1061–1073.

Efremov RG, Sazanov LA. Structure of the membrane domain of respiratory complex I. *Nature* (2011);476: 414–420.

Elluru RG, Bloom GS, Brady ST. Fast axonal transport of kinesin in the rat visual system: functionality of the kinesin heavy chain isoforms. *Mol Biol Cell* (1995); 6:21– 40.

Farrer MJ, Hulihan MM, Kachergus JM, Dächsel JC, Stoessl AJ, Grantier LL, Calne S, Calne DB, Lechevalier B, Chapon F, Tsuboi Y, Yamada T, Gutmann L, Elibol B, Bhatia KP, Wider C, Vilarino-Güell C, Ross OA, Brown LA, Castanedes-Casey M, et al. DCTN1 mutations in Perry syndrome. *Nat Genet* (2009); 41:163–165.

Fisher RP, Clayton DA. A transcription factor required for promoter recognition by human mitochondrial RNA polymerase. Accurate initiation at the heavy- and light-strand promoters dissected and reconstituted in vitro. *J Biol Chem.* (1985) Sep 15;260(20):11330-8.

Fisher RP, Clayton DA. Purification and characterization of human mitochondrial transcription factor 1. *Mol Cell Biol.* (1988) Aug;8(8):3496-509.

Galmiche L, Serre V, Beinat M, Assouline Z, Lebre AS, Chretien D, Nietschke P, Benes V, Boddaert N, Sidi D, Brunelle F, Rio M, Munnich A, Rötig A. Exome sequencing identifies MRPL3 mutation in mitochondrial cardiomyopathy. *Hum Mutat* (2011) Nov;32(11):1225-31.

Ghezzi D, Baruffini E, Haack TB, Invernizzi F, Melchionda L, Dallabona C, Strom TM, Parini R, Burlina AB, Meitinger T, Prokisch H, Ferrero I, Zeviani M. Mutations of the mitochondrial-tRNA modifier MTO1 cause hypertrophic cardiomyopathy and lactic acidosis. *Am J Hum Genet* (2012) Jun 8;90(6):1079-87.

Goedert M. Alpha-synuclein and neurodegenerative diseases. *Nat. Rev. Neurosci.* (2001);2, 492–501.

Hafezparast M, Klocke R, Ruhrberg C, Marquardt A, Ahmad-Annur A, Bowen S, Lalli G, Witherden AS, Hummerich H, Nicholson S, Morgan PJ, Oozageer R, Priestley JV, Averill S, King VR, Ball S, Peters J, Toda T, Yamamoto A, Hiraoka Y, et al. Mutations in dynein link motor neuron degeneration to defects in retrograde transport. *Science* (2003);300:808–812.

Halliwell B. Oxidative stress and neurodegeneration: where are we now? *Journal of Neurochemistry* (2006) vol. 97, no. 6, pp.1634–1658.

Hardy, J. A hundred years of Alzheimer's disease research. *Neuron* (2006);52, 3–13.

Harper ME, Bevilacqua L, Hagopian K, Weindruch R, Ramsey JJ. Ageing, oxidative stress, and mitochondrial uncoupling. *Acta Physiol Scand.* (2004) Dec;182(4):321-31.

Hirano M, Silvestri G, Blake DM, Lombes A, Minetti C, Bonilla E, et al. Mitochondrial neurogastrointestinal encephalomyopathy (MNGIE): clinical, biochemical, and genetic features of an autosomal recessive mitochondrial disorder. *Neurology* (1994); 44: 721–7.

Hirst J. Why does mitochondrial complex I have so many subunits? *Biochem* (2011); J 437: e1–e3.

Holt IJ, Harding AE, Morgan-Hughes JA. Deletions of muscle mitochondrial DNA in patients with mitochondrial myopathies. *Nature* (1988); 331: 717–19.

Holt IJ, Harding AE, Petty RK, Morgan-Hughes JA. A new mitochondrial disease associated with mitochondrial DNA heteroplasmy. *Am J Hum Genet* (1990); 46: 428–433.

Howell N, Bindoff LA, McCullough DA, Kubacka I, Poulton J, Mackey D, et al. Leber hereditary optic neuropathy: identification of the same mitochondrial ND1 mutation in six pedigrees. *Am J Hum Genet* (1991); 49:939–50.

Johnston JA, Ward CL, Kopito RR. Aggresomes: a cellular response to misfolded proteins. *J Cell Biol*(1998); 143: 1883-1898

Kaufmann, P, Engelstad K, Wei Y, Kulikova R, Oskoui M, Sproule DM, Battista V, Keller JN, Hanni KB, Markesbery WR. Impaired proteasome function in Alzheimer's disease. *J Neurochem*(2000); 75: 436-439.

Kitada T, Asakawa S, Hattori N, Matsumine H, Yamamura Y, Minoshima S, Yokochi M, Mizuno Y, Shimizu N. Mutations in the parkin gene cause autosomal recessive juvenile parkinsonism. *Nature*(1998); 392: 605-608.

Koenigsberger DY, Pascual JM, Shanske S, Sano M, Mao X, Hirano M, Shungu DC, Dimauro S, De Vivo DC. Natural history of MELAS associated with mitochondrial DNA m.3243A>G genotype. *Neurology* (2011);77, 1965–1971.

Koopman WJH, Nijtmans LG, Dieteren CEJ, Roestenberg P, Valsecchi F, Smeitink JAM, Willems PHGM Mammalian mitochondrial complex I: biogenesis, regulation and reactive oxygen species generation. *Antioxid Redox Signal* (2010);12: 1431–1470.

Langston JW, Ballard PA Jr. Parkinson's disease in a chemist working with 1-methyl-4-phenyl-1,2,5,6-tetrahydropyridine. *N Engl J Med.* (1983) Aug 4;309(5):310.

Leopold PL, McDowall AW, Pfister KK, Bloom GS, Brady ST . Association of kinesin with characterized membrane-bounded organelles. *Cell Motil Cytoskeleton* (1992); 23:19 –33.

Liu Q, Xie F, Siedlak SL, Nunomura A, Honda K, Moreira PI, Zhua X, Smith MA, Perry M. Neurofilament proteins in neurodegenerative diseases, *Cell. Mol. Life Sci.* (2004);61 3057–3075.

Mailloux RJ, Harper ME (2012) Mitochondrial proticity and ROS signaling: lessons from the uncoupling proteins. *Trends Endocrinol Metab* 23: 451–458

Mattiazzi M, D'Aurelio M, Gajewski CD, Martushova K, Kiaei M, Beal MF, et al. Mutated human SOD1 causes dysfunction of oxidative phosphorylation in mitochondria of transgenic mice. *J Biol Chem* (2002);277:29626–33.

McKusick VA Online Mendelian Inheritance in Man, OMIM <http://www.ncbi.nlm.nih.gov/omim>, <http://www.ncbi.nlm.nih.gov/omim>, (2011).

McNaught KS and Jenner P. Proteasomal function is impaired in substantia nigra in Parkinson's disease. *Neurosci Lett*(2001); 297: 191-194.

Mick DU, Fox TD, Rehling P. Inventory control: cytochrome c oxidase assembly regulates mitochondrial translation. *Nat Rev Mol Cell Biol* (2011); 12: 14–20.

Miller C, Saada A, Shaul N, Shabtai N, Ben-Shalom E, Shaag A, Hershkovitz E, Elpeleg O. Defective mitochondrial translation caused by a ribosomal protein (MRPS16) mutation. *Ann Neurol.* (2004) Nov;56(5):734-8.

Mita S, Schmidt B, Schon EA, DiMauro S & Bonilla E. Detection of “deleted” mitochondrial genomes in cytochrome-c oxidase-deficient muscle fibers of a patient with Kearns-Sayre syndrome. *Proc. Natl Acad. Sci. USA* (1989);86, 9509–9513.

Mita S, Rizzuto R, Moraes CT, et al . Recombination via flanking direct repeats is a major cause of large-scale deletions of human mitochondrial DNA. *Nucleic Acids Res* (1990); 18: 561–567.

Mitsumoto H, Santella RM, Liu X, Bogdanov M, Zipprich J, Wu HC, Mahata J, Kilty M, Bednarz K, Bell D, Gordon PH, Hornig M, Mehrazin M, Naini A, Flint Beal M, Factor-Litvak P. Oxidative stress biomarkers in sporadic ALS. *Amyotroph. Lateral Scler.* (2008); 9, 177–183.

Montoya J, Gaines GL, Attardi G. The pattern of transcription of the human mitochondrial rRNA genes reveals two overlapping transcription units. *Cell.* (1983) Aug;34(1):151-9.

Moraes CT, Ricci E, Petruzzella V, et al . Molecular analysis of the muscle pathology associated with mitochondrial DNA deletions. *Nat Genet* (1992); 1: 359–367.

Morfini GA, Stenoien, DL, Brady, ST. Axonal transport. *Basic neurochemistry* (2006); Ed 7 (Siegel G, Albers RW, Brady S, Price D, eds), pp 485–502. Burlington, MA: Elsevier Academic.

Musumeci O, Naini A, Slonim AE et al. Familial cerebellar ataxia with muscle coenzyme Q10 deficiency. *Neurology* (2001); 56:849–855.

Ng SB, Buckingham KJ, Lee C, Bigham AW, Tabor HK, Dent KM, Huff CD, Shannon PT, Jabs EW, Nickerson DA, Shendure J, Bamshad MJ. Exome sequencing identifies the cause of a mendelian disorder. *Nat Genet* (2010) Jan;42(1):30-5.

Ojala D, Montoya J, Attardi G. tRNA punctuation model of RNA processing in human mitochondria. *Nature* (1981) Apr 9;290(5806):470-4.

Okuno D, Iino R, Noji H (2011) Rotation and structure of FoF1-ATP synthase. *J Biochem* 149: 655–664

Onishi T. Structural biology: Piston drives a proton pump. *Nature* (2010); 465: 428–429.

Pagano G, Castello G. Oxidative stress and mitochondrial dysfunction in Down syndrome. *Adv Exp Med Biol* (2012); 724: 291–299.

Pasinelli P, Belford ME, Lennon N, Bacskai BJ, Hyman BT, Trotti D, et al. Amyotrophic lateral sclerosis-associated SOD1 mutant proteins bind and aggregate with Bcl-2 in spinal cord mitochondria. *Neuron* (2004);43:19–30.

Prusiner SB . Shattuck lecture – neurodegenerative diseases and prions. *N. Engl. J. Med.* (2001);344, 1516–1526.

Przedborski S, Vila M, Jackson-Lewis V Neurodegeneration: what is it and where are we? *J Clin Invest* (2003) 111: 3–10

Reid E, Kloos M, Ashley-Koch A, Hughes L, Bevan S, Svenson IK, Graham FL, Gaskell PC, Dearlove A, Pericak-Vance MA, Rubinsztein DC, Marchuk DA. A kinesin heavy chain (KIF5A) mutation in hereditary spastic paraplegia (SPG10). *Am J Hum Genet* (2002); 71:1189 –1194.

Ross CA, Poirier MA. Protein aggregation and neurodegenerative disease. *Nat. Med.* 10 (Suppl.) (2004); S10–S17.

Schon EA, DiMauro S, Hirano M. Human mitochondrial DNA: roles of inherited and somatic mutations. *Nat Rev Genet.* (2012) Dec;13(12):878-90.

Selkoe, DJ. Cell biology of protein misfolding: the examples of Alzheimer’s and Parkinson’s diseases. *Nat. Cell Biol*(2004); 6, 1054–1061.

Servidei S, Zeviani M, Manfredi G, Ricci E, Silvestri G, Bertini E, et al. Dominantly inherited mitochondrial myopathy with multiple deletions of mitochondrial DNA: clinical, morphologic, and biochemical studies. *Neurology* (1991); 41: 1053–9.

Simpson E P, Henry Y K, Henkel J S, Smith R G, Appel S H. Increased lipid peroxidation in sera of ALS patients: a potential biomarker of disease burden. *Neurology*(2004); 62, 1758–1765.

Smeitink J, van den Heuvel L, DiMauro S. The genetics and pathology of oxidative phosphorylation. *Nat Rev Genet* (2001); 2: 342–52.

Smits P, Smeitink JA, van den Heuvel LP, Huynen MA, Ettema TJ. Reconstructing the evolution of the mitochondrial ribosomal proteome. *Nucleic Acids Res.* (2007);35(14):4686-703.

Soto C. Unfolding the role of protein misfolding in neurodegenerative diseases. *Nat Rev Neurosci.* (2003) Jan;4(1):49-60.

Stacpoole PW. Why are there no proven therapies for genetic mitochondrial diseases? *Mitochondrion* (2011);11:679-85.

Stadtman ER, Oliver CN, Levine RL, Fucci L, Rivett AJ. Implication of protein oxidation in protein turnover, aging, and oxygen toxicity. *Basic Life Sci*(1998); 49, 331–339.

Susalka SJ, Pfister KK. Cytoplasmic dynein subunit heterogeneity: implications for axonal transport. *J Neurocytol* (2000); 29:819–829.

Takeuchi H, Kobayashi Y, Ishigaki S, Doyu M, Sobue G. Mitochondrial localization of mutant superoxide dismutase 1 triggers caspase-dependent cell death in a cellular model of familial amyotrophic lateral sclerosis. *J Biol Chem* (2002);277: 50966–72.

Tansey MG, McCoy MK, Frank-Cannon TC: Neuroinflammatory mechanisms in Parkinson's disease: potential environmental triggers, pathways, and targets for early therapeutic intervention. *Exp Neurol* (2007); 208(1):1-25.

Tiranti V, Savoia A, Forti F, D'Apolito MF, Centra M, Rocchi M, Zeviani M. Identification of the gene encoding the human mitochondrial RNA polymerase (h-mtRPOL) by cyberscreening of the Expressed Sequence Tags database. *Hum Mol Genet.* (1997) Apr;6(4):615-25.

Torroni A, Petrozzi M, D'Urbano L, et al. Haplotype and phylogenetic analyses suggest that one European-specific mtDNA background plays a role in the expression of Leber hereditary optic neuropathy by increasing the penetrance of the primary mutations 11778 and 14484. *Am J Hum Genet* (1997); 60: 1107–21.

Tucker EJ, Hershman SG, Köhrer C, Belcher-Timme CA, Patel J, Goldberger OA, Christodoulou J, Silberstein JM, McKenzie M, Ryan MT, Compton AG, Jaffe JD, Carr SA, Calvo SE, RajBhandary UL, Thorburn DR, Mootha VK. Mutations in MTFMT underlie a human disorder of formylation causing impaired mitochondrial translation. *Cell Metab.*(2011) Sep 7;14(3):428-34.

Vijayvergiya C, Beal MF, Buck J, Manfredi G. Mutant superoxide dismutase 1 forms aggregates in the brain mitochondrial matrix of amyotrophic lateral sclerosis mice. *J Neurosci* (2005);25:2463–70.

Vilardo E, Nachbagauer C, Buzet B, Taschner A, Holzmann W A, Rossmannith. A Subcomplex of Human Mitochondrial RNase P Is a Bifunctional Methyltransferase.-Extensive Moonlighting in Mitochondrial tRNA Biogenesis. *Nucleic Acids Research* (2012); Vol. 40, No. 22, pp. 11583-11593.

Wagey RT, Krieger C. Abnormalities of protein kinases in neurodegenerative diseases. *Prog Drug Res* (1998);51:133–183.

Wallace DC, Zheng X, Lott MT, Shoffner JM, Hodge JA, Kelley RI, Epstein CM, Hopkins LC. Familial mitochondrial encephalomyopathy (MERRF): Genetic, pathophysiological, and biochemical characterization of a mitochondrial DNA disease. *Cell* (1988a); 55: 601–610.

Wallace DC, Singh G, Lott MT, Hodge JA, Schurr TG, Lezza AM, et al. Mitochondrial DNA mutation associated with Leber's hereditary optic neuropathy. *Science* (1988b); 242: 1427–30.

Wallace DC, Brown MD, Lott MT. Mitochondrial DNA variation in human evolution and disease. *Gene* (1999); 238: 211–30.

Watanabe R, Okuno D, Sakakihara S, Shimabukuro K, Iino R, Yoshida M, Noji H. Mechanical modulation of catalytic power on F1-ATPase. *Nat Chem Biol*(2011); 8: 86–92

Watt IN, Montgomery MG, Runswick MJ, Leslie AG, Walker JE. Bioenergetic cost of making an adenosine triphosphate molecule in animal mitochondria. *Proc Natl Acad Sci USA* (2010); 107: 16823–16827

Wei YH, Lu CY, Lee HC, Pang CY, Ma YS. Oxidative damage and mutation to mitochondrial DNA and age-dependent decline of mitochondrial respiratory function. *Ann N Y Acad Sci.* (1998) Nov 20;854:155-70.

Wojda U, Salinska E, Kuznicki J: Calcium ions in neuronal degeneration. *IUBMB Life* (2008), **60**:575-590.

Youle RJ, Narendra DP. Mechanisms of mitophagy. *Nat Rev Mol Cell Biol* (2011), 12:9–14.

Zeharia A, Shaag A, Pappo O, Mager-Heckel AM, Saada A, Beinat M, Karicheva O, Mandel H, Ofek N, Segel R, Marom D, Rötig A, Tarassov I, Elpeleg O. Acute infantile liver failure due to mutations in the TRMU gene. *Am J Hum Genet.* (2009) Sep;85(3):401-7.

Zeviani M. The expanding spectrum of nuclear gene mutations in mitochondrial disorders. *Seminars in Cell and Developmental Biology* (2001); 12: 407–416.

CHAPTER 2

Adult-onset Alexander disease, associated with a mutation in an alternative GFAP transcript, may be phenotypically modulated by a non-neutral HDAC6 variant

Laura Melchionda^{1†}, Mingyan Fang^{2†}, Hairong Wang², Valeria Fugnanesi³, Michela Morbin³, Xuanzhu Liu², Wenyan Li⁴, Isabella Ceccherini⁵, Laura Farina⁶, Mario Savoirdo⁶, Pio D'Adamo⁷, Jianguo Zhang^{2,8}, Alfredo Costa⁹, Sabrina Ravaglia⁹, Daniele Ghezzi¹ and Massimo Zeviani^{1*}

¹Unit of Molecular Neurogenetics, Fondazione Istituto Neurologico 'Carlo Besta', Istituto di Ricovero e Cura a Carattere Scientifico (IRCCS), Milan, Italy.

²BGI-Shenzhen, Shenzhen, China.

³Unit of Neuropathology and Neurology 5, Fondazione Istituto Neurologico 'Carlo Besta', IRCCS, Milan, Italy.

⁴BGI-Europe, Copenhagen, Denmark.

⁵Laboratory of Molecular Genetics, G Gaslini Institute, Genoa, Italy.

⁶Department of Neuroradiology, Fondazione Istituto Neurologico 'Carlo Besta', IRCCS, Milan, Italy.

⁷Medical Genetics, IRCCS, Burlo Garofolo, University of Trieste, Trieste, Italy.

⁸T-Life Research Center, Fudan University, Shanghai, China.

⁹National Institute of Neurology, IRCCS 'C Mondino', Pavia, Italy.

Orphanet Journal of Rare Diseases 2013, 8:66

Abstract

Background: We studied a family including two half-siblings, sharing the same mother, affected by slowly progressive, adult-onset neurological syndromes. In spite of the diversity of the clinical features, characterized by a mild movement disorder with cognitive impairment in the elder patient, and severe motor-neuron disease (MND) in her half-brother, the brain Magnetic Resonance Imaging (MRI) features were compatible with adult-onset Alexander's disease (AOAD), suggesting different expression of the same, genetically determined, condition.

Methods: Since mutations in the alpha isoform of glial fibrillary acidic protein, GFAP- α , the only cause so far known of AOAD, were excluded, we applied exome Next Generation Sequencing (NGS) to identify gene variants, which were then functionally validated by molecular characterization of recombinant and patient-derived cells.

Results: Exome-NGS revealed a mutation in a previously neglected GFAP isoform, GFAP- ϵ , which disrupts the GFAP-associated filamentous cytoskeletal meshwork of astrocytoma cells. To shed light on the different clinical features in the two patients, we sought for variants in other genes. The male patient had a mutation, absent in his half-sister, in X-linked histone deacetylase 6, a candidate MND susceptibility gene.

Conclusions: Exome-NGS is an unbiased approach that not only helps identify new disease genes, but may also contribute to elucidate phenotypic expression.

Background

Alexander's disease (AD, OMIM #203450) is a rare neurological disorder characterized by a peculiar form of leukodystrophy, with infantile, juvenile and adult forms manifesting with different clinical and pathological signs [1]. AD is a sporadic or autosomal dominant condition associated in most of the cases with heterozygous mutations in the gene encoding the glial fibrillary acidic protein, GFAP, an intermediate filament component of the cytoskeleton of several cell types [2]. GFAP mutations frequently occur *de novo*, particularly in infantile cases, while in Adult-onset AD (AOAD) both *de novo* mutations and autosomal dominant transmission have been described [3]. GFAP-containing eosinophil aggregates, known as Rosenthal fibers, distributed in the white matter of the CNS, constitute the morphological hallmark of the disease [2]. Whilst the infantile form shows extensive white matter lesions and usually fatal outcome, AOAD is characterized by predominant brainstem involvement and survival into adulthood [4].

We here report the results of exome next-generation DNA sequencing (NGS) conducted on a family with two maternal half-siblings, affected by two distinct adult onset neurological syndromes: mild cognitive deterioration and movement disorder in a female patient, motor-neuron disease (MND) in her half-brother. The two patients shared the same mother, but had different, unrelated fathers, suggesting either an X-linked or an autosomal dominant condition with variable penetrance and expressivity. In spite of the diversity of the clinical features, the brain MRI features were compatible with AOAD. However, standard

sequence analysis of the nine canonical exons encoding the predominant isoform, GFAP- α , had previously ruled out mutations in both patients.

NGS is a holistic, unbiased approach that generates comprehensive information on gene variance [5]. Exome NGS analysis in our family revealed a heterozygous missense mutation in an alternative exon of the *GFAP* gene (exon 7A), which has not previously been included in the diagnostic screening of AOAD. Additional variants in other genes included a private mutation in the X-linked gene encoding histone deacetylase 6, *HDAC6*, which was present in the male, but absent in the female, patients. HDAC6 was suggested to have a modulating role in different processes related to neurodegeneration, including autophagy, proteosomal degradation, aggresome formation [6,7]. We demonstrated that the mutant HDAC6 variant has reduced deacetylase activity, which could contribute to the different phenotypes of our patients.

Patients and methods

Case reports

Patient 1, Pt1 (subject II-2 in Figure 1A) is now 68 years old. Her insidious disease onset started at 55 years, and was first characterized by psychiatric symptoms, initially as a bipolar disorder with depression alternated by hypomanic behavior (compulsive gambling), and eventually as a cognitive deterioration with apathy, neglect of personal care, and memory loss. Shortly thereafter, she manifested an ataxic gait with frequent falls, followed by progressive dysarthria,

dysphagia to liquids, drooling, and fluctuating palatal myoclonus. An Electroencephalography at 61 showed unspecific irritative abnormalities; visual evoked potentials were altered. The neurological examination disclosed a moderate ataxic gait requiring a can, dysarthria, palatal myoclonus, and hypotonia (right >left), increased tendon reflexes, a positive Babinski sign at the right foot, mild dyskinesias, mild distal dystonia. Eye movements were normal. A Mini Mental State Examination scored 16/30. The syndrome slowly progressed, with worsening of cognitive deterioration, dysarthria and dysphagia, and onset of urinary incontinence. Several Electromyography (EMG) examinations have consistently been normal over time.

Pt2 (II-4 in Figure 1A), now 60 years old, was first referred to us at 52, for insidiously progressive walking difficulties, initiated at 46 years with stiffness and weakness at the right lower limb, followed within 3-5 years by involvement of the right upper, and then left lower and upper limbs. He also reported symptoms consistent with nocturnal lower-limb myoclonus. The neurological examination at 52 years showed spastic tetraparesis, more prominent on the right side and lower limbs, bilateral pes equinovarus, normal strength, bilateral Babinski sign. His gait was paraparetic with bilateral thigh adduction; however he could still walk unassisted. He showed no muscle wasting, with the exception of bilateral atrophy of the temporalis muscle. He was diagnosed as having “primary lateral sclerosis” and started riluzole and baclofen, with no tangible benefit.

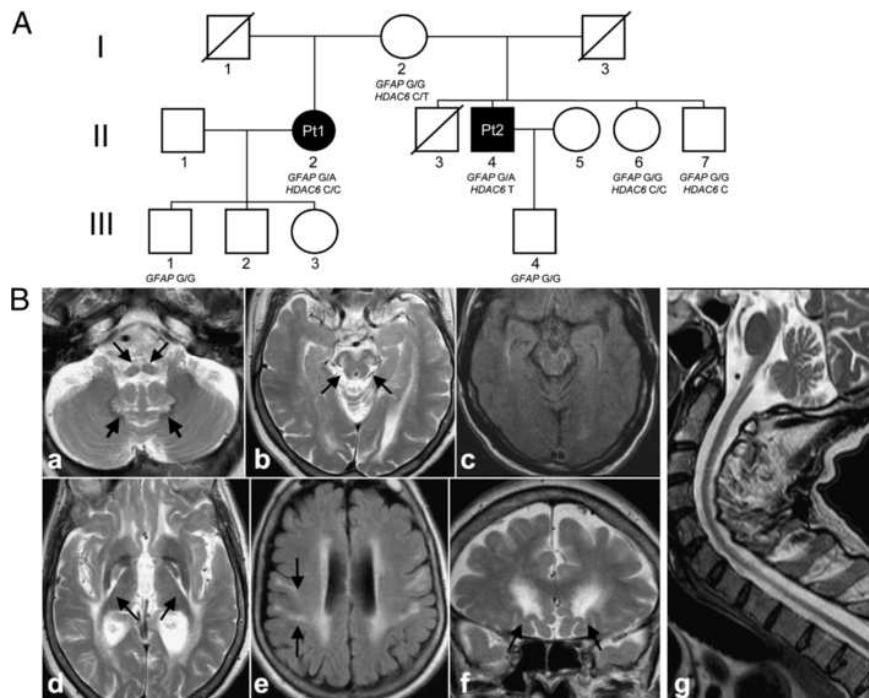


Figure 1 Pedigree and radiological features of the patients. **A:** Pedigree of the family. Black symbols indicate affected patients 1 and 2 (Pt1, Pt2). Genotypes of each tested individual are indicated under the corresponding symbols (GFAP G: wt; GFAP A: mutant; HDAC6 C: wt; HDAC6 T: mutant). I-3 died of colon cancer at 62 years of age; I-1 died of unknown causes when he was over 80; II-3 died of a cerebral stroke at 60 years of age. **B:** Brain MRI findings of Pt1 (a-f) and Pt2 (g). Atrophy of the medulla is present, with signal abnormalities of the pyramidal tract and medial lemniscus (a, arrows). In the cerebellum, the hilum of the dentate nucleus is bilaterally hyperintense (a, thick arrows). At midbrain level (b,c), substantia nigra and medial lemniscus are hyperintense (b, arrows); a sub-pial rim of high signal intensity is present in the FLAIR image (c). Symmetrical signal abnormalities involve the pallida, particularly at the interface with the posterior limb of the internal capsule (d, arrows). Hyperintensity is present in the periventricular white matter, pre- and post-central gyri (e, arrows on the right) and subcortical frontobasal areas (f, arrows). The typical tadpole appearance of the brainstem and cervical spinal cord is seen in the midline sagittal section of Pt2 (g).

Over the subsequent two years he developed mild spastic hypophonia, and moderate dysphagia for liquids, with worsening of the limb spasticity.

At 56 he became wheelchair-bound, severely dysphonic and dysphagic, with severe tetraspasticity, flexed posture, bilateral ankle clonus, bilateral Babinski, bilateral hypotrophy of *temporalis*, *interosseus* and *tibialis anterior* muscles. Sensory examination and neurovegetative tests were normal, as were the eye movements. The EMG showed neurogenic abnormalities, without spontaneous fibrillation. Nerve conduction studies showed motor axonal neuropathy at the lower limbs, whereas the peripheral sensory conduction was normal. Taken together, these findings indicate severe motor-neuron disease (MND) of limb and bulbar districts. Symptoms have slowly progressed over time. The patient has no cognitive deterioration.

The MRI findings of these patients were very similar and consistent with the diagnosis of AOAD (Figure 1B). Atrophy of the medulla oblongata and cervical spinal cord (“tadpole” appearance) and signal abnormalities were present in the brainstem, dentate nuclei and supratentorial periventricular white matter. Additional findings, peculiar to our patients, were mild atrophy of the midbrain with T2 hyperintensity of the substantia nigra and medial lemniscus, pallida, and subcortical white matter in the pre- and post-central gyri and frontobasal areas. Interestingly, Pt1, who had more marked cognitive impairment, had slightly more extensive supratentorial white matter involvement. To quantitatively express the different clinical features

of the two siblings, we used the Kurtzke scale [8] (Additional file 1), that scores several functional systems (motor, cerebellar, brainstem, urinary, visual, and cognitive) usually involved in white matter disease, including leukodystrophies.

Table 1 Clinical and instrumental assessments

	Pt1	Pt2
Current age	68	60
Age at onset	55	46
Disease duration at the time of examinations, years	13	14
Instrumental assessment *		
Cognitive: MMSE score	16/30	30/30
EMG	0	Mild motor axonal neuropathy (1)
MEPs Bulbar/UL/LL	NA/0/0	1/1/3
SEPs UL/LL	1/1	0/1
BAEPs	NA	NA
VEPs	0	0
Autonomic testing	0	0
Clinical scoring **		
Dysarthria/dysphagia	2	2
Gait abnormalities	1	3
Spasticity	0	3
Axial Ataxia	1	0
Limb dysmetria	2	0
Limb weakness	0	2
Muscle wasting	0	1
Sphincter function	2	0

* For neurophysiological assessments, values are graded as 0 (normal), 1 (abnormality not exceeding 25% of upper/lower normal ranges), 2 (between 25 and 50%), and 3 (beyond 50%).

** For clinical dysfunctions, abnormalities are graded as 0 (normal), 1 (only objective signs), 2 (mild dysfunction, not interfering with activities), 3 (severe dysfunction interfering with walking, feeding, or social interactions).

MMSE: mini-mental state examination; EMG: Electromyography; MEPs: Motor evoked potentials; SEPs: Sensory evoked potentials; UL/LL: upper/lower limbs; BAEPs: Brainstem Auditory Evoked Potentials; VEPs: visual evoked potentials.

The scores were obtained 13 years after disease onset for Pt1 and 14 years after onset for Pt2. The global functional impairment, as assessed by the final EDSS score, [9] was 3/10 for Pt1 (able to walk, moderate ataxia and cognitive impairment, not requiring institutionalization) and 8.5/10 for Pt2 (confined to bed but with some residual upper limb function). For Pt2, the source of the severe disability was predominantly due to pyramidal dysfunction: we thus assessed both patients by also using the ALS-Severity scale, [10]

which scored 33/40 for pt1 (speech 7, deglutition 6, upper limbs 10, lower limbs 10), and 17/40 for pt2 (speech 3, deglutition 8, upper limbs 4, lower limbs 2). The results of instrumental examinations are reported in Table 1.

Molecular analyses

Informed consent for participation in this study was obtained from all family members, in agreement with the Declaration of Helsinki and approved by the Ethical Committee of the Fondazione Istituto Neurologico –IRCCS, Milan, Italy.

Genomic DNA was extracted by standard methods from peripheral blood samples (I-2, II-2, II-4, II-6, II-7, III-1, III-3) and from skin fibroblasts (II-2, II-4). Whole-exome and Sanger's sequencing were performed as described [11]. Total RNA was isolated from fibroblasts (RNeasy kit, Qiagen) and then transcribed to cDNA (Cloned AMV first-strand cDNA synthesis kit, Invitrogen). Quantitative Real-time PCR (QRtPCR) was assayed on an ABI Prism 7000 apparatus (Applied Biosystems). Additional file 2 reports primers and conditions for PCR amplifications of relevant exons of human *GFAP* and *HDAC6* and for QRtPCR of *HDAC6* cDNA.

Additional file 3 reports URLs for biocomputational analysis.

A GFP tagged *GFAP* cDNA (Origene RG225707) was modified by using Quick-change Site-directed mutagenesis kit (Stratagene) to introduce either the c.1289G > A or the c.1288C > T nucleotide change in the RG225707 clone, using primers listed in Additional file 2.

Cellular experiments

Cell culture, transient transfections, western-blot analysis, and immunocytochemistry were performed as described, [12-15] using antibodies against α -tubulin (Life Science) and acetylated α -tubulin (Sigma). Patients' fibroblasts and adult control fibroblasts were grown under the same conditions, and analyzed among culture passages 5 and 8. As a positive control for tubulin acetylation, fibroblasts were pre-incubated with the specific HDAC6 inhibitor Tubacin (0, 0.2 μ M and 2.5 μ M) (Sigma) for 24 h [16]. Immunohistochemistry was carried out on 2 μ m thick sections from pellets of Pt1, Pt2 and control fibroblasts, fixed in glutaraldehyde 2.5% (Electron Microscopy Science - EMS), in 0.05 M PBS pH 7.4, dehydrated in graded acetone, and embedded in Spurr (Epoxy resin, EMS).

Transfection of U251-MG by electroporation was performed in triplicate according to the manufacturer's protocol (GenePulserII-Biorad), and about 100 cells were analyzed blindly for each experiment (a total of 324 cells for GFP-GFAP- ϵ^{wt} and 285 for GFP-GFAP- ϵ^{R430H} in a first experiment, and 460 cells for either GFP-GFAP- ϵ^{wt} or GFP-GFAP- ϵ^{R430C} in a second experiment).

Results

Mutational screening ruled out mutations in the *SPG4* and *SPG7* genes in Pt2, due to the presence of spastic tetraparesis; in the *HTT* gene in Pt1, due to the subtle onset of symptoms consistent with an affective disorder, together with cognitive dysfunction; and in the

UBQLN2 and *C9orf72* genes, recently associated to ALS/FTD, in both.

The MRI features were consistent with AOAD, but no mutation was detected in the nine exons encoding the prevalent (alpha) isoform of GFAP (GFAP- α , NP_002046.1; Figure 2A). All of the known mutations associated with Alexander's disease have so far been found in this isoform, [17] which is the only one analyzed by standard screening. However, exome-NGS revealed a heterozygous variant (c.1289G > A, p.R430H) in the alternative *GFAP* exon 7A (Ex7A) in both patients (Figure 2B). Ex7A is part of the transcript encoding the GFAP- ϵ isoform (NP_001124491.1), which differs from GFAP- α in the last 35 amino acids. A third isoform, GFAP- κ (NP_001229305.1), which contains a unique exon 7B, has also been identified (Figure 2A) [18]. The c.1289G>A nucleotide change was absent in the healthy mother and in all other tested family members. DNA samples from I-1 and I-3, fathers of Pt1 and Pt2, respectively, were unavailable. Haplotype analysis of the *GFAP* genomic region by SNPs array in the available family members confirmed that the father of Pt1 was different from that of Pt2 and of his siblings, whilst Pt1 and Pt2 share the same maternal allele (Additional file 4). Since the likelihood that the same rare variant (<0.01%) may occur independently in the two patients is negligible, the most probable hypothesis is that the mutation was transmitted by descent to both Pt1 and Pt2 by maternal germinal mosaicism, a mechanism that can also explain the healthy status of the mother. Since blood was the only source of DNA available from the mother, somatic mosaicism affecting other tissues

of this subject cannot be excluded, as recently found in an AD patient with atypical infantile clinical presentation and essentially normal MRI features [19]. However, we think that the latter hypothesis is unlikely, since no trace of mutation could be detected by an ad hoc RFLP analysis carried out in the mother's DNA (not shown) and, in contrast with the case reported by Flint et al. [19], this lady is now 87 years old and well.

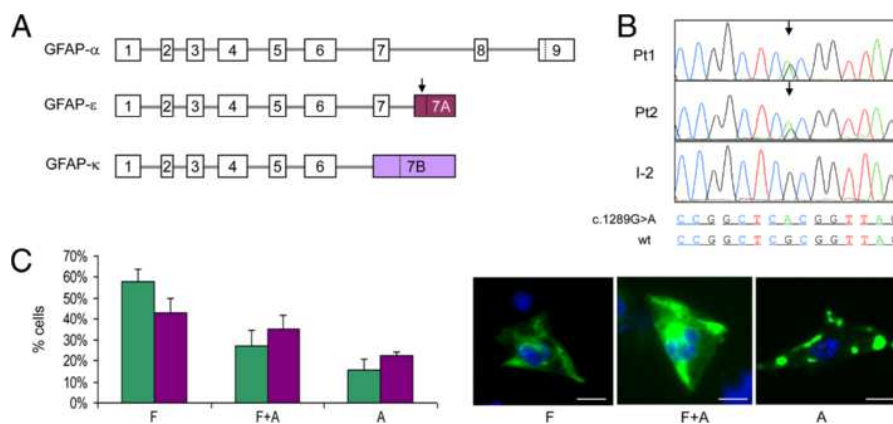


Figure 2 Characterization of the GFAP c.1289G>A/p.R430H mutation. **A:** Schematic representation of the exonic structure of different GFAP isoforms. Dotted lines indicate the termination codons. The arrows indicate the position of the c.1289G>A variant (Note that in GFAP- κ the c.1289G>A mutation is part of the 3'-UTR). **B:** Electropherograms of *GFAP* exon 7A region containing c.1289G>A variant, in patients 1 and 2 (Pt1, Pt2) and in their mother (I-2). **C:** The histogram displays the percentages of cells transfected with GFP-GFAP- ϵ^{wt} (green bars) or GFP-GFAP- ϵ^{R430H} (purple bars), classified in filamentous pattern (F), cytoplasmic aggregates on a filamentous pattern (F + A), cytoplasmic aggregates with no filamentous pattern (A). Scale bars represent 15 μ m. A total of 324 cells for GFP-GFAP- ϵ^{wt} and 285 for GFP-GFAP- ϵ^{R430H} , from 3 independent experiments, were blindly analyzed by two different operators. ANOVA test for interaction $p = 0.001$.

In contrast with a p.R430C SNP (rs 78994946), reported with a frequency of 1% in dbSNP, the p.R430H change found in our patients is absent in both dbSNP and the Exome Variant Server (EVS) database, which contains >10000 alleles (\approx 7000 of European origin). These data are compatible for p.R430H being a deleterious mutation (Additional file 5).

GFAP is an intermediate filament (IF) protein expressed mainly by astrocytes and ependymocytes. Recent data suggested that GFAP- ϵ was unable to form filaments by itself but it could participate to the formation of the GFAP network by interacting with GFAP- α [20]. Hence we analyzed the IF meshwork in human astrocytoma U251-MG cells, constitutively expressing both GFAP- α and GFAP- ϵ , by expressing GFP-tagged wt and mutated GFAP- ϵ (GFP-GFAP- ϵ^{wt} vs. GFP-GFAP- ϵ^{R430H}). Cells were assigned to three patterns: [14] (i) exclusively filamentous pattern (F), (ii) cytoplasmic aggregates on a filamentous pattern (F + A), (iii) cytoplasmic aggregates with no filamentous pattern (A). The expression of GFP-GFAP- ϵ^{wt} led to a distribution among the three groups similar to that reported for GFP-GFAP- α^{wt} [14] (Figure 2C) indicating no intrinsic damaging effect of recombinant GFP-GFAP- ϵ^{wt} in our experimental conditions. Contrariwise, expression of mutant GFP-GFAP- ϵ^{R430H} produced significant decrease in F (43% vs. 58%; test t p = 0.002) and increase in A (22% vs. 15%; test t p = 0.009) cells (Figure 2C), with a distinct distribution in the three patterns compared to GFP-GFAP- ϵ^{wt} expressing cells (ANOVA test for interaction p = 0.001).

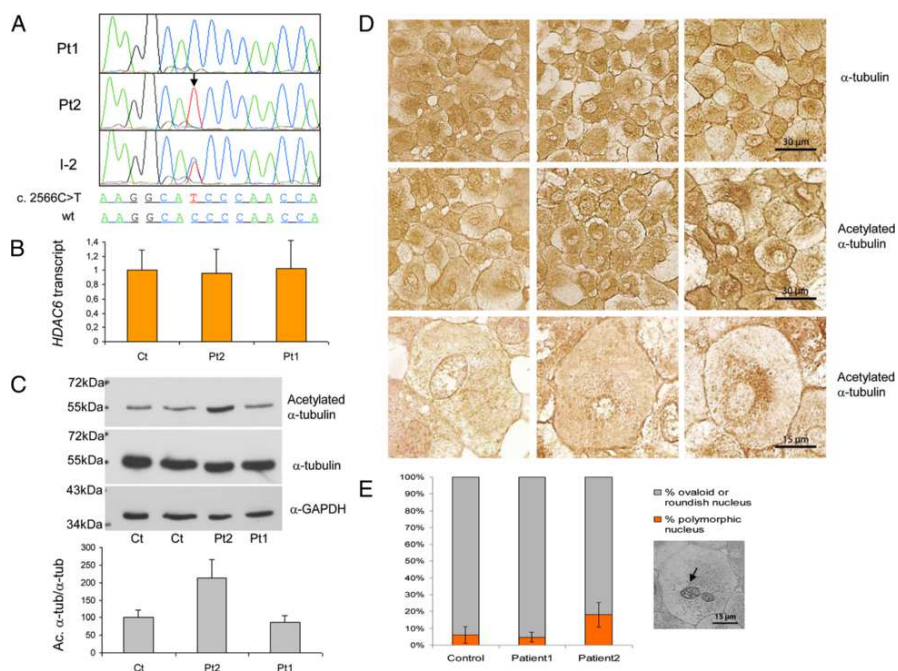


Figure 3 Characterization of the HDAC6 c.2566C>T/p.P856S variant.

A: Electropherograms of *HDAC6* exon 25 region containing the c.2566C>T variant, in patients 1 and 2 (Pt1, Pt2) and their mother (I-2). **B:** Levels of *HDAC6* transcript, normalized to that of the endogenous *GAPDH* cDNA, in controls (Ct; mean of five subjects) and patients 1 and 2 (Pt1, Pt2), obtained from 3 independent experiments. Two-tailed Student's t-tests showed no significant differences: Pt2 vs. Ct $p = 0.811$; Pt2 vs. Pt1 $p = 0.813$; Pt1 vs. Ct $p = 0.896$. **C:** Exemplifying Western-blot analysis of fibroblast lysates from control subjects (Ct1, Ct2) and patients 1 and 2 (Pt1, Pt2), using antibodies against acetylated α -tubulin (upper panel), α -tubulin (middle panel) and α -GAPDH, as loading control (lower panel). The graph represents the ratio acetylated α -tubulin/ α -tubulin obtained by densitometric analysis from 3 independent experiments: 100% corresponds to the mean value of four control subjects. Two-tailed Student's t-test Pt2 vs Ct $p = 0.002$, Pt1 vs Ct $p = 0.33$. **D:** Immunocytochemistry on fibroblasts from a control subject (Ct) and patients 1 and 2 (Pt1, Pt2), using antibodies against α -tubulin and acetylated α -tubulin. Scale bars are reported on the right for each row. **E:** Percentages of multilobated nuclei in control, Patient1 and Patient2. A total of 15 digital images (at least 600 cells for each patient) representative of the whole sections were collected and analyzed for each sample; the arrow indicates a typical multilobated nucleus. Two-tailed Student's t-test between Control vs. Pt1 showed no significant differences ($p = 0.4970$); Pt2 vs. Control $p = 0.000099$; Pt2 vs. Pt1 $p = 0.000018$ (both highly significant).

Notably, the expression of GFP-tagged GFAP carrying the R430C variant (GFP-GFAP- ϵ^{R430C}) led to a distribution amongst the three different patterns similar to that obtained with GFP-GFAP- ϵ^{wt} , i.e. non-significant (ANOVA test for interaction $p = 0.333$). These results indicate that GFAP- ϵ^{R430H} is inefficiently incorporated, and is likely to perturb the GFAP network in GFAP-expressing astrocytoma cells, whereas the GFAP- ϵ^{R430C} variant is functionally wt, but we cannot exclude the possibility that variations in the level of expression contributed to this result.

To test whether additional genes could influence phenotype expression, 18 genes with variants in Pt2 were prioritized by the Endeavour software, [21] using “training genes” associated with MND (Additional file 6). The highest score was achieved by *HDAC6*, on chromosome Xp11.23, encoding a member of the histone deacetylase family (NP_006035.2); Pt2 was hemizygous for a c. 2566C>T/p.P856S, variant, whereas Pt1, II-6 and II-7 were wt, and the mother, I-2, was heterozygous (Figure 3A). Whilst the variants in the other genes were all relatively frequent SNPs and/or present also in Pt1 (Additional file 6), the P856S change was absent in all available databases, including EVS. The amount of *HDAC6* transcripts was similar in fibroblasts from Pt2 vs. Pt1 or control subjects, indicating that neither HDAC6 expression nor stability is severely affected by the mutation (Figure 3B). However, acetylated alpha-tubulin, a HDAC6 substrate, [22] was consistently increased (Figure 3C); treatment of fibroblasts with tubacin, a selective HDAC6 inhibitor, clearly

increased the acetylation of alpha-tubulin, confirming the specificity of this assay to detect impaired HDAC6 activity (Additional file 7).

Densitometric analysis of immunoreactive bands from three independent experiments, showed that the ratio acetylated α -tubulin/ α -tubulin was significantly augmented to 213% in Pt2, compared to the mean value of four control subjects, but was unchanged (87%) in Pt1 (Figure 3C). Moreover, immunocytochemical staining showed abnormal clumps of acetylated α -tubulin in the perinuclear region of Pt2 fibroblasts (Figure 3D).

Interestingly HDAC6^{P856S} fibroblasts showed a significantly higher number of multilobated nuclei, compared to control cells, which could be consequent to altered physical connection between nuclear membrane and cytoskeletal network (Figure 3E). Taken together these results suggest dysregulation of the microtubule-organizing center (MTOC), associated with reduced HDAC6 activity [23].

Discussion

A substantial fraction of AOAD patients are sporadic, the most frequent symptoms being related to bulbar dysfunction, pyramidal involvement and cerebellar ataxia. Palatal myoclonus is frequent in, and highly suggestive of, AOAD [4]. Other findings include cognitive deterioration, sleep disorders, and dysautonomia. The course is slowly progressive and fluctuations may occur. Ultimately, the diagnosis is strongly suggested by a typical MRI pattern, and confirmed by *GFAP* gene analysis. In our family, Pt1 has been suffering of slowly

progressive cognitive impairment and mild movement disorder, whereas her younger half-brother (Pt2) has severe MND.

In spite of clinical diversity, the cardinal MRI features of AOAD [24] were present in both. The absence of mutation in the *GFAP- α* encoding gene prompted us to perform exome-NGS and eventually identify a unique mutation in alternative *GFAP* ex7A, not present in the healthy mother tested DNAs and with a deleterious outcome in a cellular model. These are in fact the first cases associated with a mutation in the *GFAP- ϵ* variant (*GFAP- ϵ ^{R430H}*). Whilst this finding supports the idea that AOAD is almost invariably associated with abnormalities of *GFAP*, it also expands the spectrum of variants that should be included in the diagnostic screening. Due to the pedigree structure, the mutation has very likely been transmitted by maternal germinal mosaicism, since it was absent in other available family members, including the healthy mother of the two patients.

The clinical diversity in our two half-siblings was as remarkable as to suggest that differential segregation of other gene variants could influence phenotypic expression. A prioritized variant found by in-silico data mining was in *HDAC6*. A hemizygous *HDAC6^{P856S}* change, found in Pt2, and absent in Pt1, was associated with decreased tubulinspecific deacetylase activity [22]. Through deacetylation of α -tubulin, HSP90, and other substrates, and binding to ubiquitinated proteins that are then transported into, and degraded by, the aggresome, *HDAC6* plays a role in a number of important homeostatic and signaling pathways, including axonal transport, redox signaling, misfoldedprotein response, and autophagy [25,26].

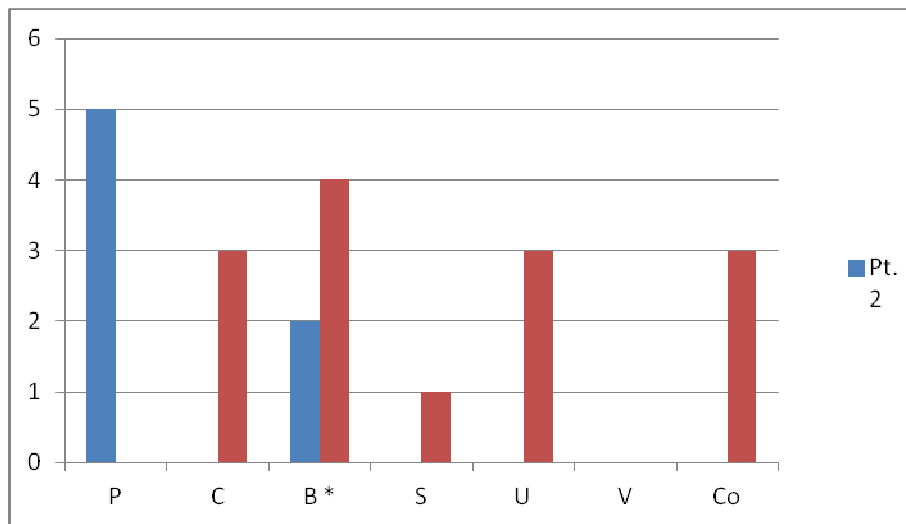
Interestingly, the RNA-binding modulator factors TDP-43 and FUS/TLS, whose mutations are associated with familial amyotrophic lateral sclerosis (ALS), have *HDAC6* mRNA as a specific substrate [27]. A *Drosophila* model in which TDP-43 is silenced shows decreased *HDAC6* expression, [28] and *HDAC6* overexpression is able to rescue the phenotype of a *Drosophila* model of spinobulbar muscular atrophy [6].

Taken together, these observations indicate HDAC6 as a master regulator of different neuroprotective mechanisms, partly mediated by controlling MTOC biogenesis and function, [23] and predict a role for defective HDAC6 in neurodegeneration, particularly in MND [26]. As for mammalian models, although a first strain of *HDAC6* knockout (KO) mice presented no sign of neurodegeneration, [29] altered emotional behaviors suggested a contribution of HDAC6 to maintain proper neuronal activity [30]. Moreover, a second KO *HDAC6* strain displayed ubiquitin-positive aggregates and increased apoptosis of brain nerve cells, both hallmarks of neurodegeneration, starting from 6 months of age [31]. These and other results suggest for HDAC6 a complex role in contributing to either neuroprotection or neurodegeneration, depending on the specific pathological condition [7,26,32]. These opposite effects can indeed hamper the development of therapeutic strategies based on HDAC6 modulation [7].

Albeit preliminary, our own results support the interesting hypothesis that the *HDAC6*^{P856S} protein variant may be acting synergistically with the GFAP- ϵ ^{R430H} mutation, conditioning the development of the severe MND phenotype of Pt2.

The mechanisms underlying the diverse etiology and expressivity of many inherited neurodegenerative disorders are still poorly understood. Exome-NGS is an unbiased approach that not only helps identify new disease genes, but may also contribute to elucidate phenotypic expression and penetrance.

Additional file 1



Clinical involvement on specific functional systems. The bars represent the score on the Kurtzke scale of the two patients (Pt1 red bars; Pt2 blue bars), 13 and 14 years after the onset of the disease (higher scores express higher disability).

* Brainstem involvement consisted of spastic dysarthria and fluids dysphagia for both patients.

P: Pyramidal ; C Cerebellar; B Brainstem; S Sensory; U Urinary; V Visual; Co Cognitive.

Additional file 2

Primers sequences and amplification conditions

<i>Amplicon</i>	<i>Forward primer</i>	<i>Reverse primer</i>	<i>PCR conditions</i>
<i>GFAP</i> exon 7A	AGATCCCTGAGCAAGCA CTG	CTGGGAAGAGGGAAGCTC AGG	Ta: 58°C; GoTaq Promega
<i>GFAP</i> exon 7B	CCCTCTCCCTCTGCTTTCT T	CGGCGTCCATTACAAT CT	Ta: 58°C; GoTaq Promega
<i>HDAC6</i> exon 25	GGGAACCCAGGGAAGG AG	GAGTGAGGGCCACCACA G	Ta: 58°C; GoTaq Promega
<i>HDAC6</i> cDNA (nt556-616)	TCGCTGCGTGTCTTTCA G	GCTGTGAACCAACATCA GCTCTT	Quantitative PCR (ABI Prism7000)
<i>HDAC6</i> cDNA (nt3605-3675)	TGGGTGTGTCTCTTTC TATCA	CCATGGTGTGGAGCAT GTG	Quantitative PCR (ABI Prism7000)
<i>Mutagenesis</i>			
<i>GFAP</i> c.1288C>T	GAACGCCGCCGGCTTGC GGTACGCGTACGC	GCGTACGCGTACCGCAA GCCGGCGCGTTC	Quick-change Site-directed mutagenesis kit (Stratagene)
<i>GFAP</i> c.1289G>A	GAACGCCGCCGGCTCAC GGTACGCGTACGC	GCGTACGCGTACCGTGA GCCGGCGCGTTC	Quick-change Site-directed mutagenesis kit (Stratagene)

Ta: Annealing temperature

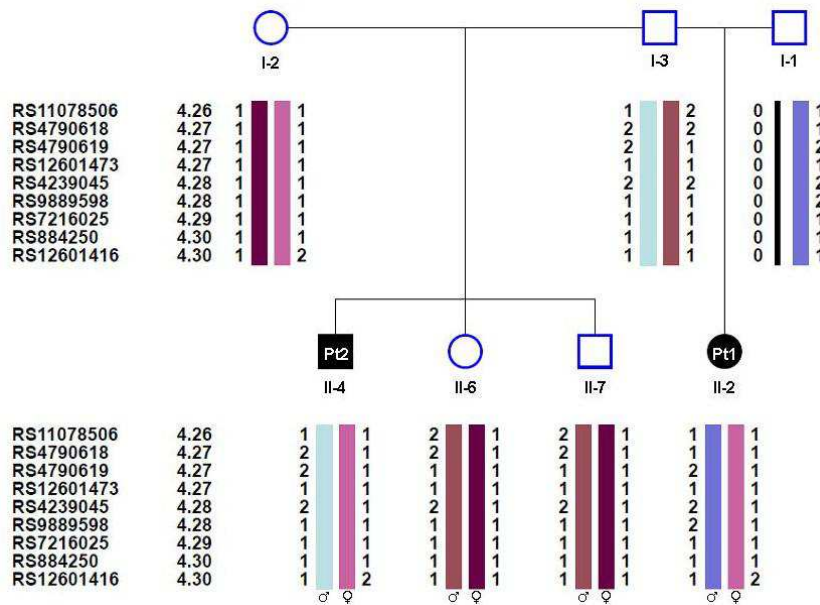
Additional file 3

URLs for biocomputational analysis

<i>Prediction softwares for mutation pathogenicity</i>	
MutPred	http://mutpred.mutdb.org
PMUT	http://mmb.pcb.ub.es/PMut
Polyphen2	http://genetics.bwh.harvard.edu/pph2
Sorting Intolerant From Tolerant (SIFT)	http://sift.bii.a-star.edu.sg

Public databases for SNPs	
dbSNP	http://www.ncbi.nlm.nih.gov/projects/SNP
Exome Variant Server (EVS)	http://evs.gs.washington.edu/EVS
HapMap	http://hapmap.ncbi.nlm.nih.gov/
Computational prioritization of candidates genes	
Endeavour	http://homes.esat.kuleuven.be/~bioiuser/endeavour/index.php

Additional file 4



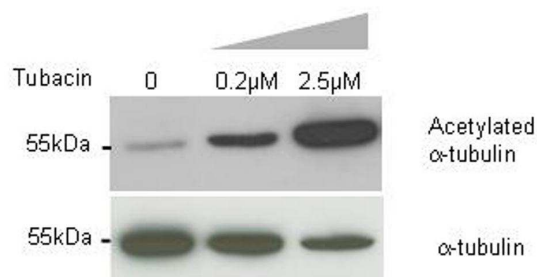
Haplotype analysis of the *GFAP* genomic region by SNPs array (ILLUMINA HumanCytoSNP-12 BeadChip). In the siblings the symbol ♂ indicates the paternal allele and ♀ the maternal allele. Individuals are numbered according to the pedigree in Figure 1A.

Additional file 5

Predictions of pathogenicity for GFAP p.R430H change

Software	Prediction result
MutPred	Probability of deleterious mutation: 0.240
PMUT	Pathological
Polyphen2	Probability of deleterious mutation: 0.564; Possibly damaging
Sorting Intolerant From Tolerant (SIFT)	Probability that the amino acid change is tolerated: 0.01

Additional file 7



Western-blot analysis of control fibroblasts, using antibodies against acetylated α -tubulin (upper panel), and α -tubulin (lower panel), after treatment for 24h with a specific inhibitor of HDAC6, tubacin, at different concentrations (0, 0.2 μ M and 2.5 μ M). Note that the α -tubulin antibody (Life Science) showed preferential immunoreactivity for deacetylated α -tubulin.

Competing interests

The authors declare that they have no competing interests.

Authors' contributions

LM performed genetic screening and protein characterization. HW, XL, WL were involved in exome-sequencing and bio-informatic analysis, under the supervision of FM and JZ. VF and MM analyzed the morphology of mutant fibroblasts. IC supplied U251 cells and suggestions for transfection studies. LF and MS evaluated the MRI. PDA performed haplotypes analysis. AC, SR and MZ evaluated the patients and wrote the case report. DG monitored genetic/protein analyses, prioritized Pt2 variants, and drafted the paper. MZ supervised all the study, drafted and revised the paper. All authors read and approved the final manuscript. LM and MF share first authorship.

Acknowledgments

This work was supported by Fondazione Telethon grants GGP11011 and GPP10005; CARIPLO grant 2011/0526. The Cell lines and DNA bank of Paediatric Movement Disorders and Neurodegenerative Diseases, member of the Telethon Network of Genetic Biobanks (project no. GTB12001), funded by Telethon Italy, provided us with specimens.

References

1. Johnson AB, Brenner M: Alexander's disease: clinical, pathologic, and genetic features. *J Child Neurol* 2003, 18:625–632.
2. Quinlan RA, Brenner M, Goldman JE, Messing A: GFAP and its role in Alexander disease. *Exp Cell Res* 2007, 313:2077–2087.
3. Li R, Johnson AB, Salomons GS, van der Knaap MS, Rodriguez D, Boespflug-Tanguy O, Gorospe JR, Goldman JE, Messing A, Brenner M: Propensity for paternal inheritance of de novo mutations in Alexander disease. *Hum Genet* 2006, 119(1–2):137–144.
4. Pareyson D, Fancellu R, Mariotti C, et al: Adult-onset Alexander disease: a series of eleven unrelated cases with review of the literature. *Brain* 2008, 131:2321–2331.
5. Laing NG: Genetics of neuromuscular disorders. *Crit Rev Clin Lab Sci* 2012, 49:33–48.
6. Pandey UB, Nie Z, Batlevi Y, et al: HDAC6 rescues neurodegeneration and provides an essential link between autophagy and the UPS. *Nature* 2007, 447:859–863.
7. Li G, Jiang H, Chang M, Xie H, Hu L: HDAC6 α -tubulin deacetylase: a potential therapeutic target in neurodegenerative diseases. *J Neurol Sci* 2011, 304:1–8.
8. Kurtzke JF: Neurologic impairment in multiple sclerosis and the disability status scale. *Acta Neurol Scand* 1970, 46:493–512.
9. Kurtzke JF: Rating neurologic impairment in multiple sclerosis: an expanded disability status scale (EDSS). *Neurology* 1983, 33:1444–1452.

10. Hillel AD, Miller RM, Yorkston K, McDonald E, Norris FH, Konikov N: Amyotrophic lateral sclerosis severity scale. *Neuroepidemiol* 1989, 8:142–150.
11. Lamperti C, Fang M, Invernizzi F, et al: A novel homozygous mutation in SUCLA2 gene identified by exome sequencing. *Mol Genet Metab* 2012, 7:403–408.
12. Tiranti V, Galimberti C, Nijtmans L, et al: Characterization of SURF-1 expression and Surf-1p function in normal and disease conditions. *Hum Mol Genet* 1999, 8:2533–2540.
13. Ghezzi D, Viscomi C, Ferlini A, et al: Paroxysmal non-kinesigenic dyskinesia is caused by mutations of the MR-1 mitochondrial targeting sequence. *Hum Mol Genet* 2009, 18:1058–1064.
14. Bachetti T, Caroli F, Bocca P, et al: Mild functional effects of a novel GFAP mutant allele identified in a familial case of adult-onset Alexander disease. *Eur J Hum Genet* 2008, 16:462–470.
15. Matucci A, Zanusso G, Gelati M, et al: Analysis of mammalian scrapie protein by novel monoclonal antibodies recognizing distinct prion protein glycoforms: an immunoblot and immunohistochemical study at the light and electron microscopic levels. *Brain Res Bull* 2005, 65:155–162.
16. Haggarty SJ, Koeller KM, Wong JC, Grozinger CM, Schreiber SL: Domain-selective small-molecule inhibitor of histone deacetylase 6 (HDAC6)-mediated tubulin deacetylation. *Proc Natl Acad Sci USA* 2003, 100:4389–4394.
17. Messing A, Brenner M, Feany MB, et al: Alexander disease. *J Neurosci* 2012, 32:5017–5023.

18. Boyd SE, Nair B, Ng SW, et al: Computational characterization of 3' splice variants in the GFAP isoform family. *PLoS One* 2012, 7:e33565.
19. Flint D, Li R, Webster LS, Naidu S, Kolodny E, Percy A, van der Knaap M, Powers JM, Mantovani JF, Ekstein J, Goldman JE, Messing A, Brenner M: Splice site, frameshift, and chimeric GFAP mutations in Alexander disease. *Hum Mutat* 2012, 33:1141–1148.
20. Kamphuis W, Mamber C, Moeton M, Kooijman L, Sluijs JA, Jansen AH, Verveer M, de Groot LR, Smith VD, Rangarajan S, Rodríguez JJ, Orre M, Hol EM: GFAP isoforms in adult mouse brain with a focus on neurogenic astrocytes and reactive astrogliosis in mouse models of Alzheimer disease. *PLoS One* 2012, 7:e42823.
21. Aerts S, Lambrechts D, Maity S, et al: Gene prioritization through genomic data fusion. *Nat Biotechnol* 2006, 24:537–544.
22. Hubbert C, Guardiola A, Shao R, et al: HDAC6 is a microtubule-associated deacetylase. *Nature* 2002, 417:455–458.
23. Perdiz Mackeh R, Poüs C, Baillet A: The ins and outs of tubulin acetylation: more than just a post-translational modification? *Cell Signal* 2011, 23:763–771.
24. Farina L, Pareyson D, Minati L, et al: Can MR imaging diagnose adult-onset Alexander disease? *Am J Neuroradiol* 2008, 29:1190–1196.
25. Lee JY, Yao TP: Quality control autophagy: a joint effort of ubiquitin, protein deacetylase and actin cytoskeleton. *Autophagy* 2010, 6:555–557.

26. D'Ydewalle C, Bogaert E, Van Den Bosch L: HDAC6 At the intersection of neuroprotection and neurodegeneration. *Traffic* 2012, 13:771–779.
27. Kim SH, Shanware NP, Bowler MJ, Tibbetts RS: Amyotrophic lateral sclerosis-associated proteins TDP-43 and FUS/TLS function in a common biochemical complex to co-regulate HDAC6 mRNA. *J Biol Chem* 2010, 285:34097–34105.
28. Fiesel FC, Voigt A, Weber SS, et al: Knockdown of transactive response DNA-binding protein (TDP-43) downregulates histone deacetylase 6. *EMBO J* 2010, 29:209–221.
29. Zhang Y, Kwon S, Yamaguchi T, Cubizolles F, Rousseaux S, Kneissel M, Cao C, Li N, Cheng HL, Chua K, Lombard D, Mizeracki A, Matthias G, Alt FW, Khochbin S, Matthias P: Mice lacking histone deacetylase 6 have hyperacetylated tubulin but are viable and develop normally. *Mol Cell Biol* 2008, 28:1688–1701.
30. Fukada M, Hanai A, Nakayama A, Suzuki T, Miyata N, Rodriguiz RM, Wetsel WC, Yao P, Kawaguchi Y: Loss of deacetylation activity of Hdac6 affects emotional behavior in mice. *PLoS One* 2012, 7:e30924.
31. Lee JY, Koga H, Kawaguchi Y, Tang W, Wong E, Gao YS, Pandey UB, Kaushik S, Tresse E, Lu J, Taylor JP, Cuervo AM, Yao TP: HDAC6 controls autophagosome maturation essential for ubiquitin-selective qualitycontrol autophagy. *EMBO J* 2010, 29:969–980.
32. Govindarajan N, Rao P, Burkhardt S, Sananbenesi F, Schlüter OM, Bradke F, Lu J, Fischer A: Reducing HDAC6 ameliorates

cognitive deficits in a mouse model for Alzheimer's disease. *EMBO Mol Med* 2013, 5:52–63.

CHAPTER 3

Mutations of the Mitochondrial-tRNA Modifier *MTO1* Cause Hypertrophic Cardiomyopathy and Lactic Acidosis

Daniele Ghezzi,^{1,7} Enrico Baruffini,^{2,7} Tobias B. Haack,^{3,4} Federica Invernizzi,¹ Laura Melchionda,¹ Cristina Dallabona,² Tim M. Strom,^{3,4} Rossella Parini,⁵ Alberto B. Burlina,⁶ Thomas Meitinger,^{3,4} Holger Prokisch,^{3,4} Ileana Ferrero,² and Massimo Zeviani¹

¹Unit of Molecular Neurogenetics, Fondazione IRCCS (Istituto di Ricovero e Cura a Carattere Scientifico) Istituto Neurologico “Carlo Besta,” 20126 Milan, Italy;

²Department of Genetics, Biology of Microorganisms, Anthropology, and Evolution, University of Parma, 43124 Parma, Italy;

³Institute of Human Genetics, Helmholtz Zentrum München, 85764 Neuherberg, Germany;

⁴Institute of Human Genetics, Technische Universität München, 80333 Munich, Germany;

⁵Rare Metabolic Diseases Unit, Pediatric Clinic, San Gerardo Hospital, University of Milano-Bicocca, 20090 Monza, Italy;

⁶Metabolic Diseases Unit, Department of Paediatrics, University of Padua School of Medicine, 35128 Padua, Italy

⁷These authors contributed equally to this work

The American Journal of Human Genetics 90, 1079–1087, June 8, 2012

Dysfunction of mitochondrial respiration is an increasingly recognized cause of isolated hypertrophic cardiomyopathy. To gain insight into the genetic origin of this condition, we used next-generation exome sequencing to identify mutations in *MTO1*, which encodes mitochondrial translation optimization 1. Two affected siblings carried a maternal c.1858dup (p.Arg620Lysfs*8) frameshift and a paternal c.1282G>A (p.Ala428Thr) missense mutation. A third unrelated individual was homozygous for the latter change. In both humans and yeast, MTO1 increases the accuracy and efficiency of mtDNA translation by catalyzing the 5-carboxymethylaminomethylation of the wobble uridine base in three mitochondrial tRNAs (mt-tRNAs). Accordingly, mutant muscle and fibroblasts showed variably combined reduction in mtDNA-dependent respiratory chain activities. Reduced respiration in mutant cells was corrected by expressing a wild-type *MTO1* cDNA. Conversely, defective respiration of a yeast *mto1Δ* strain failed to be corrected by an Mto1^{Pro622*} variant, equivalent to human MTO1^{Arg620Lysfs*8}, whereas incomplete correction was achieved by an Mto1^{Ala431Thr} variant, corresponding to human MTO1^{Ala428Thr}. The respiratory yeast phenotype was dramatically worsened in stress conditions and in the presence of a paromomycin-resistant (P^R) mitochondrial rRNA mutation. Lastly, in vivo mtDNA translation was impaired in the mutant yeast strains.

Infantile hypertrophic cardiomyopathy and lactic acidosis are key clinical features in an increasing number of mitochondrial disorders associated with severe dysfunction of oxidative phosphorylation (OXPHOS), the main energy supply pathway of cardiomyocytes. The advent of exome analysis by next-generation sequencing (NGS) technology has begun to elucidate the genetic defects underpinning this condition. Recently, exome-NGS allowed us to identify mutations in *ACAD9* (MIM 611103), which encodes mitochondrial flavin adenine dinucleotide (FAD)-dependent acyl-coenzyme-A dehydrogenase 9, in several children affected by early-onset, isolated hypertrophic cardiomyopathy (MIM 611126)¹. The role of *ACAD9* seems to be marginal for fatty-acid beta oxidation, but essential for the assembly of mitochondrial respiratory chain (MRC) complex I (CI).¹⁻³ Another recent example is mutations in *AGK* (MIM 610345), which encodes acylglycerol kinase, a mitochondrial enzyme involved in the biosynthesis of cardiolipin; these mutations are responsible for hypertrophic cardiomyopathy and congenital cataracts (Sengers syndrome [MIM 212350]).⁴ Cardiolipin is an essential component of the lipid milieu of the inner mitochondrial membrane that participates in the integrity and optimization of the activity of both the MRC complexes and the skeletal-muscle- and heart-specific solute carrier family 25 (adenine nucleotide translocator 1), *SLC25A4*. Likewise, rare, recessive mutations in *SLC25A4* (MIM 103220) also cause hypertrophic cardiomyopathy (MIM 192600), and yet another X-linked recessive condition, Barth syndrome, hallmarked by severe mitochondrial cardiomyopathy (MIM 302060), is caused by a

mutation in *TAZ* (MIM 300394), which encodes Tafazzin, an acyl-transferase, specific to cardiolipin, that optimizes its fatty-acid composition to the structural and functional needs of the MRC. Other children with severe, isolated cardiomyopathy and lactic acidosis harbor recessive mutations in *TMEM70* (MIM 612418), which encodes a bona fide assembly factor of MRC CV (ATP-synthase).⁵ Syndromic cardiomyopathy, in combination with encephalopathy, myopathy, or both, is also associated with a number of mutations of mtDNA or nuclear genes that affect MRC activities.⁶ Nevertheless, a substantial proportion of cases characterized by OXPHOS-related severe hypertrophic cardiomyopathy remains genetically undiagnosed. Through exome-NGS analysis of a selected cohort of affected individuals, we identified pathogenic mutations in *MTO1* (NC_000006.11), which encodes an enzyme involved in posttranscriptional modification of mitochondrial tRNAs (mt-tRNAs). Affected person 1 (Pt1) was the first child of nonconsanguineous, healthy parents from northern Italy. He was born at 29 weeks of gestational age, by caesarean section because of oligohydramnios and reduced fetal growth. His birth weight was 790 g, his length was 34.5 cm, and his head circumference was 25.5 cm. Immediately after birth he had an episode of metabolic failure with severe hypoglycemia (25 mg%), metabolic acidosis (pH 7.17, base excess [BE] -11.7 mEq/l), and high blood lactate (13 mM, normal values [nv] < 2.0). In the subsequent days, blood glucose levels were corrected by the infusion of dextrose, whereas plasma lactate remained high (10–15 mM), with mild hyperammonemia (195 mg%, nv < 80). Electroencephalogram

(EEG) and cerebral echography results were normal, as were those of a liver and spleen ultrasound examination. Interventricular septum hypertrophy was detected on the 15th day (6.4 mm, nv < 3). He died on the 19th day of sudden bradycardia unresponsive to resuscitation procedures. MRC activities in digitonin-permeabilized skin fibroblasts showed a reduction of CIII normalized to citrate synthase (CS) (CIII/CS = 60% of the controls' mean) and of CIV/CS (56%), whereas the other activities were within the controls' range (Table 1). Sequence analysis of muscle mtDNA revealed a normal H1t haplogroup common in Europeans.

Table 1. Biochemical Analysis of OXPHOS Activities

Muscle	CS ^a	CI	SDH	CII	CIII	CIV	CV
Ct values	80–210	13–24	10.7–17,4	15–28	60–100	120–220	130–280
Pt2	73	5 (27)	16.8 (120)	28.7 (133)	95.3 (119)	46.5 (27)	351 (171)
Pt3 (3 mo)	209	2.2 (12)	13.1 (93)	nd ^b	nd ^b	51 (30)	nd
Pt3 (17 yr)	147	1.3 (7)	13.6 (97)	26.3 (122)	75 (94)	59 (35)	144 (70)
Fibroblasts	CS ^a	CI	SDH	CII	CIII	CIV	CV
Ct values	100–200	10.7–26	6.5–14,3	8.6–18,4	70–120	70–125	65–113
Pt1	160	12.5 (68)	14.3 (137)	24.6 (182)	57 (60)	55 (56)	93 (104)
Pt2	101	10.1 (55)	11 (105)	30.3 (224)	92 (97)	111 (114)	126 (141)
Pt1 + riboflavin	142	11.6 (63)	nd	nd	53 (56)	62 (64)	nd
Pt2 + riboflavin	82	6.5 (35)	nd	nd	71 (75)	76 (78)	nd

nd, not determined; + riboflavin, fibroblasts cultured for 1 week with Dulbecco's modified Eagle's medium (DMEM) supplemented with 5.3 μM riboflavin. Parentheses indicate percentages relative to the mean control (Ct) value. Values below the control range are reported in bold. All enzymatic activities are normalized for CS activity. Two muscle biopsies were analyzed in Pt3; the first taken at 3 months of age (3 mo) and the second at 17 years of age (17 yr).
^aCitrate synthase (CS) activity, expressed as nmol min⁻¹ mg⁻¹.
^bIn Pt3 muscle, the ratio CII+CIII (succinate cytochrome c reductase)/CS was 16.6 (105% of the Ct value; normal range 12.2–19.4).

Affected person 2 (Pt2), our index case, was the younger sister of Pt1. She also was born at 36 weeks of gestational age by caesarean section because of oligohydramnios and reduced fetal growth. Her birth weight was 1,380 g, her length was 42 cm, and her head circumference was 30 cm. At birth, she was mildly hypotonic and had severe metabolic acidosis (pH 7.21, BE -13 mEq/l), with high blood lactate (17.9 mM). She was immediately started on biotin (10 mg per

day), Coenzyme Q10 (14 mg per day), thiamine (150 mg per day), and dichloroacetate (DCA; 30 mg per day). Plasma lactate stabilized to values between 6 and 10 mM. EEG and brain ultrasound results were normal. On the seventh day, she became tachycardic. Heart ultrasound findings were normal until the 38th day, when septum hypertrophy (7 mm, nv 3.5) and leftventricular-wall hypertrophy (6 mm, nv 4) were found. She died on the 40th day of sudden bradycardia unresponsive to resuscitation procedures. An autopsy showed the presence of cardiomegaly, pleural effusion, and ascites. Biochemical assays, performed on the 800x g supernatant from the homogenate of a muscle biopsy, showed a reduction of the ratios of CI/CS and CIV/CS. MRC activities in digitonin-permeabilized fibroblasts showed only the reduction of CI/CS (Table 1). Sequence analysis of muscle mtDNA revealed a normal H1t haplogroup, and Sanger sequence analysis of *ACAD9*, *TMEM70*, *NDUFS2* (MIM 602985), and *NDUFV2* (MIM 600532) showed no mutation.

Affected person 3 (Pt3), a boy, was born at term to reportedly nonconsanguineous, healthy parents originating from a small village in the alpine region of northeastern Italy. His initial clinical history has been reported elsewhere.⁷ At the age of 1 month, he developed hyperpnea, difficulty feeding, weakness, and a lack of ocular fixation. His liver was 5 cm below the costal margin; he had severe metabolic acidosis, with high blood lactate (5.5 mM, nv < 2.0). An electrocardiogram (ECG) showed signs of ischemia, and a cardiac ultrasound examination revealed marked hypertrophic cardiomyopathy, particularly affecting the posterior wall of the left

ventricle (8.5 mm, nv 4), reduced left-ventricular function, and mild pericardial effusion. Biochemical assays on the 800x g supernatant of the homogenate from a muscle biopsy taken at 3 months of age revealed severe reduction of CI/CS (12% of the controls' mean) and CIV/CS (30%) ratios, whereas succinate dehydrogenase (SDH)/CS and CII+III/CS ratios as well as CS (Table 1) and pyruvate dehydrogenase activities were normal. DCA treatment resulted in marked improvement of both metabolic acidosis and cardiomyopathy. After 9 months of DCA therapy, a cardiac ultrasound examination showed a normal-sized heart, with normal left-ventricular-wall thickness (5 mm) and function (ejection fraction 76%, systolic fraction 43%) and low blood lactate values, ranging from 1.6 to 3.1 mM. During his first years of life, Pt3 had no severe episode of metabolic acidosis, even if plasma lactate remained moderately high, ranging from 2.5 to 4 mM. His growth rate has been normal, with good neurological development and a normal brain anatomy, according to magnetic resonance imaging. He was put on a permanent treatment of DCA (200 mg per day), carnitine (1 g per day), and CoQ₁₀ (100 mg per day). Because of the possible side effects of DCA, he was monitored regularly through the evaluation of visual and brainstem auditory evoked potentials as well as electromyography and nerve conduction velocities. At the age of 7 years, ultrasound examination showed a normal systolic ejection fraction in spite of a slight dilation of the left-ventricular chamber. At 12 years, DCA was stopped because of normalization of plasma lactate. A second muscle biopsy, taken at 17 years, again showed severe reduction of CI/CS (7% of the

controls' mean) and CIV/CS (35%), whereas the other MRC activities were normal (Table 1). Sequence analysis of mtDNA showed a normal H2 haplogroup. He is now 19 years old with a normal scholastic performance. A recent ultrasound examination revealed the presence of hypertrophic cardiomyopathy with an ejection fraction of 60%. An ECG showed sinus bradycardia (45 beats per min) but a Holter ECG was otherwise normal. A neurological examination was normal, except for a reduction of skills in the execution of fine movements, more evident in the left hand. Ophthalmoscopic examination showed moderate bilateral optic atrophy. Visual-evoked potential showed an increased P100 latency, more marked in the left eye. Electromyography and nerve-conduction velocity were normal.

Informed consent for participation in this study was obtained from the parents of all individuals involved, in agreement with the Declaration of Helsinki and approved by the ethics committees of the Fondazione IRCCS (Istituto di Ricovero e Cura a Carattere Scientifico) Istituto Neurologico (Milan, Italy).

We first carried out exome-NGS in the index case. The DNA extracted from fibroblasts was processed with the SureSelect Human All Exon 50 Mb kit (Agilent) and subsequently sequenced as 76 base-pair (bp) paired-end runs to an average coverage of 120x, corresponding to 9–12 Gb of sequence data. Read alignment was performed with the use of the Burrows-Wheeler Aligner (version 0.5.8) applied to the human genome assembly hg19. Single-nucleotide variants and small insertions and deletions were detected with SAMtools (version 0.1.7). Given that mitochondrial disorders are rare

conditions, we excluded variants with a frequency > 0.2% in “in house” control exomes and public databases. Assuming an autosomal-recessive mode of inheritance, we searched for homozygous or compound-heterozygous variants, which were filtered against (1) variants known to be associated with MRC defects and (2) novel homozygous or compound-heterozygous variants affecting genes that encode mitochondrial proteins listed in MitoP2 (score > 0.5). This filtering procedure (Table S1 available online) revealed that our index case was compoundheterozygous for mutations in *MTO1*: a maternal c.1858dup (p.Arg620Lysfs*8) and a paternal c.1282G>A (p.Ala428Thr) (Figure 1A). The same mutations were also found in her affected brother.

The frameshift mutation is predicted to introduce a stop codon after an aberrant sequence of seven amino acids (aa) (Figure S1), causing the loss of the C-terminal 73 aa residues ($\approx 10\%$ of the protein size); the missense mutation affects an amino-acid residue, Ala428, which is invariant in all available animal, plant, and yeast species, including *Saccharomyces cerevisiae* (Figures S2A and S2B). In addition, the Ala428Thr change scored very highly for likelihood to be deleterious according to ad-hoc softwares for pathogenicity prediction (deleterious for Polyphen2: $p = 0.999$; Panther: 0.88041; MutPred: 0.903). The exome variant server (EVS) of the NHLBI GO Exome Sequencing Project reports a frequency of 0.028% (2/7,020) in the American population of European origin for the c.1282G>A change, whereas the c.1858dup change was not present in the database. We also excluded the missense mutation from our exome database, which

contains 973 genomes from Europeans (=1,946 alleles), and from a database of 300 alleles from consecutive control DNA samples from subjects originating from northern Italy.

To evaluate a possible influence of the two mutations on the stability of the transcript, we extracted mRNA from mutant fibroblasts of affected individuals 1 and 2 and retrotranscribed it into cDNA. Quantitative real-time PCR showed that the content of mutant MTO1 transcripts was similar to that of wild-type (WT) control samples (Figure 1B), and sequence analysis revealed the presence of comparable amounts of either mutant transcript (data not shown), indicating no RNA decay.

Next, we analyzed MTO1 on isolated mitochondria and on total cell lysates obtained from both mutant and control immortalized fibroblasts, using a polyclonal MTO1 antibody (Proteintech). MTO1 is predicted by bioinformatic tools (MitoProt, TargetP) to be imported inside mitochondria after the cleavage of a 25-aa-long mitochondrial targeting sequence. We synthesized the polypeptides corresponding to the precursor, the mature WT, and the mature p.Arg620Lysfs*8 truncated MTO1 species (TNT Transcription-Translation System kit, Promega). After performing SDS-polyacrylamide electrophoresis and electroblotting, we immunovisualized a band reacting with an MTO1 antibody in mitochondria (Figure 1C) and in fibroblast lysates (Figure S3). This band, which comigrates with a band corresponding to the 74 kDa fulllength, mature in-vitro-synthesized MTO1 polypeptide (NM_012123, NP_036255), was markedly increased in *MTO1*-overexpressing fibroblasts (Figure S3).

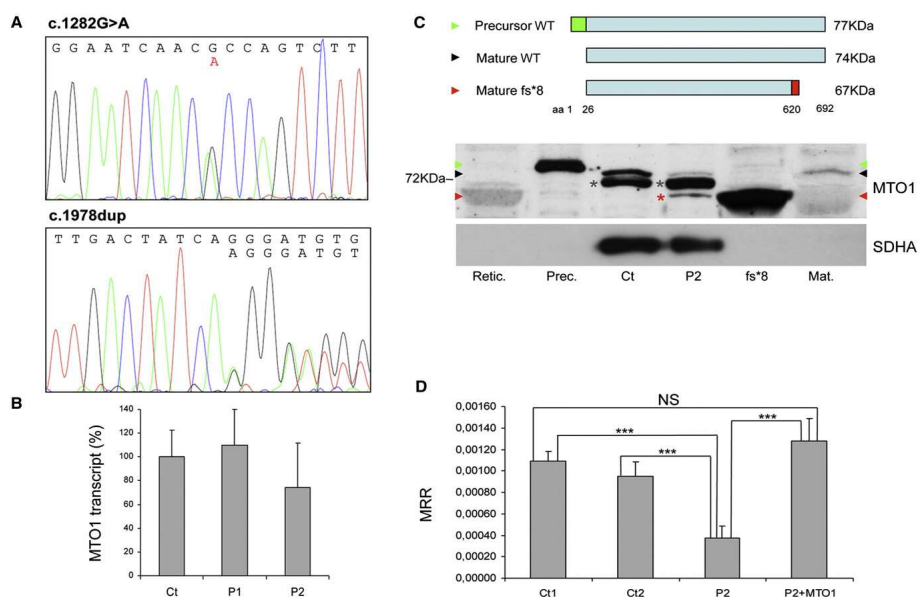


Figure 1. *MTO1* Mutations

(A) Electropherograms of *MTO1* of Pt2 showing the c.1282G>A (left) and c.1858dup (right), both in heterozygosis.

(B) Real-time PCR on retrotranscribed cDNA from fibroblasts of individuals 1 (P1) and 2 (P2). The amount of *MTO1* transcript (normalized to GAPDH levels) is comparable in mutant versus WT control samples (Ct), indicating no mRNA decay. Data are represented as mean \pm SD.

(C) Western-blot analysis of *MTO1*. Top: schematic representation of the precursor WT *MTO1* (isoform a), its mature species after cleavage of a predicted 25 aa mitochondrial targeting sequence in the N terminus, and the mature p.Arg620Lysfs*8 mutant species. Bottom: Western-blot analysis on isolated mitochondria. Retic.: reticulocyte lysate used for in-vitro protein synthesis; Prec.: in-vitro translated 77 kDa *MTO1* precursor protein (green arrowhead); Ct: isolated mitochondria from control fibroblasts; P2: isolated mitochondria from individual 2 fibroblasts; fs*8: in-vitro-translated 67 kDa mature protein carrying the truncating p.Arg620Lysfs*8 variant (red arrowhead); Mat.: in-vitro-translated 74 kDa WT mature *MTO1* (black arrowhead). A faint crossreacting band is visualized in mt P2 sample (red asterisk), corresponding to the mature p.Arg620Lysfs*8 truncated protein. An unspecific signal is present in mt samples (gray asterisks). The position of the 72 kDa molecular weight marker protein is also indicated. SDHA was used as loading control.

(D) MRR measured in immortalized fibroblasts from Pt 2, in naive condition (P2) or overexpressing *MTO1* (P2+MTO1), and in control subjects (Ct1, Ct2). MRR values are expressed as pMolesO₂/min/cells. Data are represented as mean \pm 5 SD. Two-tail, unpaired Student's t test was applied for statistical significance. ***: $p < 0.001$.

In mutant mitochondria, the amount of the 74 kDa protein was clearly reduced, whereas an additional band was detected, with the same electrophoretic mobility of the in-vitrosynthesized mature p.Arg620Lysfs*8 *MTO1* species, predicted to have a molecular weight of ≈ 67 kDa. This result suggests that the p.Arg620Lysfs*8 truncated *MTO1* is relatively stable (Figure 1C).

In order to prove the causative role of the *MTO1* variants found in the affected siblings of family 1, we first tested whether the expression of WT *MTO1* cDNA could rescue the biochemical phenotype of mutant cells. Given that the MRC defects in Pt1 and Pt2 fibroblasts were relatively mild and variable, we immortalized the Pt2 fibroblasts using pBABE-puro SV40 and evaluated the oxygen consumption through microscale oxygraphy (Seahorse Bioscience XF-96). This assay, which depends upon and reflects the cumulative proficiency of the whole set of MRC complexes, is more sensitive than individual assays of each complex.⁸ We demonstrated a clear reduction of the maximal respiration rate (MRR) in immortalized Pt2 cells compared to immortalized control fibroblasts, which returned to normal after transduction with a *MTO1*^{WT}-expressing lentivirus (pLenti6 Gateway Vector kit, Invitrogen) (Figures 1E and S3). This result indicates a pathogenic role of the *MTO1* variants found in Pt2 mutant cells.

Second, we sequenced the exons and exon-intron boundaries of *MTO1* in DNA samples from 17 individuals with early-onset hypertrophic cardiomyopathy, lactic acidosis, and defective MRC activities. We found a single individual, Pt3, homozygous for the c.1282G>A

(p.Ala428Thr) mutation, identical to that found in the paternal allele of family 1.

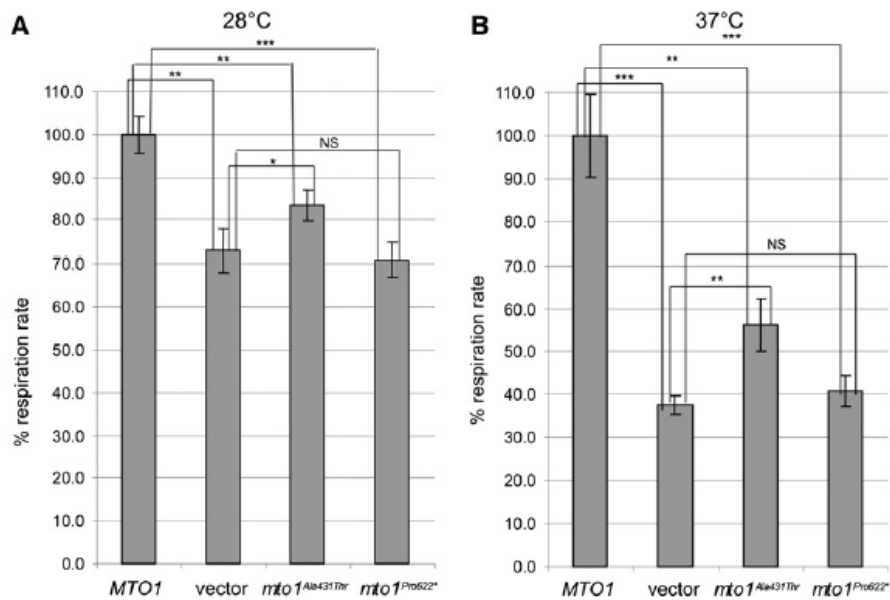


Figure 2. Respiratory Phenotypes of Yeast Mutant Strains

(A and B) Respiratory activity of yeast *mto1Δ* strains transformed with *MTO1*^{WT} recombinant vector, (empty) vector, and *mto1*^{Ala431Thr} and *mto1*^{Pro622*} recombinant vectors at 28°C (A) and 37°C (B). Respiratory rates were normalized to the WT strain, for which the respiratory rate was 38.2 nmol min⁻¹ mg⁻¹ at 28°C and 28.9 nmol min⁻¹ mg⁻¹ at 37°C. Values are the mean of at least three independent experiments. Two-tail, unpaired t test was applied for statistical significance. *: p < 0.05; **: p < 0.01; ***: p < 0.001. Data are represented as mean ± SD.

In both yeast and humans, *MTO1* encodes the enzyme that catalyzes the 5-carboxymethylaminomethylation (mnm5s2U34) of the wobble uridine base in mt-tRNA^{Gln}, mt-tRNA^{Glu}, and mt-tRNA^{Lys}.⁹ This modification is usually coupled to the 2-thiolation of the same uridine moiety, a reaction catalyzed by 2-thiouridylase, encoded by *MTO2*

(*TRMU* in humans [MIM 610230]); both these posttranscriptional modifications increase accuracy and efficiency of mtDNA translation.¹⁰ In order to further test the pathogenic role of the *MTO1* mutations, we used the yeast *Saccharomyces cerevisiae*. We first showed that the absence of *MTO1* (*mto1Δ*) was associated with decreased respiration rate in yeast incubated at 28°C (Figure 2A). Second, we demonstrated that this phenotype failed to be corrected by expression of a recombinant yeast *MTO1* cDNA encoding protein variant Pro622*, corresponding to the human Arg620Lysfs*8 change (Figure S2, Table S2). This result suggests that, although present in human mitochondria, the Arg620Lysfs*8 *MTO1* variant is functionally inactive. The respiratory phenotype of the *mto1Δ* strain was only partially corrected by expression of a yeast recombinant *MTO1* encoding protein variant Ala431Thr, corresponding to the human Ala428Thr change (Figure S2, Table S2), whereas the expression of yeast *MTO1*^{WT} led to full recovery (Figure 2A). These results were qualitatively unchanged, but dramatically amplified, in experiments carried out under temperature-induced stress conditions; i.e., at 37°C (Figure 2B). However, neither the growth of *mto1Δ* nor that of *mto1*^{Pro622*} or *mto1*^{Ala431Thr} strains on oxidative carbon sources was significantly impaired. The OXPHOS-negative growth phenotype of *mto1* mutants is in fact contingent on the presence of a C>G transversion at nucleotide 1477 of the 15S rRNA in mtDNA.¹¹ The mutation disrupts the C₁₄₇₇-G₁₅₈₃ base pairing in a functionally relevant hairpin structure, which is part of the decoding site (site A) of the ribosome, where the codon-anticodon recognition occurs.¹² This

mutation confers resistance to the antibiotic paromomycin (Figure 3) by destabilizing the hairpin and results in a synthetic phenotype with *MTO1* disruption,¹¹ most likely due to impaired interaction between unprocessed *MTO1*-dependent mt-tRNAs with ribosomal site A.¹³

The normal human mitochondrial 12S rRNA contains a hairpin structure that corresponds to the paromomycin-resistant (P^R) variant in yeast, because C₁₄₉₄ and A₁₅₅₅, which are equivalent to yeast C₁₄₇₇ and G₁₅₈₃, cannot form a pair. Incidentally, the well-known pathogenic m.1555A>G mutation of human mtDNA as well as the m.1494C>T can establish a C₁₄₉₄-G₁₅₅₅ pairing or the equivalent U₁₄₉₄-A₁₅₅₅ pairing, respectively, both of which increase the length of the hairpin structure, thus letting paromomycin (and other aminoglycosides) bind to site A (Figure 3).¹⁴ As a consequence, the m.1555A>G and m.1494C>T both confer aminoglycoside susceptibility to human mtDNA, being associated with a specific phenotype, aminoglycoside-induced nonsyndromic deafness (MIM 580000).^{15,16}

Given that human WT 12S RNA site A is structurally similar to the yeast P^R variant of the 15S RNA site A (Figure 3), we extended our complementation analysis to a m.1477C>G mutant P^R yeast strain.

We showed that, in contrast to the *mtol1Δ* paromomycin-sensitive (P^S) strain, the *mtol1Δ* P^R strain was unable to grow on oxidative carbon sources such as glycerol (Figure 4A). The oxidative growth remained abolished with the expression of a cDNA encoding Mto1^{Pro622*}, clearly reduced with the expression of a cDNA encoding Mto1^{Ala431Thr}, and fully restored with the expression of a cDNA encoding MTO1^{WT} (Figure 4A).

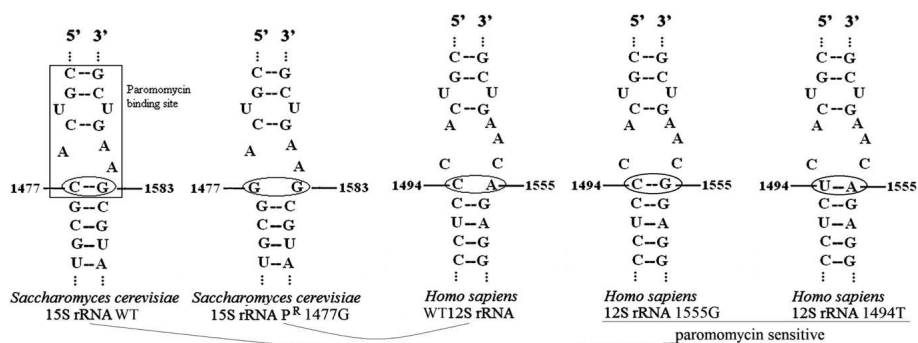


Figure 3. A-Site Structures of Yeast 15S and Human 12S rRNAs

Secondary structure of site A of the WT yeast strain 15S rRNA, of the P^R yeast strain 15S rRNA, of the WT human 12S rRNA, and of the mutant human 12S rRNA—the last two carrying either the 1555G or the 1494T mtDNA mutation, both associated with P^S. The pairing of 1477–1583 nucleotides in WT yeast rRNA corresponds to that of 1494–1555 nucleotides in mutant human rRNA and confers aminoglycoside susceptibility.

Likewise, the respiration rate, which was nearly abolished in the *mtol1* P^R strain, was not corrected by transformation with the Mto1^{Pro622*}-encoding cDNA and only partially corrected by the Mto1^{Ala431Thr}-encoding cDNA, in contrast to the full recovery obtained by expressing a MTO1^{WT} cDNA (Figure 4B). We observed no difference between MTO1^{WT} and *mtol1* mutant strains in the frequency of ‘petite’ colonies; i.e., respiration-defective clones caused by large deletions or loss of mtDNA (data not shown), which indicates that mutations in *MTO1* did not affect mtDNA stability.

Analysis in yeast clearly shows that while both mutations are detrimental for respiratory activity, the deleterious effects of the Pro622* protein variant is more severe than the Ala431Thr replacement.

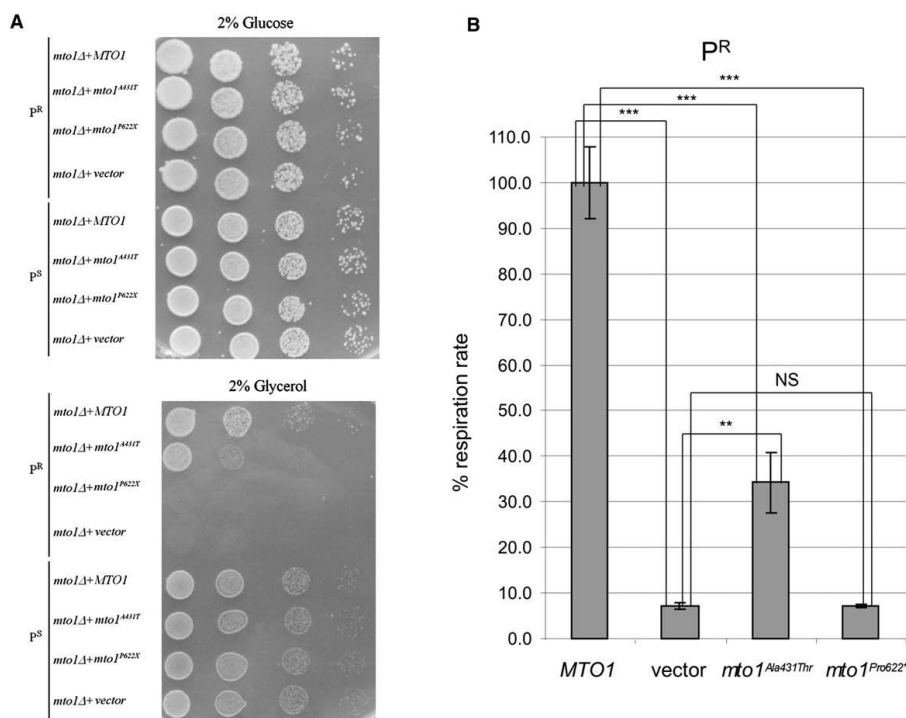


Figure 4. PR and PS Yeast Phenotypes

(A) Spot assay of *mtolΔ* P^R and P^S strains, transformed with *MTO1*^{WT} recombinant vector, (empty) vector, and *mto1*^{Ala431Thr} and *mto1*^{Pro622*} recombinant vectors. The assay was performed by spotting decreasing concentrations of yeast cells (10⁵, 10⁴, 10³, and 10²) on a medium supplemented with either 2% glucose (upper panel) or 2% glycerol (lower panel). See text for details.

(B) Respiratory activity of yeast *MTO1*^{WT} and mutant P^R strains at 28°C. Respiratory rates were normalized to the WT strain, for which the respiratory rate was 26.6 nmol min⁻¹ mg⁻¹. Values are the mean of at least four independent experiments. Two-tail, unpaired t test was applied for statistical significance. *: p < 0.05; **: p < 0.01; ***: p < 0.001. Data are represented as mean ± SD.

These results are concordant with the clinical phenotype associated with the equivalent mutations in humans: the third affected individual, homozygous for the *MTO1* mutation encoding the Ala428Thr protein variant, equivalent to the yeast Ala431Thr, is now 19 years old, and in

relatively well compensated condition, whereas individuals 1 and 2, who were compound heterozygous for the *MTO1* mutations encoding the Ala428Thr and Arg620Lysfs*8 mutations, the latter being equivalent to the yeast Pro622*, died a few days after birth of intractable congestive heart failure and severe lactic acidosis.

MTO1 encodes a FAD-containing enzyme involved in posttranscriptional modification of specific mt-tRNAs, thus contributing to the optimization of mtDNA-dependent protein synthesis. However, similar to a recent report on the effects on in-vivo mtDNA translation of *TRMU* (*MTO2*) mutations,¹⁷ we failed to show consistent alterations of mtDNA-dependent protein synthesis in Pt2 mutant fibroblasts assayed in standard conditions¹⁸ (Figure S4). Hence, we evaluated the effect on mtDNA translation of the expression of cDNAs encoding the Mto1^{Pro622*} and Mto1^{Ala431Thr} variants, versus MTO1^{WT}, in the highly sensitive *mto1Δ* P^R yeast model.¹⁹ Interestingly, the mtDNA protein synthesis in the *mto1Δ* strain expressing a cDNA encoding Mto1^{Pro622*} was markedly reduced, particularly for cytochrome *c* oxidase (Cox) subunits 1 and 2 and for cytochrome *b*, similar to, albeit lesser than, the null *mto1Δ* strain. The mtDNA translation pattern in the *mto1Δ* strain expressing a cDNA encoding Mto1^{Ala431Thr} was similar to that of the *MTO1*^{WT} strain, although some bands, such as those corresponding to the Var1 and adenosine triphosphatase (ATPase) 6 polypeptides, were slightly reduced in the mutant versus WT strains (Figure 5).

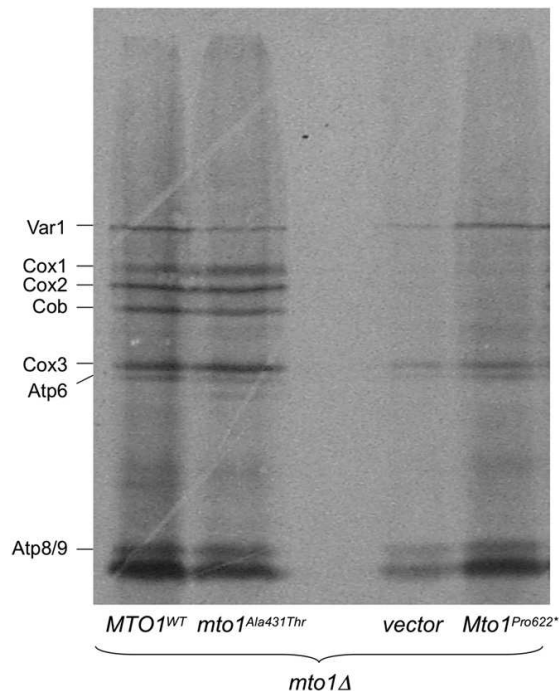


Figure 5. In-Vivo Mitochondrial Translation of P^R *mto1Δ* Strain Transformed with WT or Mutant *MTO1* Alleles

Mitochondrial gene products were labeled with [³⁵S] methionine in whole cells at 30°C in the presence of cycloheximide for 7 min.¹⁹ Equivalent amounts of total cellular proteins were separated by SDS-PAGE on a 17.5% polyacrylamide gel, transferred to a nitrocellulose membrane, and exposed to X-ray film. The *mto1Δ* strain transformed with the empty vector (vector) contained 40% of petite cells, thus reducing the overall signal. Cox: cytochrome c oxidase; Cob: cytochrome b; Atp: ATP synthase; Var1: small mitochondrial ribosome subunit. In the *mto1*^{Pro622*} strain, several bands, particularly Cox1, Cox2, and Cob, are virtually missing, and the overall pattern is similar to that of the (empty) vector. In the *mto1*^{Ala431Thr}, the intensity of some bands, including Var1 and Atp6, is slightly reduced compared to the *MTO1*^{WT} strain, but the two patterns are similar, suggesting mild impairment.

As expected, these results confirm that the effects of the Mto1^{Pro622*} truncating mutation are more deleterious on mtDNA translation than those of the Mto1^{Ala431Thr} missense mutation, in agreement with the results of the respiratory and oxidative-growth phenotypes in yeast

and of the greater severity of the clinical phenotype in individuals 1 and 2 versus that of individual 3.

The function of *MTO1* could explain the variability of the biochemical defects, ranging from isolated CI deficiency, as in Pt2 fibroblasts, to combined CI-CIV deficiency in Pt2 and Pt3 skeletal muscle, or to combined CIII-CIV deficiency in Pt1 fibroblasts. Among the 13 mtDNA-encoded proteins, seven are subunits of CI, three of CIV, two of CV, and one of CIII. This gene distribution can explain why mtDNA translation defects such as those associated with mutations of *MTO1* can predominantly impair the activity of CI, but also that of CIII and CIV. The two mtDNA-encoded subunits of CV are part of the F0 component of this complex, the function of which is not directly measured by the standard CV assay that is based on ATP-hydrolysis, a function carried out by the F1 component of CV. This could explain, at least in part, why CV activity was essentially normal in *MTO1* mutant samples.

The presence of a FAD moiety in *MTO1* opens the possibility that, as observed for other mitochondrial flavo-enzymes,^{1,3,20} riboflavin supplementation may be beneficial for correction, at least in part, of the biochemical defect and improvement of the clinical course. However, we observed neither correction of MRC biochemical activities (Table 1) nor improvement of oxygen consumption (data not shown) by growing Pt1 and Pt2 mutant fibroblasts in 5.3 mM riboflavin for 1 week. Likewise, addition of different amounts of riboflavin (0.53, 2.6, 5.3, 13.3, and 26.6 mM) to a glycerol medium had no effect on either growth or respiration of *mtol* mutant yeast

strains (data not shown). These results indicate that riboflavin supplementation is ineffective, possibly because the truncating mutation is too drastic and the missense mutation does not affect the N-terminal, FAD-binding domain of the protein.²¹

An additional source of complexity stems from the existence of transcript variants encoding at least three different MTO1 isoforms. Although isoform a is prevalent, being in fact the only one that we could detect in fibroblasts, the presence of isoforms b (NM_133645, NP_598400) and c (NM_001123226, NP_001116698) is also predicted, each retaining a different extra-exon resulting in protein sequences longer than those of isoform a.²² The existence and functional significance of these longer variants are presently unknown. Notably, both mutations found in this study affect the protein sequence common to all three isoforms, predicting overall impairment of the MTO1 function.

MTO1 and MTO2 (TRMU) take part in the same pathway involved in posttranscriptional modification of specific mt-tRNAs.¹⁰ Interestingly, specific TRMU mutations cause severe and sometimes fatal liver failure (MIM 613070),²³ and other mutations in the same gene have been associated with reversible mitochondrial myopathy.²⁴ Here we report mutations of *MTO1* associated with impairment of yet another target organ, the heart, the severity of which seems to depend on the potential deleteriousness of the mutations. The mechanisms underlying such diverse tissue and organ specificity in the same enzyme or in the same enzymatic pathway is a challenge for future work in this rapidly expanding field of mitochondrial medicine.

Supplemental Data

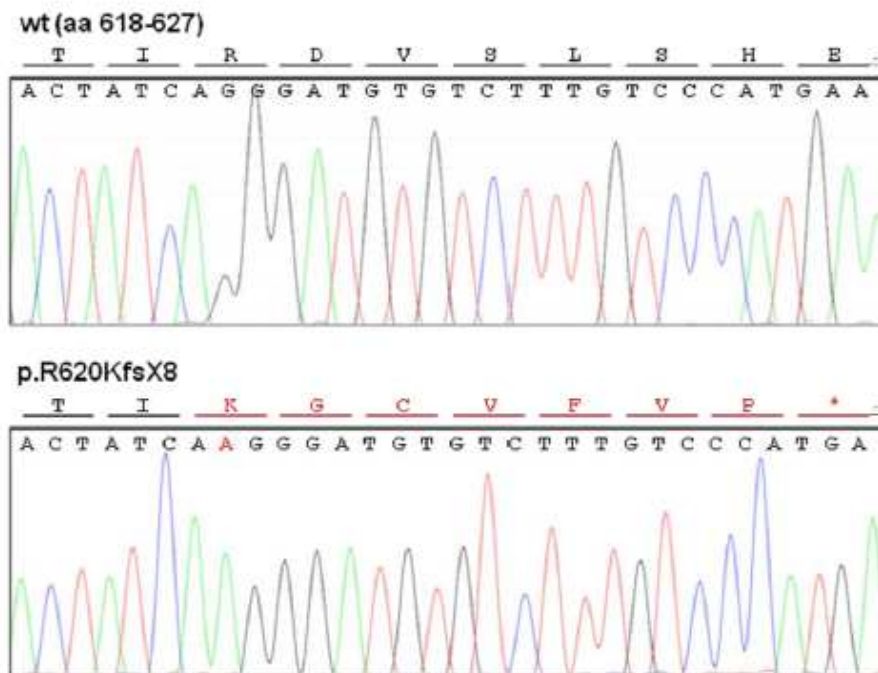


Figure S1. Sequence Analysis of c.1858dup

Electropherograms of the *MTO1* region around the c.1858dup mutation. The *MTO1* cDNA obtained by retro-transcription of RNA from fibroblasts of patient 2 was subcloned into pCR2.1 vector (Invitrogen) in order to separate the two alleles: the lower panel shows the allele carrying the c.1858dup, p.Arg620Lysfs*8 mutation; the upper panel shows a wt sequence belonging to the allele carrying the c.1282G>A, p.Ala431Thr, mutation.

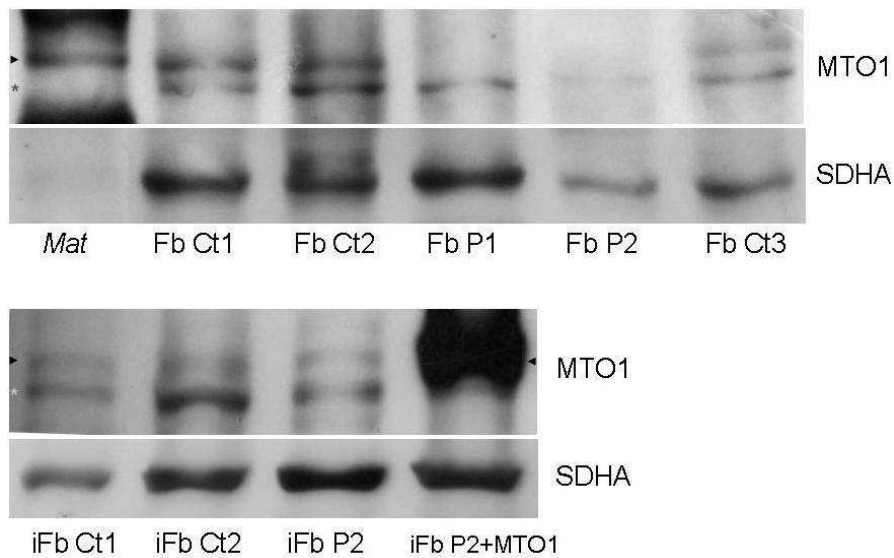


Figure S3. Western-Blot Analysis of MTO1 in Fibroblast Lysates

Top panel. Primary fibroblasts

Samples obtained from persons 1 and 2 (P1, P2) and controls (Ct1, Ct2, Ct3) fibroblasts (Fb) were loaded on 10% SDS-PAGE gel, blotted and immunovisualized with an anti-MTO1 antibody. A black arrow indicates the band corresponding to the *in vitro* synthesized mature MTO1 protein (*Mat*). An unspecific signal is present in fibroblasts (grey asterisks). SDHA was used as loading control.

Bottom panel. Immortalized fibroblasts and *MTO1* transduction

Immortalized fibroblast (iFb) lysates of person 2 (P2) and controls (Ct1, Ct2). “iFb P2+MTO1” corresponds to cellular lysate obtained from immortalized P2 fibroblasts, overexpressing wild-type MTO1. A black arrow indicates the band corresponding to mature MTO1. An unspecific signal is present in fibroblasts (grey asterisks). SDHA was used as loading control.

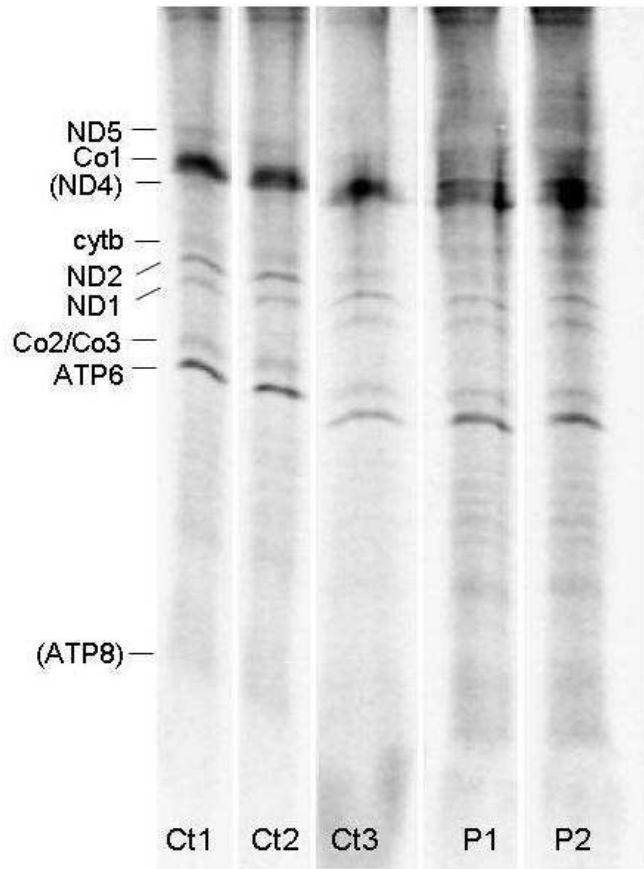


Figure S4. Mitochondrial Protein Synthesis in Fibroblasts

The assay was performed in fibroblasts from three controls (Ct1-Ct3) and persons P1 and P2. The mitochondrial translation products on the SDS-polyacrylamide gel are indicated according to ref. 7.

Table S1. Variants Identified in Individual 2 by Exome Sequencing

Individual ID	#55554
Synonymous variants	11140
NSV	10196
NSV with frequency <0.2% in “in-house” + public databases	331
≥ 2 NSV / gene	14
known disease allele	0
known MRC subunits and assembly factors	0
mitochondrial localization	1 (<i>MTO1</i>)

NSV = missense, nonsense, stop-loss, splice-site disruption, insertions, deletions; mitochondrial localization refers to proteins with a Mitop2 score > 0.5.

Table S2. Primers Used for Yeast Studies*

Name	Sequence	PCR products and notes
MTO1CFw	ggggggtcgacgcttactgccactattagtcacg	Primers amplifying the entire <i>yMTO1</i> gene, encompassing both promoter and termination regions
MTO1CRv	ggggggagctccgacagtgagttgcccttttgc	
MTO1A431TFw	ggatcattgcaggtatcaataaccggattactatcgcgccaagaacg	Primers specific for the amplification of the A431T <i>yMTO1</i> mutant variant
MTO1A431TRv	cgttcttggcgcgatagtaatccggtattgatacctgcaatgatcc	
MTO1P622*Fw	gattacgattaccgctcagttatgatagctttccactgaatgcaaac	Primers specific for the amplification of the P622* <i>yMTO1</i> mutant variant
MTO1P622*Rv	gtttgcattcagtggaagctatcataactgacggtaategtaate	

* The yeast strains used in this study are BY4741 *mto1* (*MATa his3Δ0 leu2Δ0 met15Δ0 ura3Δ0 mto1::Kan^R*) (Euroscarf collection) and W303 P^R*mto1* (*MAT trp1-1 mto1::URA3*). *MTO1* PCR-products were cloned in centromeric plasmids pFL38 or pFL39. Mutagenesis of *MTO1* was performed using the overlap extension technique (Ho et al., 1989) by using external primers MTO1CFw and MTO1CRv and internal mutagenic primers. *mto1* strains were transformed with plasmids harboring wt or mutant *MTO1* alleles by lithium acetate methods (Gietz and Woods, 2002).

Acknowledgments

We thank Alexander Tzagoloff for the generous gift of the P^R yeast strain. We are grateful to Erika Fernandez-Vizarra for help with the in vivo translation assay, to Alessia Nasca for the screening of the Italian DNA control samples, and to Ilaria D'Amato for technical support with microscale oxygraphy. This work was supported by the Pierfranco and Luisa Mariani Foundation of Italy; Fondazione Telethon grants GGP11011 and GPP10005; CARIPLO grant

2011/0526; the Italian Association of Mitochondrial Disease Patients and Families (Mitocon); the Helmholtz Alliance for Mental Health in an Ageing Society (HA-215) and the German Federal Ministry of Education and Research (BMBF)-funded Systems Biology of Metabotypes grant (SysMBo 0315494A); the German Network for Mitochondrial Disorders (mitoNET 01GM0867 and 01GM0862); and E-Rare grant GenoMit JTC2011.

Received: January 26, 2012

Revised: March 6, 2012

Accepted: April 12, 2012

Published online: May 17, 2012

Web Resources

The URLs for data presented herein are as follows:

Exome Variant Server (EVS), <http://evs.gs.washington.edu/EVS>

MitoP2, <http://www.mitop.de>

MitoProt, <http://ihg2.helmholtz-muenchen.de/ihg/mitoprot.html>

MutPred, <http://mutpred.mutdb.org>

Online Mendelian Inheritance in Man (OMIM), <http://www.omim.org>

Panther, <http://www.pantherdb.org>

Polyphen2, <http://genetics.bwh.harvard.edu/pph2>

TargetP, <http://www.cbs.dtu.dk/services/TargetP>

References

1. Haack, T.B., Danhauser, K., Haberberger, B., Hoser, J., Strecker, V., Boehm, D., Uziel, G., Lamantea, E., Invernizzi, F., Poulton, J., et al. (2010). Exome sequencing identifies ACAD9 mutations as a cause of complex I deficiency. *Nat. Genet.* 42, 1131–1134.
2. Nouws, J., Nijtmans, L., Houten, S.M., van den Brand, M., Huynen, M., Venselaar, H., Hoefs, S., Gloerich, J., Kronick, J., Hutchin, T., et al. (2010). Acyl-CoA dehydrogenase 9 is required for the biogenesis of oxidative phosphorylation complex I. *Cell Metab.* 12, 283–294.
3. Gerards, M., van den Bosch, B.J., Danhauser, K., Serre, V., van Weeghel, M., Wanders, R.J., Nicolaes, G.A., Sluiter, W., Schoonderwoerd, K., Scholte, H.R., et al. (2011). Riboflavinresponsive oxidative phosphorylation complex I deficiency caused by defective ACAD9: new function for an old gene. *Brain* 134, 210–219.
4. Mayr, J.A., Haack, T.B., Graf, E., Zimmermann, F.A., Wieland, T., Haberberger, B., Superti-Furga, A., Kirschner, J., Steinmann, B., Baumgartner, M.R., et al. (2012). Lack of the mitochondrial protein acylglycerol kinase causes Sengers syndrome. *Am. J. Hum. Genet.* 90, 314–320.
5. Cízková, A., Stránecký, V., Mayr, J.A., Tesarová, M., Havlícková, V., Paul, J., Ivánek, R., Kuss, A.W., Hansíková, H., Kaplanová, V., et al. (2008). TMEM70 mutations cause isolated ATP synthase deficiency and neonatal mitochondrial ncephalocardiomyopathy. *Nat. Genet.* 40, 1288–1290.

6. Uziel, G., Ghezzi, D., and Zeviani, M. (2011). Infantile mitochondrial encephalopathy. *Semin. Fetal Neonatal Med.* 16, 205–215.
7. Burlina, A.B., Milanese, O., Biban, P., Bordugo, A., Garavaglia, B., Zacchello, F., and DiMauro, S. (1993). Beneficial effect of sodium dichloroacetate in muscle cytochrome C oxidase deficiency. *Eur. J. Pediatr.* 152, 537.
8. Invernizzi, F., D’Amato, I., Jensen, P.B., Ravaglia, S., Zeviani, M., and Tiranti, V. (2012). Microscale oxygraphy reveals OXPHOS impairment in MRC mutant cells. *Mitochondrion* 12, 328–335.
9. Wang, X., Yan, Q., and Guan, M.X. (2010). Combination of the loss of cmnm5U34 with the lack of s2U34 modifications of tRNA^{Lys}, tRNA^{Glu}, and tRNA^{Gln} altered mitochondrial biogenesis and respiration. *J. Mol. Biol.* 395, 1038–1048.
10. Umeda, N., Suzuki, T., Yukawa, M., Ohya, Y., Shindo, H., Watanabe, K., and Suzuki, T. (2005). Mitochondria-specific RNA-modifying enzymes responsible for the biosynthesis of the wobble base in mitochondrial tRNAs. Implications for the molecular pathogenesis of human mitochondrial diseases. *J. Biol. Chem.* 280, 1613–1624.
11. Colby, G., Wu, M., and Tzagoloff, A. (1998). *MTO1* codes for a mitochondrial protein required for respiration in paromomycin-resistant mutants of *Saccharomyces cerevisiae*. *J. Biol. Chem.* 273, 27945–27952.
12. Yan, Q., Li, X., Faye, G., and Guan, M.X. (2005). Mutations in *MTO2* related to tRNA modification impair mitochondrial gene

expression and protein synthesis in the presence of a paromomycin resistance mutation in mitochondrial 15 S rRNA. *J. Biol. Chem.* 280, 29151–29157.

13. Wang, X., Yan, Q., and Guan, M.X. (2009). Mutation in MTO1 involved in tRNA modification impairs mitochondrial RNA metabolism in the yeast *Saccharomyces cerevisiae*. *Mitochondrion* 9, 180–185.

14. Qian, Y., and Guan, M.X. (2009). Interaction of aminoglycosides with human mitochondrial 12S rRNA carrying the deafness-associated mutation. *Antimicrob. Agents Chemother.* 53,4612–4618.

15. Prezant, T.R., Agopian, J.V., Bohlman, M.C., Bu, X., Oztas, S., Qiu, W.Q., Arnos, K.S., Cortopassi, G.A., Jaber, L., Rotter, J.I., et al. (1993). Mitochondrial ribosomal RNA mutation associated with both antibiotic-induced and non-syndromic deafness. *Nat. Genet.* 4, 289–294.

16. Zhao, H., Li, R., Wang, Q., Yan, Q., Deng, J.H., Han, D., Bai, Y., Young, W.Y., and Guan, M.X. (2004). Maternally inherited aminoglycoside-induced and nonsyndromic deafness is associated with the novel C1494T mutation in the mitochondrial 12S rRNA gene in a large Chinese family. *Am. J. Hum. Genet.* 74, 139–152.

17. Sasarman, F., Antonicka, H., Horvath, R., and Shoubridge, E.A. (2011). The 2-thiouridylase function of the human MTU1 (TRMU) enzyme is dispensable for mitochondrial translation. *Hum. Mol. Genet.* 20, 4634–4643.

18. Fernández-Silva, P., Acín-Pérez, R., Fernández-Vizarra, E., Pérez-Martos, A., and Enriquez, J.A. (2007). In vivo and in organelle

analyses of mitochondrial translation. *Methods Cell Biol.* 80, 571–588.

19. Barrientos, A., Korr, D., and Tzagoloff, A. (2002). Shy1p is necessary for full expression of mitochondrial COX1 in the yeast model of Leigh's syndrome. *EMBO J.* 21, 43–52.

20. Ghezzi, D., Sevrioukova, I., Invernizzi, F., Lamperti, C., Mora, M., D'Adamo, P., Novara, F., Zuffardi, O., Uziel, G., and Zeviani, M. (2010). Severe X-linked mitochondrial encephalomyopathy associated with a mutation in apoptosis-inducing factor. *Am. J. Hum. Genet.* 86, 639–649.

21. Shi, R., Villarroya, M., Ruiz-Partida, R., Li, Y., Proteau, A., Prado, S., Moukadiri, I., Benítez-Páez, A., Lomas, R., Wagner, J., et al. (2009). Structure-function analysis of *Escherichia coli* MnmG (GidA), a highly conserved tRNA-modifying enzyme. *J. Bacteriol.* 191, 7614–7619.

22. Li, X., Li, R., Lin, X., and Guan, M.X. (2002). Isolation and characterization of the putative nuclear modifier gene MTO1 involved in the pathogenesis of deafness-associated mitochondrial 12 S rRNA A1555G mutation. *J. Biol. Chem.* 277, 27256–27264.

23. Zeharia, A., Shaag, A., Pappo, O., Mager-Heckel, A.M., Saada, A., Beinat, M., Karicheva, O., Mandel, H., Ofek, N., Segel, R., et al. (2009). Acute infantile liver failure due to mutations in the TRMU gene. *Am. J. Hum. Genet.* 85, 401–407.

24. Uusimaa, J., Jungbluth, H., Fratter, C., Crisponi, G., Feng, L., Zeviani, M., Hughes, I., Treacy, E.P., Birks, J., Brown, G.K., et al. (2011). Reversible infantile respiratory chain deficiency is a unique,

genetically heterogenous mitochondrial disease. *J. Med. Genet.* 48, 660–668.

Supplemental References

Gietz RD, Woods RA. (2002) Transformation of yeast by lithium acetate/single-stranded carrier DNA/polyethylene glycol method. *Methods Enzymol*; 350:87-96.

Ho SN, Hunt HD, Horton RM, Pullen JK, Pease LR (1989) Site-directed mutagenesis by overlap extension using the polymerase chain reaction. *Gene*; 77:51-9.

CHAPTER 4

***MTO1* Mutations are Associated with Hypertrophic Cardiomyopathy and Lactic Acidosis and Cause Respiratory Chain Deficiency in Humans and Yeast**

Enrico Baruffini,^{1†} Cristina Dallabona,^{1†} Federica Invernizzi,² John W. Yarham,³ Laura Melchionda,² Emma L. Blakely,³ Eleonora Lamantea,² Claudia Donnini,¹ Saikat Santra,⁴ Suresh Vijayaraghavan,⁴ Helen P. Roper,⁵ Alberto Burlina,⁶ Robert Kopajtich,^{7,8} Anett Walther,^{7,8} Tim M. Strom,^{7,8} Tobias B. Haack,^{7,8} Holger Prokisch,^{7,8} Robert W. Taylor,³ Ileana Ferrero,¹ Massimo Zeviani,⁹ and Daniele Ghezzi²

¹Department of Life Sciences, University of Parma, Parma, Italy; ²Unit of Molecular Neurogenetics, Fondazione IRCCS (Istituto di Ricovero e Cura a Carattere Scientifico) Istituto Neurologico “CarloBesta”, Milan, Italy; ³Wellcome Trust Centre for Mitochondrial Research, Institute for Ageing and Health, Newcastle University, Newcastle upon Tyne, UK; ⁴Department of Clinical Inherited Metabolic Disorders, Birmingham Children’s Hospital NHS Foundation Trust, Birmingham, UK; ⁵Department of Child Health, Heart of England NHS Foundation Trust, Birmingham, UK; ⁶Division of Inborn Errors of Metabolism, Department of Paediatrics, University Hospital, Padua, Italy; ⁷Institute of Human Genetics, Helmholtz Zentrum München, Neuherberg, Germany; ⁸Institute of Human Genetics, Technische Universität München, Munich, Germany; ⁹MRC Mitochondrial Biology Unit, Cambridge, UK; †These authors contributed equally to this work.

HUMAN MUTATION, Vol. 34, No. 11, 1501–1509, 2013

Abstract

We report three families presenting with hypertrophic cardiomyopathy, lactic acidosis, and multiple defects of mitochondrial respiratory chain (MRC) activities. By direct sequencing of the candidate gene *MTO1*, encoding the mitochondrial-tRNA modifier 1, or whole exome sequencing analysis, we identified novel missense mutations. All *MTO1* mutations were predicted to be deleterious on MTO1 function. Their pathogenic role was experimentally validated in a recombinant yeast model, by assessing oxidative growth, respiratory activity, mitochondrial protein synthesis, and complex IV activity. In one case, we also demonstrated that expression of wt *MTO1* could rescue the respiratory defect in mutant fibroblasts. The severity of the yeast respiratory phenotypes partly correlated with the different clinical presentations observed in *MTO1* mutant patients, although the clinical outcome was highly variable in patients with the same mutation and seemed also to depend on timely start of pharmacological treatment, centered on the control of lactic acidosis by dichloroacetate. Our results indicate that *MTO1* mutations are commonly associated with a presentation of hypertrophic cardiomyopathy, lactic acidosis, and MRC deficiency, and that ad hoc recombinant yeast models represent a useful system to test the pathogenic potential of uncommon variants, and provide insight into their effects on the expression of a biochemical phenotype.

KEYWORDS: MTO1; hypertrophic cardiomyopathy; lactic acidosis; mitochondrial disorder; yeast

Introduction

Mitochondrial disorders are a group of syndromes associated with severe dysfunction of oxidative phosphorylation (OXPHOS), the main energy bioreactor of cells. Cardiomyocytes, with their extremely high request of energy, are one of the major targets of OXPHOS impairment, and infantile hypertrophic cardiomyopathy is a key clinical feature in many mitochondrial disorders. We have recently reported the first patients affected by hypertrophic cardiomyopathy and lactic acidosis carrying mutations in *MTO1* (MIM #614702) [Ghezzi et al., 2012]. Two were siblings, compound heterozygous for c.1858dup (p.Arg620Lysfs*8) and c.1282G>A (p.Ala428Thr) mutations, who died in their first days of life due to sudden bradycardia. Muscle and fibroblasts showed decreased activities of mitochondrial respiratory chain (MRC) complex I (CI) and CIV. The third patient, homozygous for the c.1282G>A (p.Ala428Thr) mutation, had also early-onset cardiac hypertrophy with severe lactic acidosis, and defective CI + CIV activities in muscle; however, he dramatically improved on a permanent treatment with dichloroacetate (DCA) and cofactors, being now 20 years old with compensated, stable hypertrophic cardiomyopathy.

MTO1 (MIM #614667), a gene conserved in all eukaryotes, encodes one of the two subunits of the enzyme that catalyzes the 5-carboxymethylaminomethylation (mnm5s2U34) of the wobble uridine base in the mitochondrial tRNAs specific to Gln, Glu, Lys, Leu(UUR), and possibly Trp [Suzuki et al., 2011; Wang et al., 2010]. The other subunit is encoded by *MSS1* in yeast and *GTPBP3* in

humans (MIM #608536). For mt-tRNAs for Gln, Glu, Lys, this modification is usually coupled to the 2-thiolation of the same uridine moiety, a reaction catalyzed by 2-thiouridylase, encoded by yeast *MTO2* or human *TRMU* (MIM #610230). Both these posttranscriptional modifications increase accuracy and efficiency of mitochondrial DNA (mtDNA) translation by influencing tRNA structure, binding to the ribosome, stabilization of the correct codon-anticodon pairing [Kurata et al., 2008; Murphy et al., 2004; Takai, 2005; Umeda et al., 2005; Urbonavicius et al., 2001; Wang et al., 2010; Yarian et al., 2000; Yasukawa et al., 2001], and tRNA recognition by the cognate aminoacyltransferase [Krüger and Sørensen, 1998; Sylvers et al., 1993].

In our previous work, we investigated the functional consequences of the *MTO1* mutations in a simple eukaryotic model system, *Saccharomyces cerevisiae* [Ghezzi et al., 2012]. The analysis was performed mainly in a mutant yeast strain harboring a C>G transversion at nucleotide 1,477 of the 15S rRNA mtDNA gene [Colby et al., 1998], which results in a synthetic phenotype with *MTO1* disruption. The mutation disrupts the C1477–G1583 base pairing in a functionally relevant hairpin structure, which is part of the decoding site (site A) of the ribosome, where codon–anticodon recognition takes place [Yan et al., 2005]. This mutation confers resistance to the antibiotic paromomycin by destabilizing the hairpin. We chose this strain because the human mitochondrial 12S rRNA contains a hairpin structure that corresponds to the paromomycin-resistant variant in yeast. We showed that the yeast Ala431Thr

change, corresponding to human Ala428Thr, reduced mitochondrial respiratory activity, whereas the mutation equivalent to human Arg620Lysfs*8 behaved as a null allele.

We present here the identification of five additional *MTO1* mutant subjects (two couples of siblings, and a sporadic case) who also present with hypertrophic cardiomyopathy and lactic acidosis, thus, strengthening a consistent genotype/phenotype correlation. We confirm the pathogenic role of the two novel mutations in the yeast model and, for the milder variant, by complementation studies in mutant fibroblasts.

Materials and Methods

Patients

Informed consent for participation in this study was obtained from the parents of all patients, in agreement with the Declaration of Helsinki and approved by the Ethical Committees of the Institutes participating in this study, where biological samples were obtained.

We studied a first cohort of 30 patients with cardiomyopathy and a biochemical defect of the MRC, affecting either CI alone or multiple complexes, and a second small group of four cases with isolated CIV deficiency and at least one affected sibling, irrespective of their clinical presentations (ranging from cardiomyopathy to encephalopathy). Table 1 summarizes the main clinical, laboratory and biochemical features of five patients from three families (Fig. 1A) with *MTO1* mutations. All these subjects showed early-onset, progressive hypertrophic cardiomyopathy, and lactic acidosis.

Table 1. Clinical Synopsis and Biochemical Features of MT01 patients

Patient	Familiarity	Gender	Age of onset	Relevant clinical features	Actual age/ Outcome	Cause of death	Metabolic findings	Biochemical MRC defects	Mutations in MTD1
#1	No	F	2 days	Psychomotor delay, hypotonia, dystonia. Late, hypertrophic cardiomyopathy. Poor feeding due to swallowing difficulties.	14 yrs	-	Lactic acidemia, hyperalaninemia.	Me ↓ CI and CIV Pbc ↓ MRR	p.[Ala428Thr]; [Arg477His]
#2	Brother of #3; consanguineous parents	M	Birth	Failure to thrive. Later, hypertrophic cardiomyopathy. Aspiration pneumonia. Hypotonia. Poor feeding due to swallowing difficulties. Failure to thrive. Early-onset hypertrophic cardiomyopathy.	+12 mo	Cardio-respiratory arrest.	Hypoglycaemia, lactic acidemia	Me ↓ CI and CIV Pbc ↓ MRR	p.[Thr411Ile]; [Thr411Ile]
#3	Brother of #2; consanguineous parents	M	Birth	Hypotonia. Early-onset hypertrophic cardiomyopathy. Bronchitic-like illness.	+3 mo	n.d.	Lactic acidemia	n.d.	p.[Thr411Ile]; [Thr411Ile]
#4	Sister of #5; consanguineous parents	F	3 mo	Encephalopathy and seizures. Upper respiratory illness. Hypertrophic cardiomyopathy and WPW. Psychomotor delay.	19 yrs	-	Lactic acidemia	Me ↓ CIV	p.[Thr411Ile]; [Thr411Ile]
#5	Sister of #4; consanguineous parents	F	5 mo	Hypertrophic cardiomyopathy with WPW.	12 yrs	-	Lactic acidemia, hyperalaninemia, ketonuria	Me ↓ CIV	p.[Thr411Ile]; [Thr411Ile]
#6	Brother of #7	M	Birth	Hypertrophic cardiomyopathy.	+19 days	Sudden bradycardia	Lactic acidemia, hyperalaninemia	Me ↓ CI and CIV Pbc ↓ CIII and CIV; ↓ MRR	p.[Ala428Thr]; [Arg620Lysfs*8]
#7	Sister of #6	F	Birth	Hypertrophic cardiomyopathy with tachycardia. Hypotonia.	+40 days	Sudden bradycardia	Lactic acidemia	Me ↓ CI and CIV Pbc ↓ CI; ↓ MRR	p.[Ala428Thr]; [Arg620Lysfs*8]
#8	No	M	1 mo	Weakness, lack of ocular fixation. Hypertrophic cardiomyopathy with sinus bradycardia. Moderate bilateral optic atrophy.	20 yrs	-	Lactic acidemia	Me ↓ CI and CIV	p.[Ala428Thr]; [Ala428Thr]

Me, muscle biopsy; Pbc, fibroblasts; MRC, mitochondrial respiratory chain; CI-CIV, complexes I-IV; WPW, Wolff-Parkinson-White syndrome.

Some did also display neurological features affecting the peripheral or the central nervous system, or both, associated with neuropathological abnormalities documented by MRI (Fig. 1B and C). Detailed case reports are described in the Supporting Information.

Molecular Analysis

Genomic DNA was extracted by standard methods. Exons and exon–intron boundaries of human *MTO1* (NM 012123.3; NP 036255) were amplified using primers listed in Supp. Table S1, and analyzed by Sanger sequencing. Whole-exome next-generation sequencing (WES) and variant filtering were performed as described [Ghezzi et al., 2012]. Nucleotide numbering reflects cDNA numbering with +1 corresponding to the A of the ATG translation initiation codon in the reference sequence, according to journal guidelines (www.hgvs.org/mutnomen). The initiation codon is codon 1. All variants reported have been submitted to LSDB (<http://www.lovd.nl/MTO1>).

Biochemical Assays

The activities of MRC complexes and citrate synthase in muscle homogenates were measured as described [Bugiani et al., 2004]. Microoxygraphy was used to measure maximal respiration rate (MRR), spare respiratory capacity (SRC), respiratory control ratio, and oxygen consumption rate (OCR)/extracellular acidification rate (ECAR) in fibroblasts, using SeaHorse FX-24 or FX-96 [Invernizzi et

al., 2012]. For transduced cells, F14medium (Euroclone), supplemented with EGF, FGF, insulin, and uridine, was used instead of DMEM.

In Silico Analysis

The pathogenicity of the human mutations was predicted by using five bioinformatic tools based on heuristic methods: PANTHER (<http://www.pantherdb.org>), SIFT (<http://sift.jcvi.org>), PolyPhen-2 (<http://genetics.bwh.harvard.edu/pph2>), SNPs&GO (<http://snps-and-go.biocomp.unibo.it/snps-and-go>), and MutPred (<http://mutpred.mutdb.org>). Structural analysis was performed using the structure of *Chlorobium tepidum* GidA (PDB ID 3CP8 at <http://www.rcsb.org/pdb/home/home.do>). Models of mutant proteins were constructed using SwissModel (<http://swissmodel.expasy.org/>) and superimposed with Swiss-Pdb Viewer Magic fit tool. Protein regions were visualized by the RasMol software package.

Analysis in Yeast

We used the yeast strain W303 P^R *mtol* (*MATa trp1-1 mtol::URA3*) [Colby et al., 1998]. *MTO1* was cloned in the centromeric vector pFL39 [Bonneaud et al., 1991] through PCR amplification of *MTO1* and digestion with *SalI* and *SacI*. The *mtol* mutant alleles were obtained by site-directed mutagenesis of a *MTO1* fragment [Ho et al., 1989], using suitable primers (Supp. Table S1). Mutant fragments were cloned in the *AvaI* and *SacI* cloning sites of pFL39-*MTO1*. The *mtol* strain was transformed with pFL39 harboring wt or

mutant *MTO1* alleles by lithium-acetate based methods [Gietz and Woods, 2002]. Respiratory activity and in vitro mt-DNA protein synthesis were performed as previously described [Barrientos et al., 2002; Goffrini et al., 2009]. Cytochrome *c* oxidase activity was measured according to Fontanesi et al., (2008) and Barrientos et al., (2009) on a mitochondrial-enriched fraction prepared according to Soto et al., (2009).

Lentiviral Transduction

The wt *MTO1* cDNA was cloned into the pLenti6.3/V5-TOPO Vector (Invitrogen, Carlsbad, CA, USA), and virions were obtained as previously described [Zhang et al., 2009]. Mutant and wt fibroblasts were infected with viral supernatant and selected upon exposure to 2 µg/ml Blasticidin (Invitrogen).

Results

Molecular and Biochemical Analyses in Human Samples

By Sanger sequencing we screened *MTO1* in a cohort of mitochondrial defective patients with cardiomyopathy, and found that Pt1 was compound heterozygous for the previously described c.1402G>A/p.Ala428Thr mutation and for a novel missense substitution (c.1430G>A/p.Arg477His), whereas siblings Pt2 and Pt3 harbored a homozygous c.1232C>T/p.Thr411Ile change (Fig. 1A). By WES analysis on a second group of familial cases with CIV

deficiency (see *Materials and Methods*) and no known genetic defect, we identified an additional case, Pt4, with the same homozygous c.1232C>T/p.Thr411Ile change. Her clinically affected sister (Pt5) was shown to harbor the identical homozygous variant (Fig. 1A).

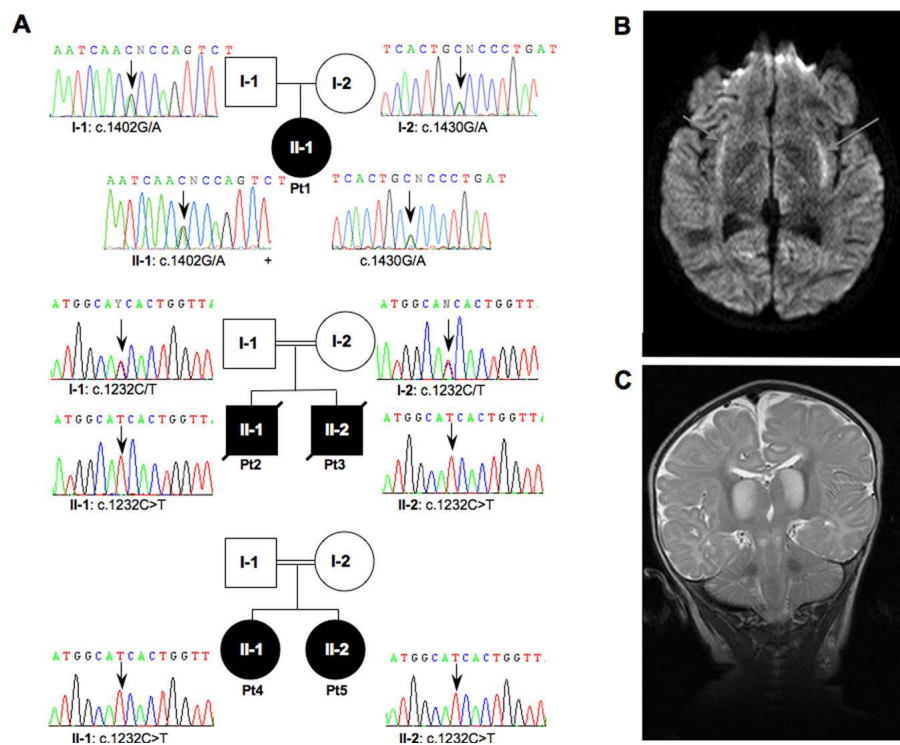


Figure 1. Pedigrees and radiological features. **A:** Pedigrees and electropherograms of the *MTO1* genomic region encompassing the nucleotide substitutions in patients and available parents. Black symbols designate affected subjects. **B:** Brain MRI of Pt1. Transverse FLAIR image showing abnormal hyperintensity in the region of the claustrum and surrounding capsulae (arrows). **C:** Brain MRI of Pt2. Coronal T2-weighted sequence showing abnormal hyperintense signals of the thalami and diffusely abnormal signal in the subcortical white matter. Lesions are also present in the brainstem. The cerebellar folia are normal.

Spectrophotometric biochemical assays of the respiratory chain complexes activities revealed defects in CI, CIV, or both (Table 1). No clear evidence of CIII deficiency was obtained in any tissue sample of the present study, in contrast with a previous study [Ghezzi et al., 2012; #6 in Table 1]. A partial but significant reduction in MRR, SRC, and OCR/ECAR was measured by SeaHorse microscale oxygraphy in fibroblast cell lines of Pt1 and Pt2 (Supp. Table S2).

In Silico Analysis

To test the potential deleterious effects of the p.Thr411Ile and p.Arg477His, we first used bioinformatic tools based on heuristic methods for predicting pathogenic variants. The prediction of a putative pathogenic change is based on evolutionary conservation, plus other features, such as predicted structural effects (Polyphen-2, MutPred), predicted functions (MutPred), and local sequence and gene ontology score (SNPs&GO). Both mutations scored a “probably pathological” prediction by each method (Supp. Table S3).

We further tested the pathogenicity of these mutations on the basis of the structure of GidA, the eubacterial ortholog of Mto1. Its structure has been resolved in *Escherichia coli*, *C. tepidum*, and *Aquifex aeolicus* [Meyer et al., 2008; Osawa et al., 2009; Shi et al., 2009]. GidA contains four domains: an α/β FAD-binding domain; a small N-terminal insertion-domain 1; a large α/β insertion-domain 2, which binds NADH; a large α C-terminal domain, which contributes to the binding of the tRNA and promotes the dimerization with MnmE, the ortholog of Mss1/Gtpbp3.

Human threonine 411 (hThr411) is part of motif 2, which is highly conserved from bacteria to eukaryotes (Fig. 2A) and is contained in the α/β FAD-binding domain. Motif 2 includes residues from the C-terminus of sheet $\beta 21$, the loop between $\beta 21$ and the residues from the N-terminal of helix $\alpha 9$. In *C. tepidum* GidA, this motif includes three conserved residues: Gln366 (hGln407, yeast Gln410), Gly372 (hGly413, yGly416), and Glu375 (hGlu416, yGlu 419), plus Ser371, which is either conserved or substituted conservatively by threonine (e.g., hThr412, yThr415). The residues are all involved in FAD binding through interaction with the FAD ribitol and pyrophosphate moieties (Gln366 and Gly372) or with the isoalloxazine ring-containing active site (Ser371 and Glu375) (Fig. 2B). Moreover, the side chain of serine 371 is oriented to the central ring of isoalloxazine, suggesting a functional role in the catalytic process and/or binding/stabilization of FAD [Meyer et al., 2008]. As a matter of fact, substitution of Thr382 in *A. aeolicus* GidA, corresponding to Ser371 in *C. tepidum* GidA, results in inability of complementing the methylaminomethylmodification at position 5 of uridine (mm⁵) during exponential growth of GidA-deficient *E. coli* [Osawa et al., 2009]. We hypothesized that the substitution of hydrophilic hThr411/yThr414 (corresponding to threonine at position 370 of GidA) with a hydrophobic, bulky isoleucine changes the position of the adjacent amino-acid residue (hThr412/yThr415 or bacterial Ser371). To support this hypothesis, we constructed a structural model in which the threonine at position 370 (yThr414) was changed to isoleucine. This change altered the orientation of the side chain of the

adjacent amino acid and increased the distance relative to the isoalloxazine ring (Fig. 2C).

We identified the hArg477 residue in humans as equivalent to *C. tepidum* Arg436, which is located in a highly conserved loop between helices $\alpha 10$ and $\alpha 11$ in the C-terminal domain (Fig. 2A). Arg436 takes part in a cluster of several basic amino acids (Lys, Arg, and His), conserved in bacteria and eukaryotes, and predicted to form a positively charged pocket, which binds the phosphates of the D-stem backbone of the incoming tRNA (Fig. 2D) [Meyer et al., 2008; Osawa et al., 2009]. The substitution of the equivalent arginine with alanine in GidA of *E. coli* is known to decrease the efficiency of mnm⁵ modification [Shi et al., 2009]. Therefore, we hypothesized that substitution of the fully charged human Arg477 with the partially charged His477 could also decrease the affinity for the incoming tRNA.

Analysis in Yeast

To confirm the pathogenic role of p.Thr411Ile and p.Arg477His mutations predicted by in silico analysis, we introduced the corresponding mutant alleles (*mtol*^{T414I} and *mtol*^{R481H}) in the paromomycin-resistant yeast strain disrupted in *MTO1* (Δ *mtol*^{P^R} strain). The parental Δ *mtol*^{P^R} strain is unable to grow on oxidative carbon sources (Fig. 3A) [Colby et al., 1998]; the expression of *mtol*^{T414I} mutant allele failed to correct this phenotype, whereas the expression of *mtol*^{R481H} was able to restore oxidative growth, although to a lesser extent than wt *MTO1* (Fig. 3A).

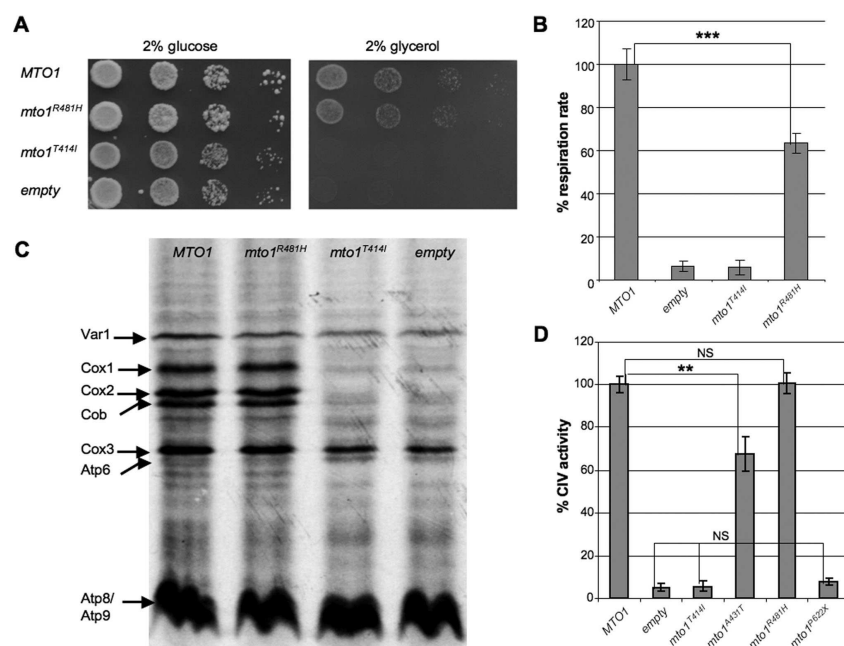


Figure 3. Yeast studies. **A:** Growth of $\Delta mto1$ strain transformed with *MTO1* wt allele, *mto1^{R481H}*, and *mto1^{T414I}* mutant alleles or empty plasmid on YP medium supplemented with 2% glucose (left panel) or 2% glycerol (left panel). Cells were pregrown on YP+glucose and plated after serial dilutions to obtain spots of 5×10^4 , 5×10^3 , 5×10^2 , and 5×10^1 cells/spot. Pictures were taken after 2 days of growth. **B:** Respiratory activity of $\Delta mto1$ strains transformed with *MTO1* wt allele, *mto1^{R481H}*, and *mto1^{T414I}* mutant alleles or empty plasmid. Respiratory rates were normalized to the strain transformed with wt *MTO1*, for which the respiratory rate was $34.7 \text{ nmol min}^{-1} \text{ mg}^{-1}$. Values are the mean of three independent experiments, each with an independent clone. Two-tail, paired *t*-test was applied for statistical significance. $***P < 0.001$. **C:** In vivo mitochondrial translation of $\Delta mto1$ strain transformed with *MTO1* wt allele, *mto1^{R481H}*, and *mto1^{T414I}* mutant alleles or empty plasmid. Mitochondrial gene products were labeled with [^{35}S]-methionine in whole cells in the presence of cycloheximide for 10 min at 28°C . Cox: cytochrome *c* oxidase; Cob: cytochrome *b*; Atp: ATP synthase; Var1: small mitochondrial ribosome subunit. **D:** Cytochrome *c* oxidase (CIV) activity of $\Delta mto1$ strain transformed with *MTO1* wt allele, *mto1^{T414I}*, *mto1^{A431T}*, *mto1^{R481H}*, and *mto1^{P622X}* mutant alleles or empty plasmid. Cytochrome *c* oxidase activities were normalized to the strain transformed with wt *MTO1*, for which the activity was 368.8 units per mg of mitochondrial proteins. Values are the mean of three independent experiments, each with an independent clone. Two-tail, unpaired *t*-test was applied for statistical significance. $**P < 0.01$.

Accordingly, mitochondrial respiration was abolished in both $\Delta mto1$ and $mto1^{T414I}$ strains, whereas it was restored by the $mto1^{R481H}$ strain to approximately 60% of the wt strain (Fig. 3B).

Since the p.Thr414Ile mutation is predicted to alter the position of the adjacent Ser371, which participates in the catalytic process involving FAD and/or in its binding/stabilization, we carried out a second set of experiments in the presence of increasing concentration of riboflavin (from 1 to 25 μM); however, neither defective oxidative growth nor reduced respiratory activity of the $mto1^{T414I}$ strain were rescued by riboflavin, suggesting that the catalytic activity of the mutant Mto1^{T414I} is fully impaired (data not show). An alternative explanation is that the mutant Mto1^{T414I} is unstable and quickly degraded; the absence of an antibody against the yeast Mto1 prevented us from evaluating the levels of Mto1 in different mutant strains.

To analyze the molecular consequences of the p.Thr414Ile and p.Arg481His MTO1 mutations, we performed in vivo mitochondrial protein synthesis (Fig. 3C). As previously observed, we detected radiolabeled bands in the $\Delta mto1$ strain corresponding to ribosomal protein Var1, cytochrome *c* oxidase subunit 3 (Cox3), and Atp subunits (Atp6, Atp8, Atp9), whose levels were similar to those of the *MTO1* strain. However, cytochrome *c* oxidase subunits 1 and 2 (Cox1 and Cox2) and cytochrome *b* (Cob) were absent. The $mto1^{T414I}$ strain behaved like the $\Delta mto1$ strain, whereas $mto1^{R481H}$ was indistinguishable from wt *MTO1*, as previously observed for $mto1A431T$. Accordingly, CIV activity of $mto1^{T414I}$ and $mto1^{P622X}$ strains was indistinguishable from that of $\Delta mto1$ strain (4%–7%

relative to *MTO1* strain), it was 70% in *mtol*^{A431T} relative to the wt, and identical to the wt in *mtol*^{R481H} strains (Fig. 3D) (Supp. Table S4). In *mtol*^{T411H} mutant strain, we measured the CI–CIII activity (following the reduction of cytochrome *c* in presence of NADH as electron donor and KCN as inhibitor of cytochrome *c* oxidase), to identify a possible explanation for the respiratory phenotype but no reduction was observed (data not shown).

Complementation in Fibroblasts

To further confirm the pathogenic role of the milder mutation p.Arg477His, we analyzed the respiration in fibroblasts from Pt1, compound heterozygous for p.Arg477His and p.Ala428Thr, after transduction with a recombinant lentiviral construct expressing the wt *MTO1* cDNA. Infected cells were cultured in F14 medium, enriched in growth factors, to facilitate the recovery after infection and speed up cell growth. In our experience, these culturing conditions increase the values for SRC, an indicator of the bioenergetic reserve, in both control and mutant cells. Infected Pt1 fibroblasts showed marked increase of MRR (+146%) up to normal values. A mild MRR increase (+34%) was also observed in *MTO1*^{wt} cells (Supp. Fig. S1). These results support a causative role for both p.Arg477His and p.Ala428Thr *MTO1* variants in defective mitochondrial respiration of Pt1.

Discussion

A quite broad phenotypic spectrum was observed in *MTO1* mutant patients: from severe, rapidly progressive, ultimately fatal presentation in two compound heterozygous children for Arg620Lysfs*8 and Ala428Thr mutations [Ghezzi et al., 2012], to fulminant postnatal phenotype, or severe, but long-lasting, encephalo-cardiomyopathy in the two families with a homozygous p.Thr411Ile mutation (this work), to benign, compensated hypertrophic cardiomyopathy with modest neurological abnormalities in patients [Pt1 in this work; Pt3 in Ghezzi et al., 2012], bearing two missense mutations.

In silico analysis suggested potential pathogenic role for the missense *MTO1* mutations identified in our patients, but the yeast model allowed us to experimentally confirm their deleterious effects, dissecting the contribution of single allelic variants and giving an idea of the severity of each mutation. As summarized in Supp. Table S4, the severity of the yeast phenotype associated with *mtol* mutations is: yArg481His (hArg477His) < yAla431Thr (hAla428Thr) << yThr414Ile (hThr411Ile) = yPro622* (hArg620Lysfs*8) \approx *mtol* Δ . In particular, the behavior of *mtol*^{R481H} mutant is intermediate between that of the *mtol*^{A431T} mutant, and that of the *MTO1* wt allele as far as oxidative growth, respiratory activity [Ghezzi et al., 2012], and CIV activity are concerned. A moderate effect of the yArg481His substitution is in agreement with the observation that the Arg versus His change is electrostatically conservative, the equivalent Arg in GidA from *C. tepidum* being predicted to participate in a positively charged pocket, formed by several Arg, Lys, and His residues, that

binds the phosphates of the D-stem backbone of the incoming tRNA. This was confirmed by the partial, but significant, reduction of oxygen consumption but virtually normal CIV and CI–CIII activities detected in the *mtol*^{R481H} mutant strain. A defect of CV in the *mtol*^{R481H} mutant is unlikely, owing to the presence of normal amount of Atp6, Atp8, Atp9, and the previous observation that yeast strains carrying mutations in ATP6, 8, or 9 display defective oxidative growth but normal respiratory activity [Dujon, 1981] or reduced respiratory activity due to an indirect decrease of CIV [Kucharczyk et al., 2009]. Both *mtol*T414I and *mtol*P622X alleles behave as the null allele as for oxidative growth, respiratory activity, mitochondrial protein synthesis [Ghezzi et al., 2012], and CIV activity, albeit it is unclear if this is due to instability or loss of function of the mutant protein. In some patients with *MTO1* mutations, the clinical presentations seemed to depend on the genotype and partly to comply with the phenotypic observations in yeast. For instance, the presence of one allele expressing the p.Ala428Thr variant, which, in yeast, is of intermediate severity, is probably not sufficient to complement the defects caused by the variant Arg620Lysfs*8, which is functionally null. Contrariwise, patients homozygous for the p.Ala428Thr mutation [Ghezzi et al., 2012] or heterozygous with the less severe p.Arg477His mutation (Pt1 in this report), have milder symptoms, and are alive and relatively well at 20 and 14 years of age respectively, although both with compensated hypertrophic cardiomyopathy. However, in spite of carrying the same mutant genotype (Thr411Ile), the disease course was very different for the patients of the two

families presented in this article. Although Pt2 and Pt3 both had perinatal onset and died very early, Pt4 and Pt5 presented with the first symptoms after only a few months of life and yet have reached adolescence, being now 19 and 12 years old, respectively. This observation highlights the importance of genetics and environmental variations in modulating the phenotype in humans. It is tempting to speculate that, in addition to protection/risk genetic factors differentially expressed in the two families, the different outcome could be due to the different pharmacological intervention, which was merely supportive in the first family, whereas included timely correction of lactic acidosis in the second, following DCA administration. Although the number of reported *MTO1* mutant patients is very low, as a matter of fact all patients that survived beyond infancy and are still alive had chronic DCA treatment starting immediately after the clinical onset. DCA was remarkably effective on metabolic acidosis, suggesting that vigorous treatment of this life-threatening condition allows compensatory mechanisms to take place, which can mitigate the effects of hypertrophic cardiomyopathy. DCA administration should therefore be considered in *MTO1* mutant patients. In spite of these encouraging effects on survival, DCA treatment could not prevent the development of neurological symptoms associated with highly deleterious mutations such as the Thr411Ile in Pt4 and 5, suggesting that neurodegeneration can progress independently from the correction of the metabolic status if *MTO1* function is severely impaired.

Given the role of MTO1 as an optimizer of mtDNA translation, *MTO1* mutations can be associated with any combination of MRC deficiency, from isolated CIV deficiency (Family 2 in this article) to combined CI + CIV deficiency, the most common biochemical signature observed in *MTO1* mutant cases, to combined CIV + CIII deficiency, as previously reported [Ghezzi et al., 2012].

A rather specific genotype/phenotype correlation has been reported for several mutant factors involved in mtDNA translation [Rotig, 2011], an observation that still requires a finer dissection of the pathomechanism. Hypertrophic cardiomyopathy seems to be the clinical hallmark of *MTO1* mutations, although in the present study most of the patients were preselected on the basis of cardiac symptoms. In addition to the heart, clinical/radiological signs of brain involvement were clearly present in several *MTO1* mutant patients. Interestingly, a recently reported patient, carrying p.Gly59Ala and p.Thr308Ala *MTO1* compound heterozygous changes, showed refractory infantile spasms and CIV deficiency, but no cardiac involvement [Vasta et al., 2012]. However, the pathogenic role of these very variants remains unproven and the c.922A>G/p.Thr308Ala is reported as a SNP (dbSNP: rs145043138) with a minor allele frequency of 0.3%.

Yeast strains harboring *mtol*^{A431T} or *mtol*^{R481H} mutant alleles did show no evident defects in mitochondrial proteins synthesis; this observation is concordant with the lack of obvious impairment in mtDNA translation found in Ala428Thr and Arg620Lysfs*8 mutant

fibroblasts [Ghezzi et al., 2012], suggesting that the pathogenic effects of *MTO1* mutations are not due to reduced levels of mtDNA encoded subunits of the respiratory chain. Likewise, mitochondrial protein synthesis was not reduced in cells carrying deleterious mutations of, or having been knocked down for, *MTO2/TRMU* [Sasarman et al., 2011]. It is possible that amino-acid substitutions, that is, qualitative alterations of the primary structure of mtDNA proteins, rather than quantitative decrease of global protein synthesis, may play a major pathogenic role in both *MTO1* and *MTO2* mutant cells. The 5-carboxymethylaminomethylation and the 2-thiolation of the wobble uridine increase the accuracy of translation when guanidine is the third base of Gln, Glu or Lys codons, and prevent codon-anticodon pairing when the third base is a pyrimidine [Kurata et al., 2008; Murphy et al., 2004; Yarian et al., 2002]. Accordingly, in Ala428Thr and Arg620Lysfs*8 compound heterozygous fibroblasts, mtDNA-dependent CI, CIII, and/or CIV showed reduced activity, in spite of quantitatively normal mitochondrial protein synthesis, suggesting that errors in translation can determine the synthesis of qualitatively altered CI, CIII, and CIV mtDNA encoded subunits [Ghezzi et al., 2012]. Likewise, CIV activity was reduced in the *mtol*^{A431T} yeast strain, although the total levels of Cox1, Cox2, and Cox3 were similar to those of *MTO1* wt. This hypothesis is testable, by systematic investigation of human or yeast mutant cells, through mass spectrometry and other proteomics approaches. Another possibility is that *MTO1* may play a second role in mitochondria besides 5-carboxymethylaminomethylation of the wobble uridine, as previously

reported for other enzymes, which modify tRNA in bacteria [Nicholson, 1999; Roovers et al., 2008] and, potentially, for MTO2 [Sasarman et al., 2011]. Alternatively, the 5-carboxymethylaminomethylation of the tRNA can have additional functions besides the optimization of mitochondrial translation, as hypothesized for the thiolation of the wobble position catalyzed by MTO2 [Sasarman et al., 2011].

This study confirmed that *MTO1* mutations are associated with a mitochondrial disorder, characterized by hypertrophic cardiomyopathy, lactic acidosis, and MRC deficiency, albeit with a broad range of severity and frequent involvement of brain, possibly depending on the treatment. Moreover, we showed that the use of a suitable recombinant yeast model can validate the pathogenic role of variants found in human patients.

SUPPORTING INFORMATION

Case reports

Patient 1

Patient 1 (Pt1) was born at 40 weeks of gestation as the first child of non-consanguineous Italian parents (Figure 1A). Birth weight was 3200g (50th percentile), length 52cm (50th percentile), head circumference 36cm (50th percentile), APGAR scores 9-10. On her second day of life the patient became apnoeic with severe metabolic acidosis and lactic acidemia (8-12mM n.v. <2). Metabolic work-up showed high plasma alanine (720μM; n.v. 180-400), and increased urinary lactate, pyruvate, and Krebs cycle intermediates. Metabolic acidosis failed to respond to intravenous sodium bicarbonate, thiamine and biotin, but markedly improvement was obtained by dichloroacetate (DCA 50 mg/kg/day initially, later lowered to 25 mg/kg/day), with dramatic reduction of plasma lactate (<3mM).

A muscle biopsy, taken at 15 days after birth, showed multiple defects of MRC complexes, with strong reduction (<5% residual activity) of CI and CIV activities. The child was discharged at the age of 1 month in good control of blood lactate levels (<3 mM) under chronic DCA treatment. The clinical course during the following years was complicated by feeding difficulties, failure to thrive and neurological symptoms, e.g. myoclonic seizures for the first years of life. Nowadays, aged 14 years, her weight is at the 10th percentile, neurological development is moderately delayed, with hypotonia, dystonia and poor speech. Several brain MRIs showed abnormal bilateral hyperintensities in the capsulae surrounding the claustra

(Figure 1B). From the age of 8 years she has suffered of hypertrophic cardiomyopathy, particularly in the posterior wall of the left ventricle (6 mm, n.v. 4) with reduced systolic fraction (40%). At age 7 years, DCA treatment was stopped because of abnormalities of visual and brainstem evoked potentials and nerve conduction velocities. Subsequent metabolic follow-up revealed mildly elevated blood lactate but no further episodes of metabolic acidosis. A second muscle biopsy at 8 years again showed severe reduction of CI (14%) and CIV (27%) activities, whereas the other MRC activities were normal. Oxygen consumption, assessed through micro-oxygraphy in cultured fibroblasts, displayed significant reduction of MRR, SRC and OCR/ECAR whereas RCR, an index of mitochondrial OXPHOS coupling, was normal (Supp. Table S2).

Patient 2

Patient 2 (Pt2) was born at 37 weeks of gestation (birth weight of 2.38kg; 4th percentile) as the male first child of 1st cousin consanguineous Pakistani parents (Family 1; Figure 1A). On the first day of life, he developed severe poor feeding and mild hypoglycaemia and was admitted to the Special Care Baby Unit. Over the first 3 months of life, he developed hypotonia, his weight gain was poor and an echocardiography (performed at 3 months of age because of the detection of a cardiac murmur) demonstrated severe left ventricular hypertrophy with posterior wall thickness (8mm). Lactic acidemia was noted, with blood lactate varying between 9.5 and 14.6 mM. Metabolic work-up showed high plasma alanine (690 μ M, n.v. <400), and increased urinary lactate, 3-methylglutaconic acid and

accumulation of Krebs cycle intermediates. A muscle biopsy, taken at 6 months of age, showed decreased staining for cytochrome *c* oxidase (COX) and severe deficiency in both CI and CIV activities (<10% residual activities). Brain MRI showed symmetrical, bilateral abnormal signals in fornices, globus pallidus, thalamus, subthalamic nucleus, substantia nigra, dorsal mesencephalon, pons and to a lesser extent dentate nuclei of the cerebellum (Figure 1C). A lactate peak was detected on [H⁺]-MR Spectroscopy. The clinical course during the following months was complicated by persistent hypotonia and failure to thrive despite nasogastric feeding. At 12 months of age the child developed pneumonia associated with worsening metabolic acidosis and died of irreversible cardiorespiratory arrest. Oxygen consumption assessed by micro-oxygraphy in cultured fibroblasts displayed significant reduction of MRR, SRC and OCR/ECAR with normal RCR (Supp. Table S2). The mtDNA sequence was normal.

Patient 3

Patient 3 (Pt3), the younger brother of Patient 2, was born at 34 weeks gestation (birth weight of 2.17kg; 25th percentile). This child was born with hypospadias and an accessory digit at the base of the palmar aspect of the left thumb. In view of the family history, plasma lactate was monitored in the neonatal period and found to be elevated (7-10 mM). An echocardiogram at 1 month of age showed mild left ventricular hypertrophy with a posterior wall thickness of 7mm. His subsequent clinical course was complicated by feeding difficulties and failure to thrive. He was admitted for nasogastric tube feeding and no further invasive investigations were performed at the family's wishes.

He received palliative care and died suddenly at home at the age of 3 months.

Patient 4

Patient 4 (Pt4) was born at term as the first female child of 1st cousin consanguineous Pakistani parents (Family 2; Figure 1A). No feeding or respiratory difficulties occurred in the perinatal period. At three months of age, she developed severe metabolic acidosis with lactic acidemia associated with bronchiolitis-like illness. Metabolic work-up showed increased urinary lactate. A muscle biopsy, taken at 3 months of age, revealed decreased histochemical reactivity for COX and a severe CIV deficiency (<10% of controls), with CI activity reported as normal. Echocardiography demonstrated mild biventricular hypertrophic cardiomyopathy, which improved on serial scans over a number of years and did not require medication. The clinical course during the following years was complicated by speech and language delay, failure to thrive and recurrent hospital admissions with lactic acidosis associated with intercurrent infections with an admission to intensive care at age 2 years due to generalised seizures and encephalopathy. Nowadays, aged 19 years, her weight is <3rd percentile, her psychomotor development is mildly delayed and she is in special secondary education. Her menarche occurred normally, at 13 years of age. The frequency and severity of admissions has reduced gradually with age and her last acute admission was aged 8 years. She has persistent fatigue with chronic lactic acidosis (5.0-8.0mM) and Vitamin D deficiency for which she takes regular ergocalciferol and

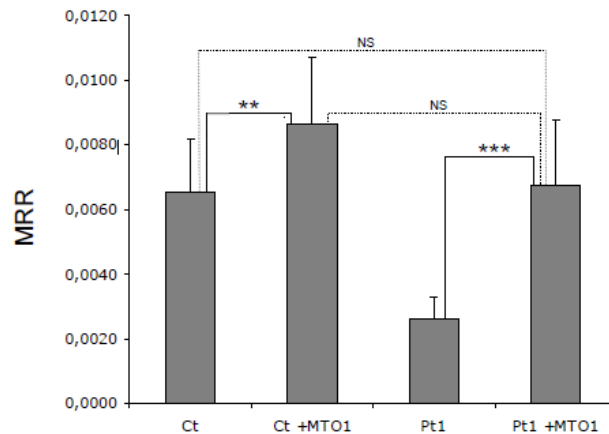
sodium bicarbonate supplements. DCA was used regularly from the age of 16 years with a reduction in resting plasma lactate levels to 4.0 mM but has now been stopped.

Patient 5

Patient 5 (Pt5), the younger sister of Patient 4 was born at term (birth weight of 2890g; 9th-25th percentile), with no perinatal respiratory or feeding difficulties. At five months of age the patient developed severe metabolic acidosis and lactic acidemia (>22.0mM), associated with an upper respiratory illness. Echocardiography demonstrated dilated cardiomyopathy with left ventricular hypertrophy and an electrocardiogram demonstrated a Wolff-Parkinson-White syndrome. Metabolic work-up showed high plasma alanine (695 μ M), and increased urinary lactate with ketonuria and dicarboxylic aciduria. A muscle biopsy, taken at 7 months of age, showed similar findings to her sister, i.e. severe COX defect. She had a further severe decompensation aged 9 months associated with bronchiolitis and was ventilated for 4 weeks with repeated attempts at extubation failing due to rising lactic acidosis and worsening cardiomyopathy (fractional shortening 15%), with pericardial effusion. She required drug treatment for cardiac failure and her lactic acidosis was successfully treated with DCA at 50mg/kg/day with plasma lactate levels falling to 3.0 mM. The clinical course during the following years was complicated by psychomotor delay, increasing lower limb spasticity, failure to thrive (needing nasogastric feeding) and recurrent hospital admissions with lactic acidosis associated with intercurrent infections. Nowadays, aged 12 years of age, her weight and height are at <3rd

percentile and psychomotor development is severely delayed. She is able to walk independently but has no speech and limited non-verbal communication; she is also in special education. The frequency and severity of admissions has reduced gradually with age and her last acute admission was at aged 11 years. Her cardiomyopathy has gradually improved with a fractional shortening of 30% and she takes only digoxin and lisinopril. Chronic DCA has been discontinued. Full mitochondrial DNA sequencing was negative in this family, as was the diagnostic screening of several COX assembly factor genes including *COX10* and *COX15*.

Supp. Figure S1.



	Pt1			Ct		
	naive	+MTO1	Fold increase	naive	+MTO1	Fold increase
MRR	41	102	2.5	100	134	1.3
SRC	52	177	3.4	100	223	2.2
RCR	93	132	1.4	100	130	1.3

Complementation in fibroblasts. Maximal respiration rate (MRR), measured in fibroblasts from Patient 1 (Pt1) and a control subject (Ct), in naive condition or overexpressing MTO1 (+MTO1). MRR values are expressed as pMolesO₂/min/cells. Data are represented as mean ± SD. Two-tail, unpaired Student's t test was applied for statistical significance. ***: p < 0.001; **: p < 0.01; NS: not significant (p > 0.01).

The percentages of maximal respiration rate (MRR), spare respiratory capacity (SRC), respiratory control ratio (RCR) in patient 1 (Pt1) compared to a control subject (Ct), are listed in naive condition and after overexpression of MTO1^{wt} (+MTO1). The values of untreated control fibroblasts were considered as 100%

Supp. Table S1. Oligonucleotides used in this work

Human <i>MTO1</i> exon	Forward primer	Reverse primer
1	TCCCTCACCAGGAAAGTAGCTC	CCCCGCTTCAGACCGG
2-3	GTAGTATATCTTTCACGTTTTCTATTTTATCAT	TCCTTGAATAAGCAACATATCTCCAC
4	ATTGCACCACTGCCCTCC	TTACAGTACTTCCTGCTGTG
5-6	TTAGTGTCTATTAAGTCAGTACGTA TCATGTG	TGACTGTAGCTAAGGCCTCCTCAC
7	TTTTTAAAGGGCATTAAAGGGTAATG	AGCCATCTCCAAACACCCCTG
8	CAATACTTGCTTTCTTCCTGTCCC	AGTGTGGTTTTTAAAGCAAATTTTTT
9	CAAGAGGATCACTTGAGGCCA	AACGGATTTTGAAAAGAAGCCAA
10	TCTTTTGGTATTTATTCTGAGATCTG ATATTAT	TGTAGGTGTGCAATGCTCTTAGC
11	AAAGGGAACACCTACCCAAC	GGCCATTATAACCCAGGTT
12	TCAGTTCCCATTTGTAAAATGAAGA	GTTTCAGTTTTAGGTTCACTGTCTCTC TC
Yeast <i>MTO1</i>	Forward primer	Reverse primer
Cloning ^a	gggggGTCGACgcttactgccactattagtcacg	gggggGAGCTCcgacagtgagttgcccttttgc
Mutagenesis	ctcactaaatcttagggcatcc	gcagatctgtttcagcctgtgg
T414I mutagenesis ^b	gccggacaataaatggtatTtacaggctacgaggaagccg	cggcttctcgtagcctgtaAtaccattattgtccgcc
R481H mutagenesis ^b	cagaattcagaatcagcgtacATgccgataacgcagacttcag	ctgaagtctgcgttatcggcATGtacgctgattctgaattg

^a In upper case the endonuclease restriction sites

^b In upper case the bases which are changed to introduce the desired mutations

Supp. Table S2. Oxygen consumption and extra-cellular acidification measurements in fibroblasts from patients 1 and 2 (Pt1 and Pt2)

	Pt1 ^a		Pt2 ^b	
	% of Ct	t-test vs Ct	% of Ct mean	t-test vs Ct
MRR	61	1.4*10 ⁻⁶	46	2.7*10 ⁻¹⁸
SRC	59	9.9*10 ⁻⁴	46	3.6*10 ⁻⁹
RCR	86	0.13	96	0.93
OCR/ECAR	40	2.1*10 ⁻³	26	6.9*10 ⁻⁹

Values are reported as percentages of the controls' (Ct) mean; unpaired two-tail Student's t-test was used for comparison between patients and controls. Measurements were performed in a Seahorse XF96 (^a) or XF24 (^b) instrument.

Supp. Table S3. In silico prediction of pathogenicity for *MTO1* mutations

	SIFT	Polyphen-2	PANTHER	SNPs&GO	MutPred
hThr441Ile (yThr414Ile)					
Prediction	Damaging	Probably damaging	0.95106/1	Disease	0.892/1
Confidence/Reliability	Low confidence		High	5/10	
hArg477His (yArg481His)					
Prediction	Damaging	Probably damaging	0.93769/1	Disease	0.710/1
Confidence/Reliability	Low confidence		High	4/10	

Supp. Table S4. Severity of the phenotypes associated with *Mto1* mutations in yeast

Human mutation	Yeast mutation	Yeast phenotype ^b				
		Oxidative growth	Respiratory activity	Mitochondrial protein synthesis	CIV activity	Severity
Arg477His	Arg481His	↓	↓	=	=	less severe
Ala428Thr	Ala431Thr	↓↓	↓↓	=	↓	intermediate
Thr411Ile	Thr414Ile ^a	↓↓↓	↓↓↓	↓↓↓	↓↓↓	most severe
Arg620Lysfs*8	Pro620* ^a	↓↓↓	↓↓↓	↓↓↓	↓↓↓	most severe

^a: Thr414Ile and Pro620* behave as the null mutation *mto1Δ*.

^b: “=” indicates that the phenotype is the same compared to *MTO1* wt, “↓↓↓” indicates that the phenotype is the same compared to the null *mto1* allele

Acknowledgments

The Cell lines and DNA bank of Paediatric Movement Disorders and Neurodegenerative Diseases, member of the Telethon Network of Genetic Biobanks (project no. GTB12001), funded by Telethon Italy, provided us with specimens.

Disclosure statement: The authors declare no conflict of interest.

Contract grant sponsors:

The Italian Ministry of Health (GR2010-2316392); Fondazione Telethon (GGP11011, GPP10005); CARIPLO (2011/0526); The Pierfranco and Luisa Mariani Foundation of Italy; The Italian Association of Mitochondrial Disease Patients and Families (Mitocon); The German Federal Ministry of Education and Research (BMBF) funded Systems Biology of Metatypes (SysMBo #0315494A); The German Network for Mitochondrial Disorders (mitoNET #01GM0867, 01GM1113C); E-rare Grant GenoMit (JTC2011, 01GM1207, FWF I 920-B13); The EU FP7 Mitochondrial European Educational Training project (Meet); The Medical Research Council (UK); A Wellcome Trust Strategic Award (906919); The UK NHS Specialist Commissioners; Medical Research Council (UK) Centenary Early Career Award.

References

- Barrientos A, Korr D, Tzagoloff A. 2002. Shy1p is necessary for full expression of mitochondrial COX1 in the yeast model of Leigh's syndrome. *EMBO J* 21:43–52.
- Barrientos A, Fontanesi F, D'iaz F. 2009. Evaluation of the mitochondrial respiratory chain and oxidative phosphorylation system using polarography and spectrophotometric enzyme assays. *Curr Protoc Hum Genet* 19:19.3.
- Bonneaud N, Ozier-Kalogeropoulos O, Li GY, Labouesse M, Minvielle-Sebastia L, Lacroute F. 1991. A family of low and high copy replicative, integrative and singlestranded *S. cerevisiae/E. coli* shuttle vectors. *Yeast* 7:609–615.
- Bugiani M, Invernizzi F, Alberio S, Briem E, Lamantea E, Carrara F, Moroni I, Farina L, Spada M, Donati MA, Uziel G, Zeviani M. 2004. Clinical and molecular findings in children with complex I deficiency. *Biochim Biophys Acta* 1659:136–147.
- Colby G, Wu M, Tzagoloff A. 1998. MTO1 codes for a mitochondrial protein required for respiration in paromomycin-resistant mutants of *Saccharomyces cerevisiae*. *J Biol Chem* 273:27945–27952.
- Dujon B. 1981. Mitochondrial genetics and functions. In: *The molecular biology of the yeast saccharomyces: life cycle and inheritance*. Cold Spring Harbor Laboratory Press. Cold Spring Harbor, NY. p 505–635.
- Fontanesi F, Jin C, Tzagoloff A, Barrientos A. 2008. Transcriptional activators HAP/NFY rescue a cytochrome *c* oxidase defect in yeast and human cells. *Hum Mol Genet* 17:775–788.

- Ghezzi D, Baruffini E, Haack TB, Invernizzi F, Melchionda L, Dallabona C, Strom TM, Parini R, Burlina AB, Meitinger T, Prokisch H, Ferrero I, Zeviani M. 2012. Mutations of the mitochondrial-tRNA modifier MTO1 cause hypertrophic cardiomyopathy and lactic acidosis. *Am J Hum Genet* 90:1079–1087.
- Gietz RD, Woods RA. 2002. Transformation of yeast by lithium acetate/single-stranded carrier DNA/polyethylene glycol method. *Methods Enzymol* 350:87–96.
- Goffrini P, Ercolino T, Panizza E, Giach`e V, Cavone L, Chiarugi A, Dima V, Ferrero I, Mannelli M. 2009. Functional study in a yeast model of a novel succinate dehydrogenase subunit B gene germline missense mutation (C191Y) diagnosed in a patient affected by a glomus tumor. *Hum Mol Genet* 18:1860–1868.
- Ho SN, Hunt HD, Horton RM, Pullen JK, Pease LR. 1989. Site-directed mutagenesis by overlap extension using the polymerase chain reaction. *Gene* 77:51–59.
- Invernizzi F, D'Amato I, Jensen PB, Ravaglia S, Zeviani M, Tiranti V. 2012. Microscale oxygraphy reveals OXPHOS impairment in MRC mutant cells. *Mitochondrion* 12:328–335.
- Krüger MK, Sørensen MA. 1998. Aminoacylation of hypomodified tRNA^{Glu} in vivo. *J Mol Biol* 284:609–620.
- Kucharczyk R, Rak M, Di Rago JP. 2009. Biochemical consequences in yeast of the human mitochondrial DNA 8993T>C mutation in the ATPase6 gene found in NARP/MILS patients. *Biochim Biophys Acta* 1793:817–824.

- Kurata S, Weixlbaumer A, Ohtsuki T, Shimazaki T, Wada T, Kirino Y, Takai K, Watanabe K, Ramakrishnan V, Suzuki T. 2008. Modified uridines with C5-methylene substituents at the first position of the tRNA anticodon stabilize U.G wobble pairing during decoding. *J Biol Chem* 283:18801–18811.
- Meyer S, Scrima A, Versées W, Wittinghofer A. 2008. Crystal structures of the conserved tRNA-modifying enzyme GidA: implications for its interaction with MnmE and substrate. *J Mol Biol* 380:532–547.
- Murphy FV 4th, Ramakrishnan V, Malkiewicz A, Agris PF. 2004. The role of modifications in codon discrimination by tRNA(Lys)UUU. *Nat Struct Mol Biol* 11:1186–1191.
- Nicholson AW. 1999. Function, mechanism and regulation of bacterial ribonucleases. *FEMS Microbiol Rev* 23:371–390.
- Osawa T, Ito K, Inanaga H, Nureki O, Tomita K, Numata T. 2009. Conserved cysteine residues of GidA are essential for biogenesis of 5-carboxymethylaminomethyluridine at tRNA anticodon. *Structure* 17:713–724.
- Roovers M, Oudjama Y, Kaminska KH, Purta E, Caillet J, Droogmans L, Bujnicki JM. 2008. Sequence–structure–function analysis of the bifunctional enzyme MnmC that catalyses the last two steps in the biosynthesis of hypermodified nucleoside mnm5s2U in tRNA. *Proteins* 71:2076–2085.
- Rötig A. 2011. Human diseases with impaired mitochondrial protein synthesis. *Biochim Biophys Acta* 1807:1198–1205.

- Sasarman F, Antonicka H, Horvath R, Shoubridge EA. 2011. The 2-thiouridylase function of the human MTU1 (TRMU) enzyme is dispensable for mitochondrial translation. *Hum Mol Genet* 20:4634–4643.
- Shi R, Villarroya M, Ruiz-Partida R, Li Y, Proteau A, Prado S, Moukadiri I, Benítez-Páez A, Lomas R, Wagner J, Matte A, Velázquez-Campoy A, et al. 2009. Structure-function analysis of *Escherichia coli* MnmG (GidA), a highly conserved tRNA modifying enzyme. *J Bacteriol* 191:7614–7619.
- Soto IC, Fontanesi F, Valledor M, Horn D, Singh R, Barrientos A. 2009. Synthesis of cytochrome *c* oxidase subunit 1 is translationally downregulated in the absence of functional F1F0-ATP synthase. *Biochim Biophys Acta* 1793:1776–1786.
- Suzuki T, Nagao A, Suzuki T. 2011. Human mitochondrial tRNAs: biogenesis, function, structural aspects, and diseases. *Annu Rev Genet* 45:299–329.
- Sylvers LA, Rogers KC, Shimizu M, Ohtsuka E, Söll D. 1993. A 2-thiouridine derivative in tRNA^{Glu} is a positive determinant for aminoacylation by *Escherichia coli* glutamyl-tRNA synthetase. *Biochemistry* 32:3836–3841.
- Takai K. 2005. Possible conformations of 5-aminomethyluridine derivatives recognizing a G at the third position of the codon. *Nucleic Acids Symp Ser (Oxf)* 49:317–318.
- Umeda N, Suzuki T, Yukawa M, Ohya Y, Shindo H, Watanabe K, Suzuki T. 2005. Mitochondria-specific RNA-modifying enzymes responsible for the biosynthesis of the wobble base in

- mitochondrial tRNAs. Implications for the molecular pathogenesis of human mitochondrial diseases. *J Biol Chem* 280:1613–1624.
- Urbonavicius J, Qian Q, Durand JM, Hagervall TG, Björk GR. 2001. Improvement of reading frame maintenance is a common function for several tRNA modifications. *EMBO J* 20:4863–4873.
- Vasta V, Merritt JL 2nd, Saneto RP, Hahn SH. 2012. Next-generation sequencing for mitochondrial diseases: a wide diagnostic spectrum. *Pediatr Int* 54:585–601.
- Wang X, Yan Q, Guan MX. 2010. Combination of the loss of mnm5U34 with the lack of s2U34 modifications of tRNA^{Lys}, tRNA^{Glu}, and tRNA^{Gln} altered mitochondrial biogenesis and respiration. *J Mol Biol* 395:1038–1048.
- Yan Q, Li X, Faye G, Guan MX. 2005. Mutations in MTO2 related to tRNA modification impair mitochondrial gene expression and protein synthesis in the presence of a paromomycin resistance mutation in mitochondrial 15 S rRNA. *J Biol Chem* 280:29151–29157.
- Yarian C, Marszalek M, Sochacka E, Malkiewicz A, Guenther R, Miskiewicz A, Agris PF. 2000. Modified nucleoside dependent Watson-Crick and wobble codon binding by tRNA^{Lys}UUU species. *Biochemistry* 39:13390–13395.
- Yarian C, Townsend H, Czestkowski W, Sochacka E, Malkiewicz AJ, Guenther R, Miskiewicz A, Agris PF. 2002. Accurate translation of the genetic code depends on tRNA modified nucleosides. *J Biol Chem* 277:16391–16395.

- Yasukawa T, Suzuki T, Ishii N, Ohta S, Watanabe K. 2001. Wobble modification defect in tRNA disturbs codon–anticodon interaction in mitochondrial disease. *EMBO J* 20:4794–4802.
- Zhang JC, Sun L, Nie QH, Huang CX, Jia ZS, Wang JP, Lian JQ, Li XH, Wang PZ, Zhang Y, Zhuang Y, Sun YT, Bai X. 2009. Down-regulation of CXCR4 expression by SDFKDEL in CD34(+) hematopoietic stem cells: an antihuman immunodeficiency virus strategy. *J Virol Methods* 16:30–37.

CHAPTER 5

Summary, conclusions and future perspectives

SUMMARY

The scope of my thesis was the identification of genes responsible for an adult-onset neurological syndrome occurring in two half-siblings, and for a hypertrophic cardiomyopathy and lactic acidosis in infantile patients with mitochondrial respiratory chain defects.

For both groups, the identification of the corresponding disease gene was carried out by whole-exome-sequencing (WES). This technology has revolutionized biology and medicine, accelerating considerably the discovery of disease genes. The great challenge of WES is represented by the enormous amount of variants identified per sequenced exome. To reduce the amount of variants, we used appropriate filtering, such as mode of disease inheritance, segregation in families, possible correlation with clinical symptoms, and, for mitochondrial diseases, localization of the corresponding protein in the organelle.

When possibly causative variants were identified, the second step was the demonstration of the pathogenic role of mutated proteins, by appropriate experimental procedures. In particular, for the characterization and complementation assays we used cellular models in both the studies, while the yeast model was used for the mitochondrial disorder.

An additional step, which can increase the relevance of single WES studies, was the screening of the identified disease-genes in patients with similar clinical phenotypes. In this sense we have obtained good

results for the screening of *MTO1*, the gene responsible for the above described mitochondrial cardiomyopathy.

GFAP and HDAC6

We studied a family with two half-siblings, sharing the same mother, affected by a progressive adult-onset neurological syndrome. The elder patient (P1) had a mild movement disorder with cognitive impairment, while her brother (P2) had a severe motor-neuron disease of limb and bulbar district without cognitive deterioration. Although they presented different clinical features, the MRI of both patients was compatible with AOAD. However, the screening of the canonical isoform of the gene responsible for this disease, GFAP- α , ruled out mutations.

WES analysis revealed a heterozygous variant (c.1289G>A, p.R430H) in GFAP- ϵ isoform in both patients. This nucleotide change was absent in the healthy mother and in all tested family members. In addition, these two patients have a different father, so the more consistent hypothesis is that the mutation was transmitted by maternal germinal mosaicism.

Because GFAP- ϵ is an IF protein that participates with GFAP- α in the formation of the GFAP network, I evaluated the damaging effect of the mutation in GFAP- ϵ isoform. I transfected astrocytoma U251-MG cells (expressing endogenous GFAP- α) with GFP-GFAP- ϵ^{wt} or GFP-GFAP- ϵ^{R430H} and then I analyzed the IF meshwork. The result was that GFP-GFAP- ϵ^{R430H} , on the contrary of GFP-GFAP- ϵ^{wt} , is

inefficiently incorporated and perturbs the GFAP network in astrocytoma cells.

Since P2 showed different clinical features, we analyzed further gene variants present in P2 but not in P1, by a prioritization software, using “training genes” associated with MND. The highest score was achieved by *HDAC6*, on chromosome Xp11.23, encoding deacetylase 6. The P865S change does not alter the *HDAC6* transcript levels, but damages its deacetylase activity. In fact, acetylated alpha-tubulin levels, its main substrate, was consistently increased and immunocytochemical staining showed abnormal clumps of acetylated alpha-tubulin in the perinuclear region of P2 fibroblasts.

MT01

We started this project studying a family with two siblings affected by infantile hypertrophic cardiomyopathy and lactic acidosis with mitochondrial respiratory chain deficiency mainly affecting CI and CIV. Unfortunately, both patients died about 1 month after birth because of sudden bradycardia unresponsive to resuscitation procedures.

First of all, we sequenced known genes associated to mitochondrial cardiomyopathy, such as *ACAD9*, *AGK*, *SLC25A4*, *TAZ* and *TMEM70*, without any positive results. So we carried out WES in one of these patients. To obtain the causative variant of disease, we excluded variants with a frequency >0.2% in public SNP databases, being mitochondrial diseases rare conditions, and we considered

homozygous or compound-heterozygous variants, assuming an autosomal-recessive mode of inheritance. In addition, variants were prioritized taking into account if 1) they affected proteins with a link to mitochondrial functions and 2) they are computationally predicted to alter protein function. This filtering analysis revealed that our patients were compound-heterozygous for mutations in *MTO1*: a maternal c.1858dup (p.Arg620Lysfs*8) and a paternal c.1282G>A (p.Ala428Thr).

MTO1 protein is involved in the posttranscriptional modification of the wobble uridine base in mt-tRNA^{Gln}, mt-tRNA^{Glu}, and mt-tRNA^{Lys}, necessary for accuracy and efficacy of mtRNA translation.

In order to prove the causative role of *MTO1* variants, we studied whether the expression of wt *MTO1* cDNA could rescue the biochemical phenotype of mutant immortalized fibroblast from P2. The evaluation of the oxygen consumption showed a reduction of maximal respiration rate (MRR) in immortalized fibroblast, which returned to normal after transduction with a *MTO1*^{wt}-expressing lentivirus.

To test the pathogenic role of the *MTO1* mutations we used also the yeast *Saccharomyces cerevisiae*, assessing oxidative growth, respiratory activity, mitochondrial protein synthesis, and CIV activity. In particular, we used a *mto1Δ* paramomycin-sensitive (P^R) strain because human 12S RNA site A is structurally similar to the yeast 15S RNA site A of the P^R strain. We showed that the yeast Ala431Thr change, corresponding to human Ala428Thr, reduced MRC activities,

whereas the mutation equivalent to human Arg620Lysfs*8 behaved as a null allele.

Finally, we tried to treat patients' fibroblast and *mtol* mutant yeast strains with riboflavin, precursor of FAD, since MTO1 owns a FAD moiety and for other mitochondrial flavoproteins (for instance ACAD9) the supplementation of riboflavin gave improvements in both cellular models and patients. Unfortunately, we did not see any positive effect.

After the identification and characterization of these mutations, we sequenced *MTO1* in DNA samples from 17 individuals with early onset hypertrophic cardiomyopathy, lactic acidosis and defective MRC activities. With this screening we found a single individual (P3) homozygous for the c.1282G>A, the identical missense mutation present in the two siblings. But the clinical condition of P3, now about 19, is less severe, probably because both his alleles produce a partial functioning protein. Moreover, to counteract metabolic acidosis, P3 was put on a permanent treatment with Dichloroacetate (DCA), a potent lactate-lowering drug.

After the first paper on MTO1, in a second work we reported further five patients with *MTO1* mutations (P1, compound heterozygotes for p.Arg477His and p.Ala428Thr; and two couples of siblings, P2-P3 and P4-P5, homozygotes for p.Thr411Ile). Besides hypertrophic cardiomyopathy, lactic acidosis and MRC defect, these patients showed different neurological symptoms (i.e. myoclonic seizures, hypotonia, dystonia, encephalopathy) and brain MRI abnormalities. Moreover, P1, P4 and P5 received early DCA treatment.

We tested the potential deleterious effect of the new found *MTO1* mutations (p.Thr411Ile and p.Arg477His) again in a $\Delta mto1$ P^R strain. The result was that p.Thr411Ile gave the mildest effect, while the behavior of p.Arg477His is similar to a null allele.

For P1, I also performed a complementation assay in fibroblasts, demonstrating that the expression of wt *MTO1* could rescue the respiratory defect in mutant fibroblast.

DISCUSSION and CONCLUSIONS

Since the release of the first draft of the human genome in 2001 followed, few years later, by the development of new DNA sequencing technology, we have been facing a “genetic revolution”.

From the mapping of Huntington disease gene to the short arm of chromosome 4 by using restriction fragment length polymorphisms and linkage in a large family in 1983 (Gusella et al., 1983) or the identification of the gene for Duchenne muscular dystrophy (DMD) (Koenig et al., 1987) in 1986–1987, one of the first genes discovered to be responsible for an inherited disorder, we witnessed numerous disease gene discoveries, which strongly increased during the last ten years.

Today, a lot of inherited disorders can be diagnosed by a simple DNA test on peripheral blood, providing patients with a definitive diagnosis. Moreover, the molecular diagnosis allows relatives of patients to ask for genetic counseling and for preimplantation or prenatal genetic testing.

GFAP- ϵ and HDAC6

Alexander disease is a rare disorder of the nervous system and it is mainly caused by mutation in GFAP- α . Probably, the pathogenesis of disease is linked to toxic gain-of-function of mutant GFAP, perhaps related to abnormal protein aggregation (Wang L et al., 2011). This observation agrees in principle with our experiments, where the

expression of mutated GFP-GFAP- ϵ in human astrocytoma cells led to an increase of cytoplasmic aggregates, perturbing the IF meshwork.

All known GFAP mutations are heterozygous and both *de novo* mutations, autosomal dominant transmission and germline mosaicism have been described.

This is the first report of mutation in GFAP- ϵ isoform causing an adult-onset Alexander disease. Till now, all missense mutations, insertions or deletions identified in AxD patients have been found in the canonical isoform GFAP- α .

Precisely, the lack of mutations in the nine canonical exons encoding GFAP- α , in contrast with a MRI pattern that strongly suggested a AOAD common to the two half-siblings, prompted us to perform WES and to search possibly deleterious variants shared by these patients.

The identification of GFAP- ϵ ^{R430H} mutation well fitted with the AOAD but did not clarify the different clinical features of P2. While P1 suffered from slowly progressive cognitive impairment and a mild movement disorder, a typical pattern of AOAD, P2 had severe MND. Therefore, we hypothesized that a differential segregation of other gene variants could influence the phenotypic expression. After a prioritization analysis, using “training genes” associated to MND, we focused on *HDAC6*. We demonstrated that P2 HDAC6^{P856S} mutation is associated with decrease tubulin-specific deacetylases activity.

Several papers suggest a role for HDAC6 in the pathogenesis of MND, although its effective role in neurodegeneration is very controversial.

It was reported that deletion of *Hdac6* in SOD1 (G93A) mouse model of ALS significantly extended the survival of the mice enhancing axonal transport via hyperacetylation of tubulin (Taes I et al, 2013). In contrast, other studies found that HDAC6 inhibition can have detrimental effects, for example slowing axonal growth in cultured hippocampal neurons (Tapia M, 2010) and reducing neurite outgrowth in SH-SY5Y cells (Fiesel, F C, 2011). In fact, HDAC6 activity is necessary to maintain axonal growth rate and for the polarized localization of proteins to the axon initial segment.

Moreover, both TDP43 and FUS/TLS, typical proteins associated to ALS, were found to co-regulate *HDAC6* mRNA (Kim SH et al., 2010).

For these reasons, although the mechanism of action is not fully understood, we think that P856S HDAC6 variant is really implicated in motor neuron disease of P2, acting with the GFAP- ϵ mutation to determine the precise phenotype of this patient.

MTO1

Mitochondrial diseases are rare conditions and their clinical manifestations are extremely heterogeneous, making the diagnosis arduous even in cases with mutations in known disease genes.

These disorders can arise from mutations in mtDNA or nDNA, affecting MRC subunits, assembly factors or proteins involved in mitochondrial replication transcription or translation.

Many mitochondrial diseases are associated with defective mitochondrial protein synthesis, which can result from mutations in

tRNA, rRNA, aminoacyl-tRNA synthetases, translation factors, ribosomal proteins etc. Typical examples of diseases due to tRNA mutations are MELAS, caused by a tRNA^{Leu(UUR)} mutation, and MERRF, caused by a tRNA^{Lys} mutation.

One key event for mammalian mitochondria gene expression is tRNA maturation, which requires many modifications necessary for proper functioning of tRNAs, including structure stabilization, aminoacylation and codon recognition. Different editing enzymes are involved in post-transcriptional modifications mainly affecting the first base of the anticodon. Mutations of *PUS1*, a pseudouridine synthase, cause mitochondrial myopathy, lactic acidosis and sideroblastic anemia, while mutations of *TRMU*, responsible for the 2-thiolation of the wobble U in mt-tRNA^{Lys}, mt-tRNA^{Glu}, mt-tRNA^{Gln}, are associated with an infantile mitochondrial hepatopathy (Zeharia A et al., 2009).

Thanks to WES, we identified the first mutations in *MTO1* encoding an optimizer of mtDNA translation, which catalyses the mnm⁵s²U34 of the wobble uridine base in mt-tRNA^{Lys}, mt-tRNA^{Glu}, mt-tRNA^{Gln}, modification usually coupled to the 2-thiolation of the same uridine moiety, catalyzed by TRMU.

We noticed a rather specific genotype/phenotype correlation; in fact all patients with *MTO1* mutations reported in our two papers presented hypertrophic cardiomyopathy and lactic acidosis with reduction of mitochondrial respiratory chain. Since MTO1 is involved in mitochondrial protein synthesis, its impairment may affect each

complex subunit encoded by mtDNA. However our patients mainly showed reduction of CI and CIV.

Including all described patients, four different *MTO1* mutations have been found. Interestingly, the severity of the yeast phenotype associated with *mtol* mutations (hArg477His < hAla428Thr << hThr411Ile = hArg620Lysfs*8 \approx *mtol* Δ) correlated with phenotypic spectrum observed in *MTO1* mutant patients: from severe, rapidly progressive, ultimately fatal presentation in two compound heterozygous children for Arg620Lysfs*8 and Ala428Thr mutations, to fulminant postnatal phenotype, or severe, but long-lasting, encephalo-cardiomyopathy in the two families with homozygous p.Thr411Ile mutation, to benign, compensated hypertrophic cardiomyopathy with modest neurological abnormalities in the two patients respectively for Ala428Thr and Arg477His.

In addition, the analysis of our patients suggests that, besides the particular *MTO1* mutations, the different outcome could be due to the different pharmacological intervention. In fact, all the surviving patients received DCA treatments.

Since the less severe *MTO1* mutations did not clearly affect the mtDNA in vitro translation, it is possible that their pathogenic effects are linked to qualitative alterations of the primary structure of mitochondrial proteins (due to lower fidelity in the recognition of the correct codon-anticodon pair), rather than quantitative decrease of global mitochondrial protein synthesis. Moreover, another possibility is that MTO1 may play a second role in mitochondria besides 5-carboxymethylaminomethylation of the wobble uridine.

FUTURE PERSPECTIVES

Neurological diseases include heterogeneous group of disorders ranging from pediatric neurodevelopment diseases, heterogeneous monogenic disorders (i.e. mitochondrial diseases) to late-onset neurodegenerative diseases, most of which are poorly understood and the treatment, since the cure is not available, will at best delay progression.

Mitochondrial disorders are a group of syndromes characterized by high genetic and clinical heterogeneity and relatively loose genotype/phenotype correlation. On the contrary most of late-onset neurodegenerative diseases (such as PD, AD and ALS) are complex neurological diseases where several genes with rare and/or common variants can influence disease risk as well as environmental factors can contribute to disease development.

Thanks to new sequencing technologies many new genes associated to inherited conditions, including several neurological diseases, have been identified in the last few years and will be identified in a more rapid turnaround time, bypassing many problems typical of the traditional approaches, for example the requirement of large pedigrees (Johnson JO et al., 2010; Zimprich, A. et al., 2011).

The rapid progress in this area of biotechnology has led to improvement in accuracy and throughput of hardware platforms, target-enrichment procedures, and coverage in sequence depth. Marked expansion of biocomputational tools, including publicly available or in-house DNA sequence variant databases, and the

development of effective predictive softwares for mutation pathogenicity, has been increasing filtering capacity and accuracy. NGS is applicable to small families and even singleton cases, allowing its use in all patients with inherited disorders. Moreover, the continuous improvement of NGS technology will make soon WES of large collections of samples both feasible and affordable.

The identification of the disease gene/protein and the understanding of its role is the first step for the development of effective cure. Moreover, the identification of disease gene can be immediately translated to diagnostic workup, with improvement in management of patients, counseling of families, and epidemiological survey of disease.

The identification of mutation in GFAP- ϵ isoform opens new perspectives towards the molecular diagnosis of AxD. So far the molecular diagnosis was based on screening of the nine exons encoding the predominant isoform GFAP- α ; our data suggest to extend the spectrum of the GFAP isoforms that should be included in the diagnostic screening.

Moreover, the identification of *HDAC6* variant in P2, that we believe to be the cause of his different phenotype, is a further evidence of HDAC6 role in moto-neuron disease. Although there are many papers that give it a controversial role, it is evident the involvement of HDAC6 in neurodegenerative diseases, which may be clarified with further studies on animal models and possibly identifying other patients with mutation in this gene. In this regard, to extend the

research of new patients with *HDAC6* mutations, we started a collaboration with a consortium (ARISLA), that has been carrying out exome sequencing on a large number of familial ALS patients. Unfortunately, in the first 50 samples, no mutations have been identified in *HDAC6*.

The identification of the first *MTO1* mutations and their association with typical clinical features, characterized by hypertrophic cardiomyopathy and lactic acidosis with MRC defects, has permitted and will permit to provide patients of molecular diagnosis. Moreover, we obtained preliminary information on the positive effects of metabolic intervention based on dichloroacetic acid (DCA).

Although the number of reported *MTO1* patients is very low, as a matter of fact all patients that survived beyond infancy and are still alive had DCA treatment starting immediately after the clinical onset. Therefore, the DCA administration should be considered in *MTO1* mutant patients, aware of the fact that neurodegeneration can progress independently from the correction of metabolic status if *MTO1* function is severely impaired.

Indeed, the possibility of a second function for *MTO1* is an interesting point to investigate, as could explain the absence of mitochondrial protein synthesis defects in cellular or yeast models carrying less severe *MTO1* mutations.

Finally, together with a group (Dr. Klopstock in Munich) that has already created a *Mto1* KO mouse model, we will try to use this mouse as a suitable model for therapy, using cardiotropic adeno-

associated virus (AAV) vector expressing wt *MTO1* in the heart. AAVs are attractive option for gene therapy for several reasons: they are not pathogenic, there are several tissue-specific serotypes, and they remain episomal upon infection. Therefore, the AAV based gene replacement seems to be a very promising and transferable approach to cure.

REFERENCES

Fiesel, F. C., Schurr, C., Weber, S. S., and Kahle, P. J. TDP-43 knockdown impairs neurite outgrowth dependent on its target histone deacetylase 6. *Mol. Neurodegener.* (2011); 6, 64.

Gal J, Chen J, Barnett KR, Yang L, Brumley E, Zhu H. HDAC6 regulates mutant SOD1 aggregation through two SMIR motifs and tubulin acetylation. *J Biol Chem.* (2013) May 24;288(21):15035-45.

Gusella JF, Wexler NS, Conneally PM, Naylor SL, Anderson MA, Tanzi RE, Watkins PC, Ottina K, Wallace MR, Sakaguchi AY, et al. A polymorphic DNA marker genetically linked to Huntington's disease. *Nature* (1983) Nov 17-23;306(5940):234-8.

Johnson J O, Mandrioli J, Benatar M, Abramzon Y, Van Deerlin VM et al. Exome sequencing reveals VCP mutations as a cause of familial ALS. *Neuron* (2010); 68, 857–864.

Kim SH, Shanware NP, Bowler MJ, Tibbetts RS. Amyotrophic lateral sclerosis-associated proteins TDP-43 and FUS/TLS function in a common biochemical complex to co-regulate HDAC6 mRNA. *J Biol Chem* (2010) Oct 29;285(44):34097-105.

Koenig M, Hoffman EP, Bertelson CJ, Monaco AP, Feener C, Kunkel LM. Complete cloning of the Duchenne muscular dystrophy (DMD) cDNA and preliminary genomic organization of the DMD gene in normal and affected individuals. *Cell* (1987) Jul 31;50(3):509-17.

Taes I, Timmers M, Hersmus N, Bento-Abreu A, Van Den Bosch L, Van Damme P, Auwerx J, Robberecht W. Hdac6 deletion delays disease progression in the SOD1G93A mouse model of ALS. *Hum Mol Genet.* (2013) May 1;22(9):1783-90.

Tapia, M., Wandosell, F., and Garrido, J. J. Impaired function of HDAC6 slows down axonal growth and interferes with axon initial segment development. *PLoS ONE* (2010); 5, e12908.

Wang L, Colodner KJ, Feany MB. Protein misfolding and oxidative stress promote glial-mediated neurodegeneration in an Alexander disease model. *J Neurosci.*(2011) Feb 23;31(8):2868-77.

Zeharia A, Shaag A, Pappo O, Mager-Heckel AM, Saada A, Beinat M, Karicheva O,

Mandel H, Ofek N, Segel R, Marom D, Rötig A, Tarassov I, Elpeleg O. Acute infantile liver failure due to mutations in the TRMU gene. *Am J Hum Genet* (2009) Sep;85(3):401-7.

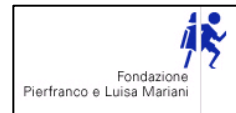
Zimprich, A. Benet-Pagès A, Struhal W, Graf E, Eck SH, Offman MN, Haubenberger D, Spielberger S, et al. A mutation in VPS35, encoding a subunit of the retromer complex, causes late-onset Parkinson disease. *Am. J. Hum. Genet.* (2011); 89, 168–175.



The research presented in this thesis was performed at the Unit of Molecular Neurogenetics, of the Foundation IRCCS Neurological Institute Carlo Besta, Milan, Italy, from January 2011 until January 2014.

I want to thank Dr. Massimo Zeviani for giving me the opportunity to pursue a PhD in his lab, for his experience and precious advice. A special thanks goes to Dr. Daniele Ghezzi for having followed me throughout the period of PhD research, for the continuous availability and for the critical reading of this manuscript.

This work was supported by Fondazione Telethon grants GGP11011 and GPP10005; CARIPLO grant 2011/0526; Pierfranco and Luisa Mariani foundation; Italian Association of Mitochondrial Disease Patients and Family (Mitocon).



All rights reserved. No part of this publication may be reproduced, stored in a retrieval system, or transmitted in any form of by any means, electronic, mechanical, photocopying, recording, or otherwise, without prior written permission of the holder of the copyright.